UNIVERSIDAD DE CANTABRIA

ESCUELA TÉCNICA SUPERIOR DE INGENIEROS DE CAMINOS, CANALES Y PUERTOS

DEPARTAMENTO DE CIENCIAS Y TÉCNICAS DEL AGUA Y DEL MEDIO AMBIENTE

PROGRAMA DE DOCTORADO EN CIENCIAS Y TECNOLOGÍAS PARA LA GESTIÓN DE LA COSTA

TESIS DOCTORAL

ANÁLISIS DE LA VARIABILIDAD CLIMÁTICA EN PARQUES EÓLICOS MARINOS

Presentada por:

Fernando del Jesus Peñil

Dirigida por:

Dr. Raúl Guanche García

Dr. Íñigo J. Losada Rodríguez

Santander, Julio de 2016

A Amparo, a mi familia y a mis amigos,
por vuestra comprensión y apoyo.

Agradecimientos

El documento que sostiene en sus manos reúne y resume una gran cantidad de trabajo desarrollado durante los últimos años y el autor, siendo consciente de que sin la inestimable aportación, no siempre técnica, de muchas personas no habría sido capaz de llegar hasta aquí, quisiera aprovechar estas líneas para agraceder el esfuerzo de todas esas personas y, si los hubiere, los elogios que a la postre pueda recibir. Por ello, gracias a todos los que de una forma u otra me habéis traído hasta aquí. Serán muchos los que nombre y otros tantos los que, por las prisas y el despiste, se queden en el tintero. Aprovecho este momento para agradecer y homenajear vuestro esfuerzo anónimo.

Comenzaré nombrando a mis directores, Raúl Guanche e Íñigo Losada. Gracias Raúl por haber aportado tu punto de vista, por haberme ayudado a mostrar de forma clara los mensajes más relevantes y por los debates y comentarios que han enriquecido este trabajo y de los que, sin ninguna duda, he aprendido mucho. Gracias Íñigo por haber aportado tu experiencia y haberme ayudado a ordenar las ideas en mi cabeza para que acabaran desembocando en este documento. Gracias a vosotros este trabajo es mucho más completo. Espero haber sido digno de vuestro tiempo y dedicación.

No quisiera olvidarme de Raúl Media, quien hace ya cinco años me ofreciera la oportunidad de entrar en un mundo tan interesante y entretenido como es el de las energías renovables y desarrollar mi doctorado en el grupo de Energías Marinas e Ingeniería Offshore.

A todos los compañeros del grupo de Energías, por soportar mis delirantes discursos y por ser tan generosos con su tiempo siempre que hice uso de él. Gracias Javi, Gema, Michele, Arantza, Víctor, José, Lucía, Carlos, Alfonso, Dani; y

en especial a los que consiguieron hacer de esta mi segunda casa y que el doctorado haya sido una experiencia inolvidable: Pimi, Adrián y José Miguel.

Hay más gente dentro del Instituto de Hidráulica de la que no me puedo olvidar. Gracias a Melisa y a Roberto, por su gran aportación, enriqueciendo algunas de las contribuciones de mayor interés. Gracias a Javi y a Rafa, que siempre han estado echando una mano para arreglar todo lo que mis manazas han roto. A Erica y a Íñigo, por los buenos ratos.

No debería olvidarme de dar las gracias a la Fundación Iberdrola y su programa de ayudas a la investigación en energía y medio ambiente. Dos veces me consideraron merecedor de dicha ayuda, otorgándome la libertad necesaria para centrarme en desarrollar todo este trabajo. He de nombrar en este momento a Luis Prieto Godino, por facilitarme el acceso a información indispensable para la realización de la Tesis. Gracias a Cayetano, por mostrar interés desde el primer momento y por echarme una mano a la hora de apartar algunos obstáculos del camino.

Gracias a José Azcona, que apareció en un momento crítico para echar una mano permitiéndonos reducir los tiempos de aprendizaje con la herramienta FAST.

También quiero agradecer a INORE la oportunidad que me ha dado de conocer a otros que, como yo, se encuentran inmersos en su doctorado. Además, he sido miembro de su comité como responsable del área de investigación, lo que me ha permitido conocer a gente muy interesante y adquirir conocimientos y capacidades que, estoy seguro, me servirán de mucho más adelante.

El doctorado no es simplemente una serie de horas dedicadas a una labor, es un estado en el que queda uno inmerso durante su ejecución. Esto conlleva que las alegrías cuando las cosas funcionan y tienen sentido, pero también las frustraciones que llevan a uno a la desesperación, se marcan en el rostro y en el estado de ánimo. Me siento realmente agradecido por haber tenido a mi lado a grandes amigos que han sabido acompañarme y apoyarme, incluso cuando yo se lo he puesto

difícil. Gracias a Leticia, Paula, Blanca, Virginia, Luis, Laura, Jaime, Chencho, Guillermo, Andrés, Javier y otros tantos.

Y cuando se habla de tener que soportar los estados de ánimo de quien escribe estas líneas, sin duda alguna, la familia se lleva el premio gordo. Tengo la suerte de compartir mi vida con una persona que saca lo mejor de mi en cada momento y ha sabido ayudarme a gestionar los ánimos. Gracias Amparo por hacer de mi un mejor marido, un mejor amigo, un mejor hijo, un mejor hermano, un mejor profesional. En definitiva, una mejor persona. Gracias a mi padre, por enseñarme a pensar con sentido común y el significado de profesionalidad. Gracias a mi madre, que me ha enseñado a prestar atención, a ser honesto, a tener personalidad y lo importante que es hacer las cosas con cariño. Gracias a Juan por su lealtad, por su buen humor y por su generosidad, siempre dispuesto a ayudar. Gracias a Manu, por haber puesto el listón tan alto, motivándome para llegar más lejos, por enseñarme que el esfuerzo siempre tiene recompensa, por contagiarme su insaciable curiosidad, por mostrarme que la excelencia es el camino y por haber sido un apoyo y una ayuda dentro del IHCantabria. Gracias a Miriam por las charlas en las que arreglábamos el mundo y por su inagotable buen humor. Gracias a mis abuelos por inculcarme el esfuerzo y la dedicación. A Juan y a Amelia por conseguir que su mensaje calara hondo: ’hijo, estudia, que todo eso es para ti’. Y a Miguel y Carmen, por haber sido un ejemplo de devoción y por enseñarme a disfrutar de las pequeñas cosas.

Mil gracias,
Fernando
Julio 2016

Resumen

Las energías renovables se han erigido como líderes del cambio de modelo energético cuyo objetivo es reducir la dependencia de los recursos fósiles. Además, la creciente preocupación relacionada con el cambio climático, del que el uso de las energías fósiles es protagonista, ha dado un impulso a la apuesta por estas energías alternativas.

Una de las fuentes de energía que más está creciendo dentro de este contexto es la energía eólica. Las políticas comunitarias, en el caso de la Unión Europea, apuestan fuertemente por esta tecnología, elevando el protagonismo de la eólica hasta el nivel de otras fuentes de energía clásicas. Para ello plantea desbloquear el potencial energético del recurso eólico en el mar, abriendo un abanico de oportunidades para el desarrollo de tecnologías innovadoras, investigación de nuevas metodologías, optimización de recursos, mejora de capacidades, etc.

En los países avanzados, que desde hace décadas apuestan por la construcción de parques eólicos en tierra, se está librando una batalla por liderar la implantación y por tanto, el conocimiento, de parques eólicos en el mar. En la actualidad, la mayor parte de los grandes parques marinos se han implantado en el Mar del Norte, gracias a su poca profundidad a disponer de un recurso eólico alto y constante. Estos primeros pasos en la implantación de la tecnología eólica en el mar se han apoyado sobre el vasto conocimiento proveniente de la industria de la extracción del petróleo y el gas.

En este trabajo se ha llevado a cabo una profunda revisión del estado del conocimiento relacionado con la energía eólica, especialmente centrado en la eólica marina. Este análisis ha permitido detectar potenciales mejoras dentro de la metodología general de diseño de parques eólicos marinos, desde la evaluación

del recurso eólico hasta el análisis de la viabilidad económica de los parques.

El principal objetivo de esta Tesis es evaluar la influencia, sobre diferentes aspectos del diseño de parques eólicos marinos, de la variabilidad climática, especialmente del viento. Para ello, en primer lugar se ha estudiado el comportamiento del recurso eólico, contando con fuentes de datos únicas en el mundo, tanto provenientes de medidas instrumentales como de modelos numéricos, y la influencia de la topografía costera sobre el mismo. El conocimiento adquirido hasta este punto se ha aplicado en la mejora de las metodologías de diseño de plataformas flotantes y en la evaluación de la viabilidad económica de parques eólicos marinos.

Abstract

Renewable energy has become leader of the energy model change in order to reduce the dependency of fossil fuels. Furthermore, the increasing concern about climate change (fossil fuels are considered one of the main reasons) is speeding up the development and implementation of renewable energy.

One of the energy sources that is increasing the most is the wind energy. Governments, and more precisely, European Union, are making a big effort to increase the wind energy quote to the level of classical sources of energy. One of the main ideas to achieve this aim is to unlock the offshore wind energy potential, opening a huge field of improvement in the development of innovative technologies, research in new methodologies, optimization of the resources, improvement of the equipments and capacities, etc.

Developed countries, which have build for last years onshore wind farms, are trying to lead the development of offshore wind. Currently, the great amount of power capacity is installed in the North Sea due to the shallow waters and the great energy potential. These first steps in offshore wind are based on the Oil and Gas sector know-how.

In this research a deep review of the state of the art in offshore wind has been carried out. This review has allowed highlighting potential contributions to the general methodology for offshore wind farm design, from the wind resource assessment to the feasibility assessment.

The main objective of this Thesis is to evaluate the influence of met-ocean conditions variability on several aspects of the offshore wind farms design and implementation. For this purpose, the wind resource behavior has been studied at

first, based on unique sources of data both numerical and instrumental. It has been payed special attention to the influence of coastal topography on wind resource. The knowledge acquired has been applied to the improvement of the floating platform design and the economical feasibility assessment of offshore wind farms.

Contents

List of Figures

LIST OF FIGURES

Index of tables

CHAPTER

0

Resumen

Con el objetivo de cumplir con las condiciones establecidas para la consecución de la mención de ***Doctor*** *en la Normativa de los Estudios de Doctorado de la Universidad de Cantabria, aprobada por la Junta de Gobierno el 12 de Marzo de 1999 y actualizada el 18 de Diciembre de 2013, en este capítulo se recogen:*

- *El resumen de la tesis doctoral redactada en español (Resumen).*
- *Las conclusiones de la tesis doctoral redactadas en español, que consiste en el Capítulo 7 íntegramente traducido al español en el apartado final del resumen (Resumen/Conclusiones).*

Análisis de la Variabilidad Climática en Parques Eólicos Marinos

0.1 Introducción

Como respuesta a la aceleración del calentamiento global ocasianada por la emisión de gases de efecto invernadero asociada, principalmente, a la explotación de las energías fósiles (GWEC (2012)), se está aumentando la inversión en las energías renovables en general y, en la eólica en particular. Destacando la puesta en marcha de parques eólicos en el mar.

La búsqueda de localizaciones más energéticas lideró la puesta en funcionamiento de parques eólicos en alta mar. En un primer momento, estos parques se desarrollaron en zonas con escasa profundidad y que permitían adaptar las tecnologías utilizadas en tierra. En los últimos años han tomado protagonismo varias iniciativas para el desarrollo de estructuras flotantes para el soporte de turbinas de viento (EWEA (2013)). El objetivo de todas ellas es desbloquear el potencial energético del viento en aguas profundas.

Tres proyectos se encuentran a la cabeza en el desarrollo de plataformas flotantes para el soporte de turbinas de viento (Table 1.1). Por un lado, el proyecto $Hywind$ desarrollado por la empresa noruega Statoil. Está basado en el concepto conocido

como $spar$ y soporta una turbina con una potencia instalada de 2,3 MW. Por otro lado, el proyecto $Windfloat$ de Principle Power y EDP, está equipado con una turbina de 2 MW y se enmarca dentro del concepto de plataforma semisumergible. Por último, el proyecto $FukushimaSimpuu$, también basado en una semisumergible, se instaló en Japón en 2015 equipado con una turbina de 7MW.

De todas formas, el sector de la eólica marina aún se encuentra en un estadío poco maduro de su desarrollo. Por esta razón, ha de enfrentarse aún a numerosos retos para alcanzar la etapa comercial.

La asociación europea de la energía eólica (EWEA por sus siglas en inglés), propone una serie de retos. A continuación se enumeran los que tienen mayor relevancia con esta Tesis.

- Desarrollo y validación de herramientas de modelado del conjunto turbina-plataforma-sistema de fondeo.
- Avance en las investigaciones sobre el sistema de anclaje.
- Desarrollo de nuevas herramientas y técnicas de medida adaptadas a las aguas profundas.

Esta tesis se apoya en estas propuestas para contribuir al avance del conocimiento en el campo de la eólica marina. Todo ello aplicado al estudio de la influencia de la varibilidad espacial y temporal de las condiciones meteoceánicas.

En el capítulo 2 se lleva a cabo una revisión del estado del conocimiento en relación a los retos propuestos por la EWEA. Posteriormente, en el capítulo 3, se plantean los objetivos y la metodología seguida en esta Tesis. El estudio de la variabilidad espacial y temporal de las condiciones de viento se desarrolla en el capítulo 4. En este capítulo, además, se presta especial atención a la evaluación del error a largo plazo asociado a las medidas de la velocidad de viento tomadas por un mástil meteorológico flotante. En el capítulo 5, se analiza el comportamiento de una plataforma flotante de referencia, centrándose en las cargas sobre el fondeo y en la influencia de la variabilidad de las condiciones meteoceánicas. La

influencia de la variabilidad del viento sobre algunos parámetros financieros de especial relevancia se analiza en el capítulo 6. Por último, las conclusiones finales del trabajo se presentan en el capítulo 7 y las líneas de investigación futuras en el capítulo 8.

0.2 Estado del conocimiento

La energía eólica marina se basa en la adaptación de las tecnologías terrestres al medio marino. Por esta razón, las turbinas eólicas se diferencian poco entre sí. Al igual que en tierra, las turbinas utilizadas son de eje horizontal con tres palas enfrentadas al viento. Las principales diferencias se encuentran en el tipo de soportes que se utilizan. En aquellos emplazamientos con profundidades inferiores a 50 metros, los monopilotes, las jackets (celosías) y las cimentaciones por gravedad son los más comunes. A mayores profundidades, el coste de implementación de estas tecnologías es inasumible. Como respuesta, aparecen las tecnologías flotantes: spar, semisumergible y TLP. En función del uso de una tecnología u otra, el sistema de fondeo puede variar. Se pueden encontrar fondeos con catenarias, tendones o líneas tensionadas, sistemas mixtos o de anclaje a un solo punto.

0.2.1 Condiciones del viento en aguas profundas

La caracterización de las condiciones de viento es un paso necesario para la correcta implementación de parques eólicos marinos. Del viento se derivan, tanto la energía producida como parte de las cargas sufridas por el sistema. Para el análisis del viento es necesario tener acceso a fuentes de datos, tanto instrumentales como numéricas. En el primer caso, los datos pueden provenir de:

- anemómetros de cazoleta o ultrasónicos
- medidas de sistemas basados en láser o sistemas sónicos
- satélite

En los primer y segundo casos, los dispositivos se montan sobre plataformas. En el caso de la eólica en grandes profundidades, estas plataformas son flotantes en forma de boyas meteorolólgicas o mástiles flotantes. Este hecho da lugar a la aparición de nuevas fuentes de incertidumbre debidas al movimiento del cuerpo. En la tabla 2.1, se enumeran las bases de datos numéricas más relevantes y utilizadas como punto de partida para la generación de bases de datos con mayor resolución espacial.

A partir de los datos disponibles se puede llevar a cabo el análisis de las condiciones de viento siguiendo uno de los ocho métodos identificados en Landberg *et al.* (2003). De forma más concreta, el método más común utiliza por un lado, los datos numéricos para llevar a cabo un estudio regional, con una mayor o menor resolución, pudiendo ser en algunos casos de escasos kilómetros; y por otro lado, los datos instrumentales, que se utilizan para validar los datos numéricos y para la caracterización local de las variables meteoceánicas.

Uno de los parámetros más relevantes a escala regional es la influencia de la topografía. En algunos casos, la influencia de la topografía costera en el comportamiento del viento alcanza decenas de kilómetros aguas adentro. En Parish (1982) se estudió la relación entre Sierra Nevada y los flujos de viento en forma de chorro paralelo a la cadena montañosa. En el caso de Overland & Bond (1993), los autores estudiaron el efecto de la topografía costera en el desplazamiento de tormentas.

0.2.2 **Comportamiento de plataformas flotantes**

El desarrollo de tecnologías flotantes como soporte de turbinas eólicas se apoya en dos pilares principales: los métodos propuestos por las normativas y las herramientas numéricas que permiten simular el comportamiento de los cuerpos flotantes.

0.2.2.1 **Revisión de los estándares**

Dos de las principales normativas del sector nacieron como adaptaciones del conocimiento del sector petrolero: IEC y DNV. En la tabla 2.2 se enumeran las

condiciones a partir de los parámetros meteoceánicos. La combinación de estas condiciones de los parámetros meteoceánicos da lugar a los casos de carga (2.3), que permiten analizar la respuesta del dispositivo ante diferentes estados de mar.

El hecho de que la base de estas normativas provenga de otro sector permite un margen de mejora de algunos de los métodos que en ellas se proponen. En el caso del método IFORM (Inverse First Order Reliability Method), en Mínguez *et al.* (2013a) se propone una nueva aproximación para mejorar la estimación de los extremos. La aplicación directa del método, tal y como se propone en la normativa, da lugar a errores de relevancia en los estados de mar más energéticos, incrementando los valores de los parámetros de cálculo. La aplicación de distribuciones de extremos, y no de valores medios como propone la normativa, permite mejorar la estimación, precisamente, de los valores asociados a cincuenta años de período de retorno, objetivo del método.

En la normativa, además, no se identifica claramente cómo se ha de proceder para el cálculo de los valores asociados a altos períodos de retorno cuando se dispone de datos instrumentales y datos numéricos. La normativa, en estos casos, deja en manos del diseñador la decisión de usar los datos de mayor calidad.

0.2.2.2 **Modelado numérico y ensayos de laboratorio**

Para la correcta simulación de dispositivos flotantes, son necesarios los modelos numéricos, que permiten simular el comportamiento de dichos dispositivos frente a diferentes condiciones meteoceánicas; y los ensayos de laboratorio, que simulan el comportamiento del cuerpo en condiciones controladas y a escala. Normalmente, los resultados obtenidos en laboratorio se utilizan para calibrar y validar los modelos numéricos.

0.2.3 **Viabilidad económica**

Las inversiones necesarias para poner en marcha parques eólicos marinos son mucho mayores que en tierra. Por ejemplo, en Young (2009), se plantea unos costes de puesta en marcha de 5M€/MW y unos costes de operación y manteni-

miento de 120K€/MW. Estos altos costes dan lugar a la participación de muchos agentes de diferente índole. Por esta razón, es necesario llevar a cabo un exhaustivo estudio preliminar de los costes potenciales de la inversión. En Couñago *et al.* (2010), los autores presentan un interesante trabajo para determinar los costes de la implementación de un parque eólico marino en la costa gallega. Hacen uso de información de calidad, proveniente de la propia industria. Otra guía de gran interés es la presentada por The Crown State (BVGA (2010)). En ella se proponen costes de todos los elementos de un parque de una forma muy detallada.

0.3 **Objetivos y metodología propuesta**

El objetivo principal de la presente Tesis es:

Caracterizar la influencia de la variabilidad espacial y temporal de las condiciones climáticas en diferentes fases del ciclo de vida de parques eólicos marinos.

Se plantean, además, objetivos secundarios que permitan llevar a cabo el trabajo de la presente Tesis. Los objetivos se reúnen siguiendo el esquema presentado en la figura 3.1.

- Condiciones del viento en aguas profundas
  - Análisis de la calidad de las medidas procedentes de sistemas flotantes
  - Caracterización de la variabilidad de las condiciones de viento
  - Evaluación de la influencia de la topografía costera en las condiciones de viento
- Comportamiento de plataformas flotantes
  - Estudio del método IFORM propuesto en la normativa
  - Adaptación de los modelos de extremos para la estimación de los parámetros de diseño.
- Viabilidad económica
  - Análisis de la influencia de la variabilidad del viento en los estimadores económicos

La metodología planteada para alcanzar los objetivos antes presentados se divide también teniendo en cuenta los tres grandes capítulos del documento.

- Condiciones del viento en aguas profundas
  En primer lugar, es necesario seleccionar las bases de datos, tanto numéricas como instrumentales, que se encuentran a disposición para llevar a cabo el estudio de las condiciones de viento. En este caso, las bases de datos numéricas son de alta resolución (Menéndez *et al.* (2014)), mientras que las bases de datos instrumentales provienen de dispositivos flotantes; tanto de boyas meteorológicas como de mástiles meteorológicos flotantes (Guanche *et al.* (2011)). Los datos instrumentales procedentes de dispositivos flotantes (en mayor medida en lo que se refiere a los mástiles flotantes) introducen nuevas fuentes de error debido al propio movimiento de la estructura soporte. Por esta razón, se lleva a cabo el análisis del error a largo plazo debido a estos movimientos. Se estudiará, gracias a las bases de datos disponibles, la influencia de la orografía en el comportamiento del viento, además del análisis de la variabilidad espacial y temporal de las condiciones del viento.

- Comportamiento de plataformas flotantes
  El análisis de las normativas en lo referente a la estimación de los casos de carga extremos es el primer paso de esta parte de la metodología. Se prestará especial atención a los métodos IFORM y de extremos. Para evaluar el impacto de las contribuciones en la estimación de las cargas es necesario el uso de un modelo numérico. Una vez dicho modelo sea calibrado y validado, servirá para simular el comportamiento de la plataforma flotante y del sistema de fondeo a lo largo del área de estudio permitiendo, por tanto, evaluar la variabilidad espacial y temporal de las cargas en el sistema de fondeo.

- Viabilidad económica
  Se desarrollará un modelo económico para llevar a cabo un estudio basado en simulaciones de vidas útiles de un parque eólico marino tipo. Teniendo en cuenta el estudio llevado a cabo en el capítulo 4 y el modelo de plataforma flotante del capítulo 5, se realiza un estudio de la influencia de la

variabilidad espacial y temporal de las variables meteoceánicas en los principales estimadores económicos.

0.4 Análisis de las condiciones del viento en aguas profundas

El análisis y evaluación de las condiciones de viento es un paso necesario para la estimación de las localizaciones óptimas de parques eólicos marinos. Uno de sus pilares son las bases de datos, tanto numéricas como instrumentales. En el caso de las aguas profundas, al tratarse de un campo inmaduro, las diferentes tecnologías adaptadas a este medio están poco caracterizadas. En concreto, las tecnologás flotantes, en las que el movimiento es una nueva fuente de incertidumbre en las medidas.

0.4.1 Error asociado a las medidas de viento en aguas profundas

Las tecnologías flotantes se espera que sean utilizadas también para la monitorización de las variables meteoceánicas, tal y como se lleva a cabo hoy en día con las boyas meteorológicas. El uso de dispositivos flotantes como soporte de los sistemas de instrumentación da lugar a la aparición de nuevas fuentes de error, principalmente relacionadas con el movimiento.

Se propone una metodología para determinar numéricamente el error de largo plazo asociado a las medidas de viento:

- Teniendo en cuenta la técnica propuesta en Guanche *et al.* (2014c), los estados de mar y viento más representativos se seleccionan.
- Para cada estado de mar se genera una serie temporal sintética de viento y oleaje.
- Se simula numéricamente la respuesta del dispositivo flotante ante dichas series temporales. La simulación se lleva a cabo con un modelo numérico calibrado con ensayos de laboratorio.
- Teniendo en cuenta los movimientos del dispositivo flotante se calcula el error en la medida de viento debido a los movimientos.

- El error de largo plazo se reconstruye aplicando Guanche *et al.* (2014c).
- Finalmente, se analiza el error de largo plazo debido al movimiento de la estructura.

Las principales hipótesis que se tienen en cuenta son:

- Las series temporales sintéticas hacen las veces de viento de referencia, es decir, que se tomarán como las medidas de la anemometría de un mástil fijo.
- El campo de viento sólo tiene componente horizontal.
- Para reducir la complejidad del análisis se supone que el viento y el oleaje son colineales.

En primer lugar, se lleva a cabo la selección de los estados de mar y viento más representativos (500 casos, Guanche *et al.* (2014a)) aplicando el algoritmo MAXDISS (Camus *et al.* (2011b), Snarey *et al.* (1997)). Posteriormente, el modelo hidrodinámico SESAM-DeepC (desarrollado por DNV) se utiliza para simular la respuesta del mástil flotante en los casos representativos. El cálculo del error asociado a las medidas de viento debido al movimiento del mástil flotante se divide en tres pasos:

- Error debido a la altura del anemómetro
  La altura del anemómetro (figura 4.2) en cualquier instante se determina por medio de la expresión 4.1. La velocidad del viento en la posición instantánea del anemómetro se calcula interpolando entre las series sintéticas. Por tanto, el factor de corrección es la relación entre ambos valores (expresión 4.3).
- Error asociado a la inclinación del anemómetro
  Los anemómetros de cazoleta miden la componente de viento en su propio plano. Si se tiene en cuenta el movimiento constante de la estructura flotante esto da lugar a una pérdida de información, ya que la componente de viento que se mide en todo instante no se corresponde con la componente horizontal. Por esta razón, las cazoletas se calibran dando lugar a la

curva coseno (figura 4.3) que permite relacionar el ángulo de inclinación de la cazoleta con el factor corrector a aplicar al viento observado.

- Error debido a la velocidad relativa
  El movimiento del anemómetro introduce una componente de velocidad relativa entre el propio anemómetro y el viento. Es necesario conocer la velocidad del anemómetro en todo momento para corregir el viento observado (expresión 4.7).

Una vez se determina la forma de evaluar el error asociado a las medidas de viento se propone el estudio del impacto del movimiento de un mástil flotante en las medidas de viento a largo plazo. Los resultados de los casos de velocidad de viento asociados a 50 años de período de retorno se muestran en la tabla 4.1, para 2 años de período de retorno en la tabla 4.2 y, por último, para el viento medio en la tabla 4.3.

La reconstrucción de las series temporales de error en las medidas de viento permite el estudio estadístico de largo plazo. En la figura 4.9, se muestra el scatter de la velocidad de viento medio horario y del viento máximo diezminutal. Permiten ver que las desviaciones en la velocidad de viento observada con respecto al viento real se da principalmente en velocidades superiores a los 20 metros por segundo.

El error se mantiene por debajo del 0.5% dentro del rango de funcionamiento de turbinas eólicas (0 m/s$< V <$ 25 m/s) (figura 4.10).

0.4.2 **Variabilidad espacial y temporal de las condiciones de viento**

El estudio de la variabilidad espacial y temporal de las condiciones de viento se lleva a cabo en la costa de Cantabria (Norte de España). Esta región se caracteriza por tener la Cordillera Cantábrica relativamente cerca de costa y paralela a ella, destacando los Picos de Europa. Además, siete valles perpendiculares a la costa y a la cordillera dan lugar a zonas de confluencia de vientos y estructuras del flujo que permanecen incluso varios kilólmetros mar adentro.

0.4.2.1 **Bases de datos**

Para el estudio del comportamiento del viento y su variabilidad espacial y temporal se han utilizado dos bases de datos numéricas:

1. Seawind 2: Es una base de datos horaria de reanálisis para la región del Mediterráneo y el Atlántico europeo de 15 km de resolución espacial de las variables relacionadas con el viento.

2. Seawind HR: Es una base de datos horaria de reanálisis de 500 días del norte de España con una resolución espacial de una milla naútica (1,8km aproximadamente) de las variables más importantes relacionadas con el viento.

0.4.2.2 **Influencia de la orografía costera**

El análisis de la influencia de la topografía costera se lleva a cabo en tres pasos: estudio del perfil de viento, análisis de la energía del viento y caracterización del factor de capacidad.

En el primer caso, se analizan los parámetros asociados a los perfiles potencial (ecuación 4.17) y logarítmico (ecuación 4.18). A partir de los datos de los mástiles meteorológicos y de los datos de velocidad de viento numéricos, se obtienen rosas direccionales del valor de los parámetros asociados a ambos perfiles. En la figura 4.32, se muestra el exponente α para el caso de la base de datos numérica en la Virgen del Mar. Se observa que los vientos del sur, afectados por la topografía costera, aumentan el valor del exponente, lo que implica que el gradiente de velocidades del perfil es importante. Esto ocurre en Ubiarco (figura 4.33) en los vientos de suroeste, relacionados directamente con los vientos provenientes de la zona de los Picos de Europa. Los valores altos asociados a los vientos de sur se pueden encontrar también en las rosas asociadas a los mástiles meteorológicos flotantes de Virgen del Mar (figura 4.35) y Ubiarco (figura 4.34). En cuanto al perfil logarítmico, en la figura 4.36 se muestra el valor de z_0 para los datos del mástil en Ubiarco. Se observa que es mayor para los vientos de sur. El mismo parámetro se muestra para los datos del mástil en Virgen del Mar (figura 4.38) y para los datos numéricos en Virgen del Mar (figura 4.39) y en Ubiarco (figura

4.37). en todos los casos se observa que este parámetro alcanza valores mayores cuando el viento proviene de tierra.

El factor de capacidad se analiza en cinco puntos a lo largo del cantábrico (Tabla 4.4). Los valores de factor de capacidad más altos se alcanzan en la costa gallega para una turbina de 2MW.

En la figura 4.40, se muestra la energá asociada al viento para situaciones de viento sur aisladas (imagen superior) y para el total (imagen inferior). Permite observar que el impacto de la orografía costera se deja notar en situaciones de viento sur, principalmente. Da lugar a valores menores de la energía del viento en la zona influenciada por los Picos de Europa.

0.4.2.3 **Variabilidad temporal de las condiciones de viento**

Las condiciones de viento se estudian destacando las situaciones sinópticas, que permiten de un vistazo destacar las condiciones de viento más comunes y que mayor variabilidad explican (figura 4.43). En la figura 4.44 se muestran las situaciones sinópticas asociadas a condiciones de viento sur. En ellas se observa la disminución de la intensdidad de velocidad de viento ocasionada por los Picos de Europa. También se lleva a cabo un análisis estacional de las situaciones sinópticas (figuras 4.46 y 4.50) donde se observan patrones similares en primavera y verano, por un lado y, otoño e invierno por otro.

0.4.3 **Conclusiones**

- El análisis llevado a cabo para determinar el error medio de largo plazo en los mástiles meteorológicos flotantes de Idermar muestra que, dentro del rango de funcionamiento de turbinas eólicas, permanece por debajo de un 0.5%.

- La combinación de datos numéricos y datos instrumentales permite aprovechar las ventajas de ambas bases de datos. Las series numéricas, gracias a su longitud permiten estimar los valores asociados a los periodos de retorno

altos, mientras que los datos instrumentales miden valores extremos que se utilizan para mejorar la estimación de dichos valores.

- La influencia de la topografía costera queda constatada y, se determina que puede llegar a influencia el flujo de viento incluso a más de ochenta kilómetros de costa.
- El uso de las situaciones sinópticas permite reducir el volumen de datos con los que llevar a cabo el estudio sin disminuir la calidad de la caracterización del viento.

0.5 Análisis del comportamiento de plataformas flotantes

Los conocimientos de partida de la energía eólica flotante provienen, principalmente, del sector petrolero y gasístico. Este hecho permite un rango de mejora de los métodos de estudio de las plataformas flotantes, adaptándolos a las nuevas necesidades del sector.

0.5.1 Actualización del método IFORM

El método presentado en Mínguez *et al.* (2014) propone una mejora para la estimación de los estados de mar, definidos como parejas de altura de ola significante y velocidad de viento, asociados a largos períodos de retorno. Su propuesta consiste en utilizar una distribución de extremos para el cálculo de la función de distribución de altura de ola condicionada a la velocidad de viento. En este trabajo se aplican ambas versiones del método en cuatro localizaciones (ver figura 5.1 y tabla 5.1). En las figuras de la 5.3 a la 5.10 se muestran los resultados. Se observa en todos los casos que el método propuesto en la normativa no estima correctamente los estados de mar asociados a largos períodos de retorno que se encuentran en la rama derecha de la distribución, asociados también a la mayor energía.

Se muestra en las figuras de la 5.11 a la 5.16 la distribución espacial de las variables altura de ola significante y velocidad de viento para determinados puntos de la curva de cincuenta años de período de retorno.

0.5.2 **Modelo mixto de extremos**

En Mínguez *et al.* (2013a), se presenta un método para mejorar la estimación de los valores asociados a grandes períodos de retorno combinando datos instrumentales y numéricos. En este caso, los autores llevan a cabo el ajuste de los extremos haciendo uso de una distribución GEV, que selecciona los máximos anuales. En este trabajo se tiene en cuenta la falta de series instrumentales suficientemente largas para poder trabajar tan solo con los máximos anuales y se propone llevar a cabo el método haciendo uso de una distribución GPD (Generalized Pareto Distribution), lo que permite marcar un umbral y utilizar todos los picos sobre dicho umbral para ajustar la distribución. De esta manera se aumenta el número de datos para la estimación.

Este método también se aplica en los cuatro puntos en los que se aplica el método IFORM revisado. Los resultados se muestran en la figuras 5.19, 5.20, 5.21, 5.22 y en la tabla 5.3.

0.5.3 **Comportamiento de una plataforma flotante: variabilidad espacial**

Se selecciona una plataforma de referencia (figura 5.23) y una turbina tipo (Jonkman *et al.* (2009)) como sistema de partida. Para la simulación de la plataforma flotante se utiliza el modelo FAST (Jonkman (2009)). A este modelo hay que alimentarlo con ficheros provenientes de WAMIT o, en nuestro caso de WADAM, módulo de cálculo hidrodinámico utilizado por el software SESAM.

En primer lugar, se lleva a cabo la calibración del modelo numérico utilizando los test de laboratorio. Se comienza con los seis grados de libertad para garantizar la correcta simulación de los períodos propios (figuras 5.27 y 5.28). Posteriormente se comprueba el comportamiento del modelo numérico en un caso de oleaje regular (figura 5.30) y, por último en un caso de oleaje irregular (figura 5.31).

Una vez dado por bueno el modelo numérico, se lleva a cabo el análisis espacial de las cargas sobre el sistema de fondeo. Para ello se seleccionan los cien

estados de mar de una hora más representativos aplicando el algoritmo de máxima disimilitud (Camus *et al.* (2011b)) para todo el cantábrico. Posteriormente, se simulan dicho casos y se obtienen las series temporales de las cargas sobre el sistema de fondeo. Se realiza una estadśtica de los picos de la serie para disminuir el volumen de información. Se calcula el valor medio, el valor máximo, el valor mínimo, el valor significante y la desviación estándar. Por último, se reconstruyen las series temporales de estos parámetros a lo largo del cantábrico.

En las figuras de la 5.37 a la 5.41 se muestra la distribución espacial de los parámetros seleccionados. Se observa la relación directa entre las cargas en el sistema de fondeo y las variables meteoceánicas. Es importante destacar la importancia del período del oleaje, ya que es una de las variables que más condiciona el comportamiento hidrodinámico de la plataforma flotante.

0.5.4 **Conclusiones**

- Hay un importante margen de mejora de los métodos propuestos en las normativas para la estimación de los casos de carga de diseño.
- El método mixto de extremos mejora la estimación de los valores asociados a largos períodos de retorno.
- Se propone llevar a cabo un análisis completo de sensibilidad del método propuesto en Mínguez *et al.* (2014) para determinar su rango óptimo de aplicación.
- El período de pico parece ser la variable meteoceánica más relevante en el comportamiento del sistema de fondeo.

0.6 **Análisis de viabilidad económica**

En este capítulo de la tesis, se lleva a cabo el análisis de la influencia de las condiciones meteo-oceánicas sobre la viabilidad económica de parques eólicos marinos. Teniendo en cuenta como valor de referencia un coste de 5M€/MW para la eólica marina, es necesario mejorar en la medida de lo posible la estimación

de los costes de inversión de los parques marinos, con el objetivo de reducir la incertidumbre asociada a tan grandes inversiones.

Para estudiar la variabilidad espacial y temporal de los costes de inversión se lleva a cabo la siguiente metodología:

1. Se generan series temporales de velocidad de viento por Monte-Carlo, a partir de las series temporales horarias numéricas de sesenta años.

2. Se calcula, posteriormente, la producción energética asociada a cada serie temporal generada.

3. Se simulan los flujos de caja para cada vida útil en cada nodo y se obtienen los principales parámetros financieros.

4. Por último, se calculan parámetros estadísticos de los parámetros financieros en cada nodo.

Son cuatro los parámetros financieros elegidos para llevar a cabo el análisis de la variabilidad espacial y temporal del comportamiento financiero en relación a la implantación de parques eólicos marinos: la tasa interna de retorno, el valor presente neto, el período de devolución de la inversión y el coste de la energía.

Para el cálculo de los costes del parque se han tomado como valores de referencia los presentados en Couñago *et al.* (2010) (ver resumen en tabla 6.1). Además, se tienen en cuenta una serie de parámetros de relevancia a la hora de calcular los costes asociados al parque. Por un lado, la distancia del parque a puerto y la distancia del parque a costa, que afectan en los costes de construcción de diferentes sistemas. Por otro lado, la profunidad que afecta, principalmente, al sistema de fondeo.

0.6.1 **Estructura del estudio**

El análisis econmico llevado a cabo se divide en dos tests:

- Test 1: Análisis espacial de los parámetros financieros suponiendo un precio de la energía.
- Test 2: Análisis espacial marcando una rentabilidad mínima esperada por el inversor.

0.6.2 **Variabilidad espacial e interanual de la producción**

En primer lugar, en la figura 6.7 se muestra el recurso disponible en el área de estudio. Se observa una clara dependencia del recurso de la topografía costera. Posteriormente, se seleccionan cinco puntos a lo largo de la costa de estudio para evaluar la variabilidad interanual de la producción (figura 6.8) De la tabla 6.2 se concluye que aquellas localizaciones con un gran potencial tienen la menor variabilidad relativa a lo largo de la zona de estudio.

En la figura 6.9, se muestra el coste de la energía producidad por un parque eólico de 500 MW. Los costes más bajos se encuentran en la costa atlántica gallega, mientras que frente a la costa de Asturias y del País Vasco se alcanzan los precios más altos de la energía.

0.6.3 **Test 1**

Dentro del primero de los tests propuestos, se analiza el comportamiento espacial de la tasa interna de retorno (figura 6.10), del valor presente neto (figura 6.11) y del período de devolución de la inversión (figura 6.12). Los valores más interesantes se alcanzan en la costa gallega, donde se encuentran las mejores condiciones para la implantación de parques eólicos marinos en el norte de la península.

0.6.4 **Test 2**

En el segundo test, se calcula el precio de la energía para asegurar una tasa interna de retorno del 10%. El resultado se puede observar en la figura 6.13, donde el precio de la energía varía de los 15c€/KWh en Galicia a los 75c€/KWh en algunas áreas de Asturias y del País Vasco.

0.6.5 **Conclusiones**

- El modelo económico utilizado se trata de un modelo simplificado y, por tanto, con una aplicación limitada. Su concepción generalista permite su adaptación para mejorar la simulación de algunos costes relacionados con la operación y el mantenimiento del parque, entre otros.

- La metodología para el análisis del comportamiento económico de parques eólicos desarrollada en este trabajo permite llevar a cabo una evaluación detallada de los emplazamientos potencialmente rentables.

- Como se concluye del análisis, en el área de estudio considerada, la costa de Galicia reúne las condiciones necesarias para ser considerada una zona de interés para la implantación de parques eólicos marinos.

0.7 **Conclusiones generales**

En este trabajo se ha llevado a cabo el análisis de la variabilidad de las condiciones meteo-oceánicas. Para ello, en primer lugar se ha llevado a cabo una revisión de las aportaciones más relevantes de la literatura (capítulo 2) en relación a los contenidos de esta tesis. Gracias a esta revisión se han podido destacar una serie de potenciales contribuciones, marcadas como objetivos en el capítulo 3.

En el capítulo 4, se ha llevado a cabo el análisis de las condiciones de viento en aguas profundas. En primer lugar, se ha estudiado el impacto del movimiento de los sistema de medida sobre mástiles meteorológicos flotantes en el error de largo plazo de las medidas. Tras esto, se han combinado fuentes de datos únicas en el mundo, provenientes de bases de datos de reanálisis de alta resolución y medidas instrumentales en aguas profundas para llevar a cabo una validación de los datos numéricos y así poder extender el estudio a una escala regional. Uno de los puntos relevantes considerados en este trabajo es la influencia de la topografía costera sobre el comportamiento del recurso eólico, además del análisis estacional e interanual.

Como uno de los aspectos más relevantes en el campo de la energía eólica marina, en el capítulo 5 se ha llevado a cabo el análisis espacial de las cargas sobre el sistema de fondeo de una turbina eólica sobre una plataforma semisumergible. La naturaleza de las normativas da pie a la mejora de algunos de los métodos para la estimación de los parámetros de diseño. En este capítulo se han analizado mejoras en la estimación de los parámetros de diseño relativos al método IFORM y a la estimación de los parámetros asociados a períodos de retorno largos cuando los datos instrumentales son escasos (Método Mixto de Extremos). Para poder comparar la influencia de las contribuciones se ha simulado el comportamiento de una turbina flotante con un modelo numérico. Gracias a estas simulaciones se ha obtenido el valor de las cargas sobre el sistema de fondeo y se ha podido llevar a cabo el análisis espacial de las mismas a lo largo de la zona de estudio.

En el capítulo 6 se ha llevado a cabo la evaluación econmica de la implantación de parques elicos marinos en la zona de estudio. La revisión del estado del conocimiento ha permitido destacar los modelos y metodologías que permiten una mejor simulación de los costes de un parque eólico marino. A partir de estos modelos, se han simulado multitud de vidas útiles con el objetivo de incluir la influencia de la variabilidad climática en los parámetros financieros más relevantes.

A continuación se presentan las conclusiones generales de la tesis:

- Análisis de las condiciones del viento en aguas profundas (capítulo 4)
  - Del análisis del error asociado a las medidas instrumentales registradas con mástil meteorológico flotante, se concluye que esta tecnología puede ser una alternativa competitiva a la hora de caracterizar el recurso eólico, ya que el error relativo a la velocidad media del viento no supera el 0.5% dentro del rango de funcionamiento clásico de las turbinas eólicas.
  - El uso combinado de datos de reanálisis y medidas instrumentales permite llevar a cabo los análisis de largo plazo y de corto plazo de las condiciones de viento.

  - La influencia de la topografía se ha demostrado que tiene una gran relevancia en la caracterización de las condiciones de viento.
  - La aplicación de los patrones sinópticos ha demostrado ser una alternativa de análisis que reduce el volumen de datos con los que trabajar sin disminuir la calidad del resultado final.

- Análisis del comportamiento de una turbina flotante
  - Se ha demostrado que aún hay espacio en las normativas relativas a energía eólica marina para la propuesta de mejoras y nuevos métodos.
  - Aún hay margen de mejora en los modelos de simulación del comportamiento de turbinas flotantes.
  - En el caso de la caracterización de extremos, se ha evaluado un método propuesto por Mínguez *et al.* (2014) en el que se aplican distribuciones de extremos para la estimación de los estados de mar asociados a grandes períodos de retorno. El método mejora la estimación de los mismos pero es muy sensible al umbral escogido y, por tanto, requiere de un análisis más profundo de su aplicabilidad.
  - Se ha desarrollado un método de estimación de parámetros de carga de diseño que combina la longitud de los datos de reanálisis y las medidas instrumentales. El método ha sido adaptado para dar respuesta a la escasez de datos de campo que caracterizará el futuro de la eólica flotante.

- Análisis económico
  - El modelo de simulación de vidas útiles para parques eólicos marinos desarrollado en esta tesis es una herramienta adecuada y que permite analizar de una forma óptima y a escala regional el comportamiento de dichos parques con el objetivo de localizar los mejores emplazamientos. Además, esta herramienta permite su adaptación a cada caso de forma sencilla, otorgando una importante capacidad de análisis a los diseñadores.

CHAPTER

1

Introduction

Nowadays, one of the most important challenges that our society must face is global warming, which is mostly due to the emission of greenhouse gases. These gases are related to the exploitation of fossil fuels for energy supply and transport. In fact, the power sector is responsible for more than the 40% of all carbon dioxide emissions (GWEC (2012)). Indeed, the society is facing a scenario where renewable energy is a valuable solution. Currently, more than a 13% (IEA (2013)) of the primary energy supply relies on renewable sources. Wind energy, due to its maturity is positioned as one of the key renewable energy resource to reduce the dependency of fossil fuels.

Wind energy has advantages and disadvantages. On one hand, wind energy is a clean energy, very consistent from year to year. But on the other hand, it should be included as part of a diverse energy mix because it has significant short-term variability. The better behavior of offshore wind, more homogeneous and powerful, and the level of maturity already achieved in onshore applications are motivating a great development of this technology in the ocean. Europe, and more precisely the North Sea area, is the location where offshore wind has been most extensively deployed due to the favorable conditions related to water depth (depth

$<$ 40 m) and wind intensity.

Nowadays, offshore wind is one of the fastest growing maritime sectors. Its installed wind capacity was 5 GW by the end of 2012, and it is expected to be eight times higher by 2020, reaching 40 GW, i.e. 4% of the European electricity demand. By 2030, offshore wind capacity is expected to be 150 GW, the 14% of the EU's total electricity consumption (EWEA (2013)).

As it was highlighted, wind at offshore sites has a greater potential than onshore (Sempreviva *et al.* (2008)). This fact is the principal reason to explain the growth of the investments in offshore wind energy. Moreover, offshore wind farms are being planned farther and deeper at each time. This is because at far offshore sites greater power potential can be found due to the reduction of coastal areas influence.

In figure 1.1, the wind power potential at coastal areas of some countries are shown. The information is shown taking into account the water depth. As it can be noticed, deep locations (blue bars) have a much greater power potential. In some cases, such as Russia, Canada or Norway the increase at deeper sites is very significant.

Globally, the wind power potential at shallow waters (0 - 30 m) is 6,928.7 GW, 10,455 GW at translational waters (30 - 60 m) and 56,785 GW at deep waters (60 - 100 m) (Arent *et al.* (2012)). Consequently, wind power potential at deep waters is 326% related to shallow and transitional waters. Because of that, deep waters is one of the targets of the offshore wind sector.

Figure 1.2 shows how the trend followed by offshore wind is moving to farther and deeper locations. Several offshore wind farms under construction are, already, being constructed at more than 80 km offshore. Depth at these locations is around 40 m, near the limit of fixed structures (50 m, EWEA (2013)) feasibility.

Offshore wind started by adapting the onshore technology to offshore loca-

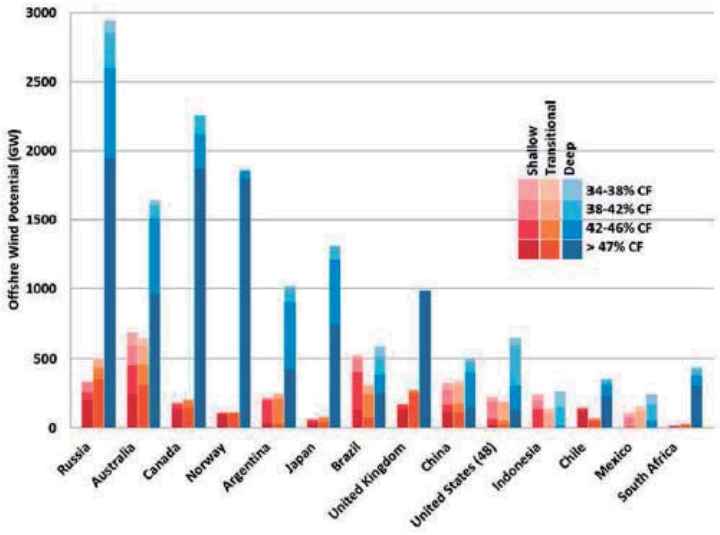

Figure 1.1: Wind potential (GW) by wind resource class (annual-average capacity factor bin) and water depth for selected countries (Arent *et al.* (2012)).

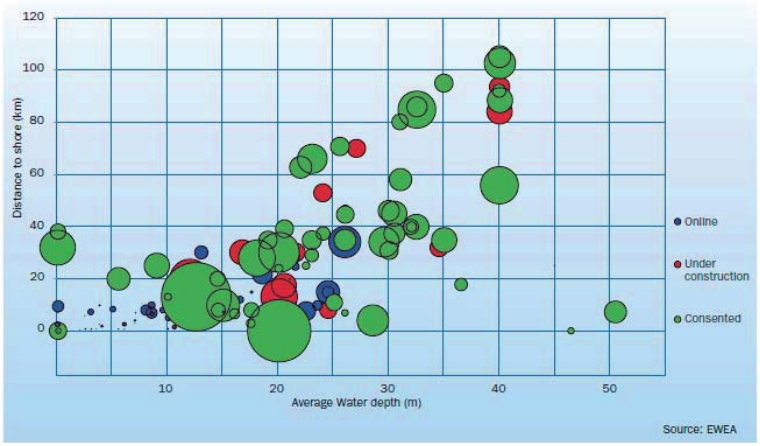

Figure 1.2: Average water depth and distance to shore for online, under construction and consented offshore wind farms (bubble size represents the total capacity of the wind farm) (EWEA (2013)).

tions. Therefore, wind turbines were deployed on fixed support structures, such as: monopiles, tripods, gravity-based foundations (GBF), jackets or tri-piles (figure 1.3, EWEA (2013)); in shallow waters.

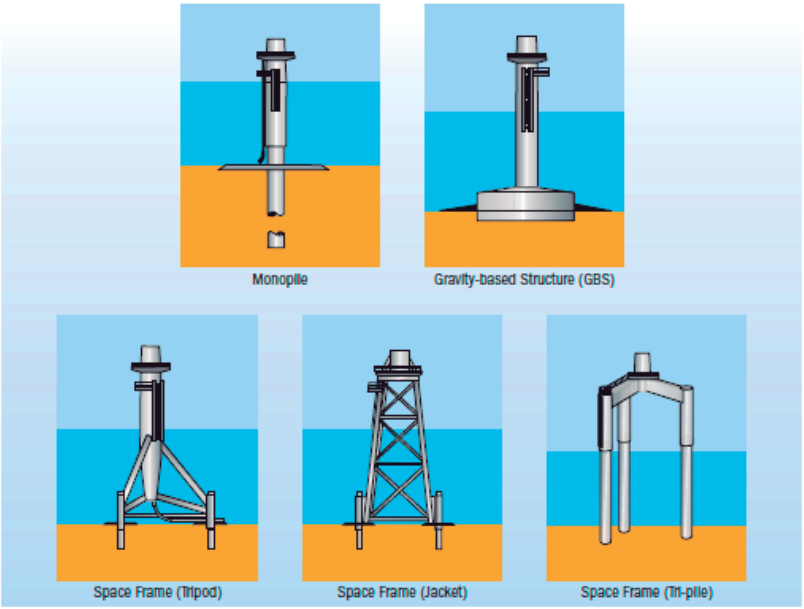

Figure 1.3: Fixed structures (EWEA (2013)).

As water depth increases new technologies must be developed: floating technology. At the end of 2015, there were few grid connected floating wind turbines: Hywind ,Windfloat and Fukushima Shimpuu, are the main examples.

- Hywind is a concept developed by Statoil installed in 2009. It is equipped with a 2.3 MW Siemens turbine. It was installed in Norway at a depth of 150m. It is based on a spar-type floating technology.
- Windfloat was installed offshore the Portuguese coast in 2011. It is developed by Principle Power and EDP equipped with a 2 MW Vestas wind turbine. It is based on a semisubmersible technology.
- Fukushima Shimpuu was installed offshore the coast of Japan in 2015. It is

equipped with a 7MW wind turbine. It is developed by a Japanese consortium and based on a semisubmersible technology.

Country	Project Name	Technology
Japan	Fukushima	Spar
Japan	Kabhasima Island	Hybrid Spar
Japan	Wind Lens	Floater
Japan	Mitsui Zosen	TLP
Japan	MODEC	Floater
Japan	Hitachi Zosen	Semisubmersible
Japan	National Maritime Research Institute of Japan	Spar
Japan	Shizimu Corporation	Semisubmersible
Norway	Hywind	Spar
Norway	Sway Floating Tower	Spar
Norway	WindSea	Floater
Norway	Pelagic Power	Floater
Denmark	Poseidon	Floater
Netherlands	Blue H	TLP
Nehterlands	Gusto Trifloater	Semisubmersible
France	Vertiwind	Floater
France	IDEOL	Floater
France	Technip INFLOW Floater	Floater
France	Nass et Wind Winflo	Floater
France	DIWET	Semisubmersible
Spain	FLOTTEK	TLP
Spain/Germany	HiPR Wind	Semisubmersible
Germany	GICON SOF	TLP
Sweden	Sea Twirl	Spar
Sweden	Hexicon	Floater
United Kingdom	Xanthus Energy Ocean Breeze	TLP
U.S.A.	DeepCwind VolturnUS	Semisubmersible
U.S.A.	Pelastar	TLP
U.S.A.	Nautica windpower AFT	TLP
U.S.A./Portugal	Windfloat	Semisubmersible

Table 1.1: Principal projects of the semi-submersible technologies.

There are several ongoing floating offshore wind projects: SeaTwirl, SWAY, Blue H, Poseidon, Kabashima Island, WindLens and DeepCwind, among others. They are shown in table 1.1 together with other projects at different phases of development. As shown in table 1.1 nine projects are based on floater technology whereas seven are designed considering a Tension Leg Platform (TLP). However, spar and semisubmersible projects are the most developed with several prototypes at different scales being tested under real conditions.

Nevertheless, the offshore wind sector is still at a very early stage of development. Many technical and scientific challenges must be faced before becoming a fully commercial source of energy.

The European Wind Energy Association (EWEA) proposed some technical recommendations for offshore wind development related to the contents of this introduction. In this section, some of them are highlighted:

- *New measuring techniques and tools should be developed to assess the wind and wave conditions at wind farm locations.*

- *More research must be done on mooring and anchoring systems.*

- *Modeling tools and numerical codes that simulate the whole structure's behavior should be developed and validated to improve design.*

The present work is based on these three technical recommendations given by EWEA in 2013 (EWEA (2013)) proposing a common core of analysis: the influence of wind conditions variability. Hence, it will try to study the influence of met-ocean conditions variability at several stages of the offshore wind design process: from the resource assessment to the economical evaluation of an offshore wind farm implementation.

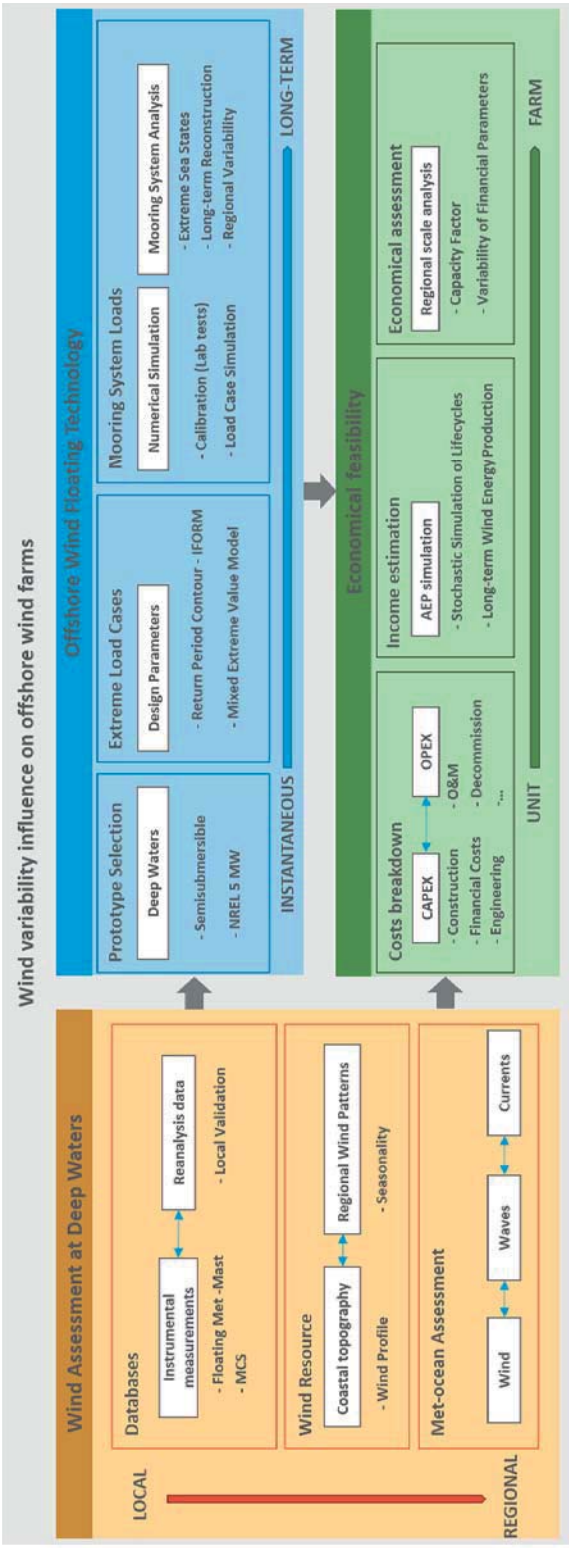

Figure 1.4: Contents of the Thesis.

In figure 1.4 the structure and the contents of the thesis are shown. This work is based on three main content blocks:

- The assessment of offshore wind conditions at locations characterized by deep and very deep waters.
- The analysis of floating technology performance and, more precisely, the response of the mooring system.
- The spatial analysis of the economical feasibility of offshore wind farms.

In the first block, the wind resource assessment at deep and very deep water locations is presented. It is based on the combination of unique sources of data both instrumental and numerical. The most interesting and innovative sources of data are related to the wind speed measurements from three floating meteorological masts. These met-masts are the first floating technology with this aim in the world. They were deployed in 2009, 2010 and 2011.

The combination of wind speed measurements from these three floating met-masts and some other devices with high resolution reanalysis wind speed databases allowed validating the numerical databases and increasing the spatial resolution from local scale to regional scale in order to evaluate the influence of coastal topography on local wind shear and regional wind patterns, including the analysis of the seasonality of wind resource and its link with the characteristics of the coast.

The information and results of this first part of the Thesis are directly applied in the rest of the work. For instance, the offshore wind floating technology performance assessment is based on the met-ocean conditions, including wind, waves and currents for the numerical simulation of a semisubmersible platform for offshore wind turbines. In this block some new methods to improve the estimation of the design parameters for extreme load cases are presented and evaluated. Selection and reconstruction algorithms are applied to evaluate the long-term mooring system load behavior at regional scale.

The third and last block is based on the economical feasibility of the implementation of offshore wind farms. It requires all the information generated in the

other chapters to estimate accurately the real costs of an offshore wind farm and the energy production. The analysis is done regionally in order to locate the most promising sites in the area of study.

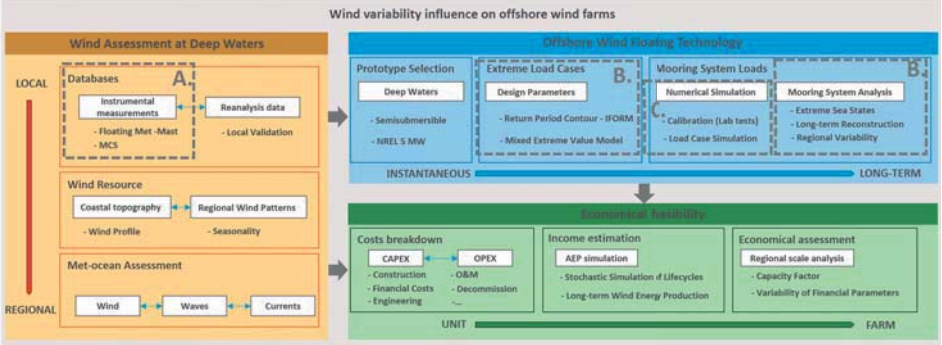

Figure 1.5: Contents of the Thesis and their relation to EWEA challenges.

The contents of this work and the challenges proposed by EWEA (figure 1.5) are interrelated. In the first block the analysis of the floating met-masts data and the development of a movement compensation algorithm is directly related to the first challenge noticed, the development of new measuring devices to characterize offshore wind resource.

In the second block new methods to estimate the design parameters for the mooring system are proposed. This is related to the second challenge outlined, which aim is to improve the knowledge and understanding of the mooring system and its numerical design.

The third challenge proposed by EWEA is focused on the numerical simulation of floating technologies for the unlocking deep and very deep locations. In this work, the numerical simulation of the complete system: turbine, floating platform and mooring system, is carried out using a calibrated numerical tool.

In figure 1.6 the contents of the thesis are included in their respective chapters. Although, first of all the state of knowledge concerning to the offshore wind

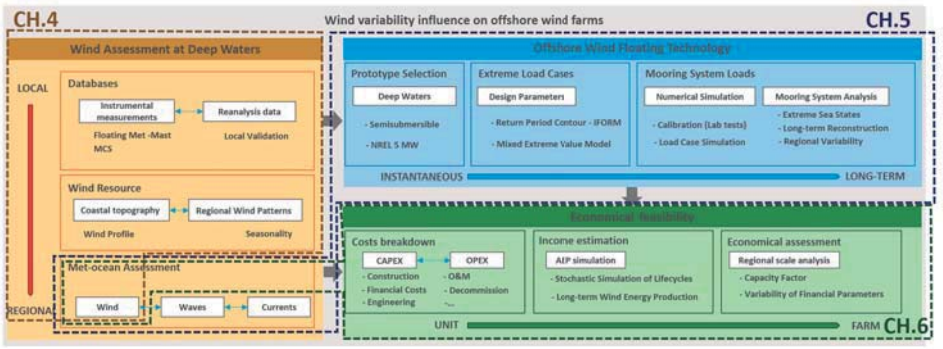

Figure 1.6: Contents and structure of the Thesis.

design methodology is reviewed in chapter 2. The review will be focused on three main topics: the wind conditions assessment, the estimation of design parameters and the analysis of offshore wind farms feasibility. Afterwards, main and partial objectives will be explained in chapter 3, including the general description of the methodology followed in this work.

Chapter 4 includes the evaluation of the temporal and spatial variability of offshore wind conditions at deep water areas in order to finally validate the numerical reanalysis databases that are applied in the rest of the work.

Floating platforms for wind energy purposes performance are analyzed in chapter 5 supplied by the met-ocean conditions analyzed and generated in chapter 4.

In order to characterize the influence of wind conditions variability, in chapter 6, the economical assessment is applied to several virtual offshore wind farms in the Cantabrian Sea (North of Spain).

In figure 1.7, the main contributions of the thesis are outlined on the contents scheme for more clarity. The first contribution is related to the development of the algorithm for the movement compensation system, although in this work it is

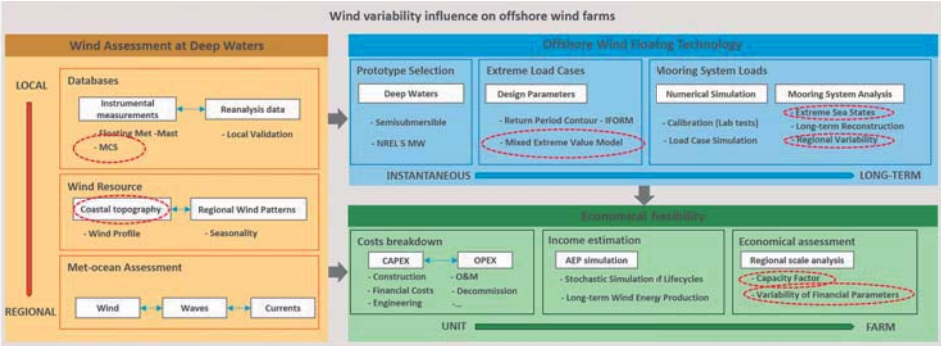

Figure 1.7: Contents of the Thesis and main contributions.

used to evaluate the long-term error related to floating measuring devices. Another main contribution is the analysis of the coastal topography influence on offshore wind, paying attention to the first kilometers from the shore, in the area where the influence of the coastal topography is more important. In the second content block, several contributions are highlighted: the development of new methods to improve the estimation of design parameters related to long return level which are directly applied to the simulation of extreme sea states. Moreover, this information is applied to evaluate the regional variability of mooring system loads due to wind, waves and currents loads. Finally, in the last content block an analysis of the capacity factor is done in order to increase the understanding of wind energy production assessment and the optimization of wind farm implementation. Moreover, the spatial variability assessment of the main financial estimators would help decision makers to select wind farm sites.

Finally, the general conclusions of the work will be summarized in chapter 7. Some future lines of research, based on the work presented in this thesis, are proposed in chapter 8.

CHAPTER

2

State of the art

In the present chapter, the state of the art of offshore wind farm aspects related to wind conditions and its influence on farm performance will be reviewed. This includes wind conditions assessment, which is the base for the rest of the work; the analysis of floating structure performance and the economical assessment. Special attention will be paid to variability and uncertainty due to met-ocean conditions. Moreover, this chapter is allocated to determine potential gaps to propose improvements in following chapters. The structure of this chapter is as follows:

- Fundamentals of Wind Energy
- Offshore Wind Conditions
- Floating Platform Performance Assessment
- Economical Feasibility Assessment

2.1 Fundamentals of wind energy

Global winds are caused by pressure differences across earth's surface due to the unequal heating by sun radiation. In addition, the rotation of the earth around the sun and around its own axis turns out seasonal variations in air circulation patterns. Furthermore, there are spatial differences in heat transfer from the earth's surface to the atmosphere. Therefore, an atmospheric pressure field is created, causing air flowing from high pressure areas to low pressure areas.

The available power in the wind that can be extracted is expressed by the next equation:

$$P_w = \frac{1}{2}\rho A u^3 \tag{2.1}$$

where ρ is the air density, A is the area and u is wind speed. Power (P_w) is measured in W (watts). It has to be highlighted that wind power depends on cubed wind velocity. Therefore, small discrepancies on wind definition leads to high differences on power assessment.

A wind turbine (figure 2.1), as defined in Manwell *et al.* (2009), is a machine which converts the power of the wind into electricity. Today, the most common design is the horizontal axis wind turbine (HAWT); upwind, which means that wind passes through blades before it passes through the nacelle; and three bladed.

To explain how wind turbines extract energy from wind some concepts about aerodynamics should be explained. Air flow over a stationary airfoil produces two forces, a *lift* force perpendicular to the air flow and a *drag* force in the direction of air flow (figure 2.2). If these forces are split into a parallel component to movement and another perpendicular, the parallel force to movement will be the one which moves the airfoil and, to it, the rotor.

The fraction of power extracted from wind by a wind turbine is given by the coefficient of performance (C_p). Therefore, the power extracted by a real turbine can be expressed as follows:

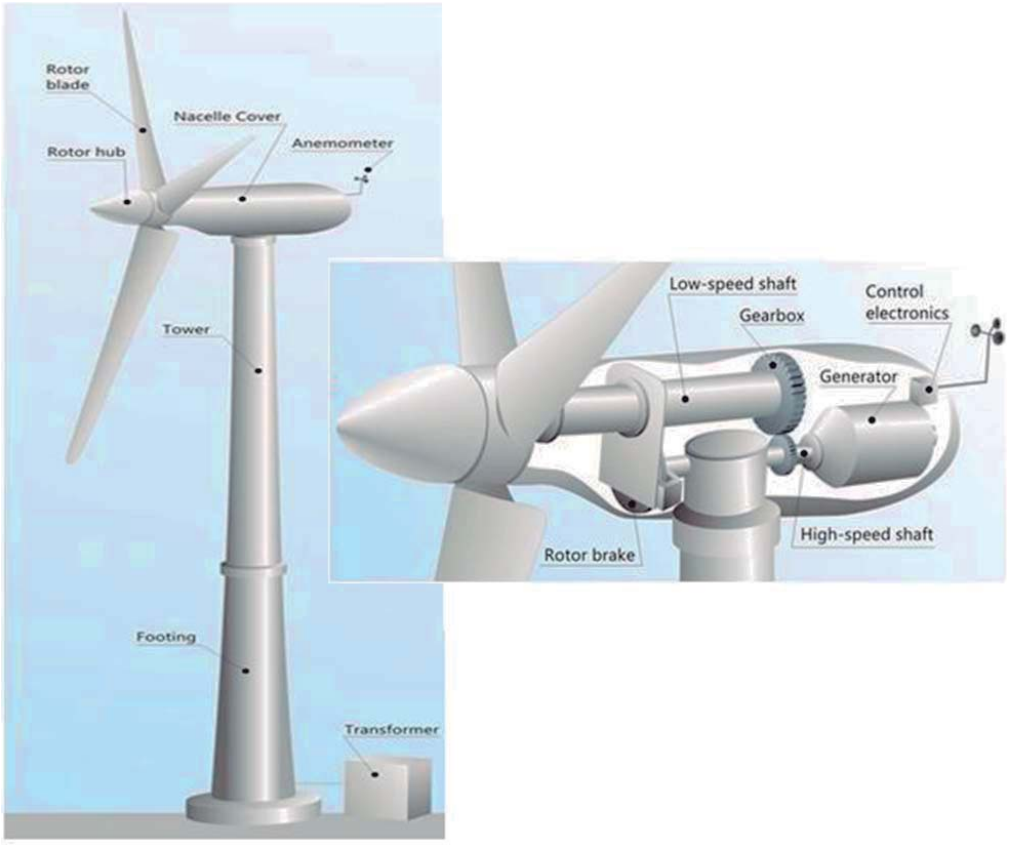

Figure 2.1: Simple scheme of HAWT components (Manwell *et al.* (2009)).

$$P_{extracted} = C_p \frac{1}{2} \rho A u^3 = C_p P_{available} \tag{2.2}$$

The coefficient of performance depends on wind speed, rotational speed and turbine blade parameters.

Wind turbine technology is directly applied to offshore sites with some upgrade to adapt wind turbines to more severe conditions of corrosion. However, when wind turbine technology is applied to offshore locations the foundation takes importance. As commented in chapter 1, wind turbines could be deployed on fixed or floating supporting structures depending on water depth, with different

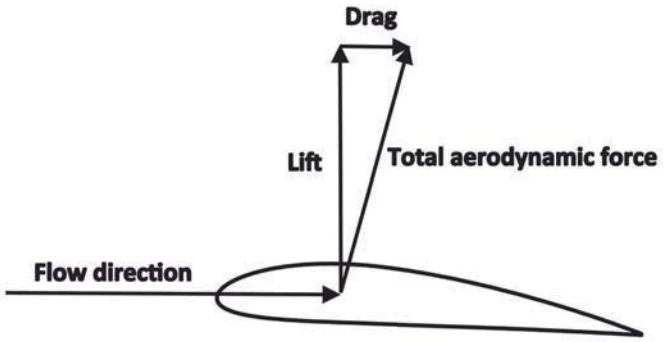

Figure 2.2: Lift and drag forces.

consequences. Fixed foundations may be considered as adaptations of the onshore know-how to offshore locations, whereas floating technology supposes the adaptation of the oil and gas experience. The most important fixed systems are: monopile, jacket and gravity base foundation. In the case of floating foundations, recommended for sites deeper than 50 meters, the most important concepts may be grouped in three types (Figure 2.3): spar, tension leg platform (TLP) and semi-submersible; which are based on three general physical principles used to achieve static stability: ballast, mooring lines and buoyancy, respectively.

- The spar concept is a large deep draft, cylindrical floating caisson designed to support the topside loads.
- Semi-submersible marine structures are multi-legged floating structures with a large deck. These legs are interconnected at the bottom underwater with horizontal buoyant elements called pontoons or branes.
- The mooring system of a TLP is vertically moored compliant platform, and consists of tubular steel members called tendons. The group of tendons at each corner of the structure is called tension leg.

One key point in the applicability of floating technologies is the mooring system. The most important aim of this system is to keep the position of the platform,

Figure 2.3: Offshore wind platforms concepts: (left) spar, (center) semisubmersible and (right) TLP

reducing its movements without introducing large loads to the system and transmitting them to the seabed. Four principal mooring systems can be used (Figure 2.4): catenary, taught leg, tension leg and single-point moorings.

- Catenary: the horizontal stiffness of the mooring lines is provided by the distributed weight over the length of the line, and to less extent the axial stiffness of the line itself.
- Taught leg: in this case, the horizontal stiffness of the mooring is provided by the axial stiffness of the mooring system, sometimes in combination with the vertical displacement of the floating platform.
- Tension leg: this system is vertically oriented and consists of tubular steel members called tendons. The principle of the tension leg mooring system is that platform's buoyancy exceeds the weight of it and hence causes a pretension in the vertical cables which keep the platform on location.
- Single point: a single point mooring (SPM), is a loading buoy anchored offshore, that serves as a mooring point and interconnects for tankers loading

or offloading gas or liquid products. SPMs are the link between geostatic sub-sea manifold connections and water tankers.

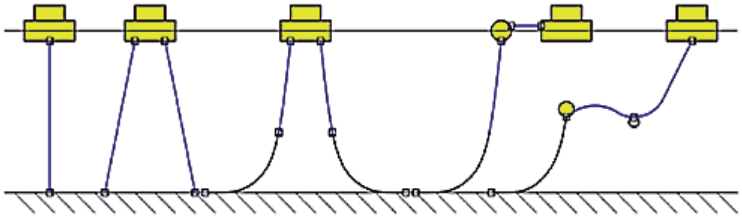

Figure 2.4: Mooring system schematic concepts (Karimirad *et al.* (2015))

2.2 Offshore Wind Conditions

As noticed in Sempreviva *et al.* (2008), planning an offshore wind farm requires a careful analysis of wind climatology, wind profile and turbulence. In this context, detailed wind data is basic. Wind data can be available from field measurements and numerical simulations. Normally, both are required to characterize the resource in order to combine their advantages. Numerical databases are, commonly, formed by long time series which allow characterizing wind performance in the long-term, whereas, instrumental measurements characterize more accurately turbulence and load anomalies. Using both, high quality rates in the wind resource assessment can be achieved, and therefore, in the energy production estimation.

2.2.1 Numerical wind databases

Resource assessment at global, regional and local scales require the use of numerical databases. This is due to the coarse spatial resolution of measurements sets. Reanalysis data is used with this purpose, whereas synoptic data is applied for lower resolutions, such as micro-scale. Atmospheric reanalysis consists of the assimilation of observational atmospheric data worldwide. When this data is assimilated it is used as input for Numerical Weather Prediction models commonly known as General Circulation Models (GCM) in order to create uniformly spaced time instants for describing the state of the atmosphere. There are several global databases that are summarized in table 2.1.

2.2.2 Instrumental measurements

Variables related to wind, such as, speed, direction, temperature, humidity, among others, may be measured by several devices available in the market. The first one, wind speed, is the most important parameter. In fact, wind energy depends, mainly, on it, as mentioned in section 2.1.

There are two main kinds of devices for measuring wind speed (figure 2.5). Intrusive devices such as cup anemometers and ultrasonic anemometers and remote sensing devices, such as LiDAR and SODAR. Another non-intrusive type of

Name	Scale	Period	Spatial Res.	Time Res. (h)
NCEP/NCAR Reanalysis 1	GLOBAL	1948-present	2.5° x 2.5°	6
NCEP/DOE Reanalysis 2	GLOBAL	1948-1979	2.5° x 2.5°	6
NCEP/CFSR NCEP/CFSv2	GLOBAL	1979-present	0.5° x 0.5°	1
NOAA-CIRES	GLOBAL	1869-2010	2° x 2°	6
MERRA	GLOBAL	1979-present	0.33° x 0.5°	1
ERA-Interim	GLOBAL	1979-present	0.75° x 0.75°	6
ERA-40	GLOBAL	1979-present	1.125° x 1.125°	6
JRA-25	REGIONAL	1979-2004	1.125° x 1.125°	6
JRA-55	REGIONAL	1958-2012	1.125° x 1.125°	6
WRF FNL	REGIONAL	2000-present	4km x 4km	1
WRF ERA-Interim	REGIONAL	1992-present	6km x 6km	1

Table 2.1: Numerical databases

data can be included, namely, satellite data, which is treated independently in this section due to its singularities.

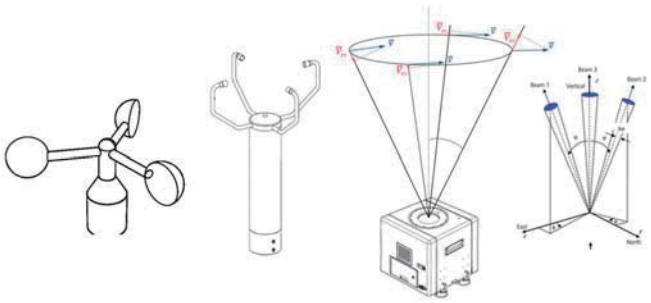

Figure 2.5: Scheme of different measuring devices (from left to right): cup anemometer, sonic anemometer, LiDAR and Sodar.

The first technology developed for measuring wind speed was cup anemometry. Because of that, its behavior is well understood and its sources of error are well known. The errors in cup anemometry caused by wind turbulence have been discussed by many authors. In L.Kristensen (1998) a review of these errors and the dynamics of cup anemometers was made. Four types of biases are discussed:

1. Over-speeding causing too high wind speeds measurements because cup anemometer responds more quickly to an increase in the wind than to a decrease of the same magnitude.
2. DP error (data-processing error) explained in P. B. MacCready (1965). It is due to the difference between the wind speed component in the cup anemometer plane and the real wind speed.
3. Vertical wind speed bias as cup anemometers only measure wind in their plane.
4. Stress bias which are equal to zero only if the anemometer has an ideal cosine response. Cup anemometers are not ideal. Consequently, this means that there will be a systematic error due to the tilt.

It is important to notice that L.Kristensen (1998) analyzed the behavior of fixed anemometers. Future offshore wind developments are based on floating structures. Due to this, moving anemometry uncertainty needs to be studied in depth.

The sonic anemometer measures wind speed by detecting ultrasonic sound pulses Kaimal & Finnigan (1994). Sonic anemometers solve the problems related to cup anemometers explained above by getting rid of moving parts. The principal sources of error of sonic anemometers are that their own probe head distorts the flow, requiring wind tunnel investigations (Kraan & Oost (1989), Mortensen & Larsen (1994), Grelle & Lindroth (1994), Mortensen & Hojstrup (1995)). Other sources of uncertainty are interferences between rain and measurements.

Light Detection and Ranging (LiDAR) as defined in Hsuan *et al.* (2014) is a remote wind sensing technology capable of measuring three-dimensional relative

wind velocity at multiple fixed distances from the optical transceiver. It is formed by two principal components: i) a sensor which transmits laser beams that interact with the existing particles in the atmosphere such us dust, aerosols, and pollen; and ii) the receiver, known as backscatter, which receives the laser light reflected back by the interaction with the particles in the atmosphere. The wind speed and direction are represented in the velocity of the backscatter. Using the concept of time-of-flight the wind speed may be deduced. The accuracy of LiDAR systems has been tested against meteorological masts with wind sensors in both onshore and offshore settings (Standridge *et al.* (2013), Jaynes *et al.* (2007)).

The sound detection and ranging (SODAR) is a ground-based remote sensor for the detection of vertical profiles of wind and turbulence data (Vogt & Thomas (1995)). A SODAR emits short pulses of acoustic waves in the audible frequency range into the atmosphere. A small fraction of the transmitted energy is backscattered by inhomogeneities of the refractive index of the air generated by turbulent fluctuations and by differences in humidity and temperature of the air. The backscattered signals are received and processed in such a manner that the Doppler spectrum is obtained by means of a fast Fourier transformation. From the Doppler spectrum the component of the wind velocity in the direction of the transmitted energy is determined.

Wind speed is not a direct measurement in satellite data so it is not included in the groups already presented. The most extended or popular satellite data available is QuikSCAT, which receives the same name as the satellite launched on 1999. The main mission of the scatterometer carried onboard, called SeaWinds, was to measure the wind near the sea surface. It was operational until the end of 2009. Another SeaWinds scatterometer was launched onboard the ADEOS-II satellite. These scatterometers are radars that send microwaves pulses to the Earth's surface where they are scattered back to the satellite. Depending on the sea surface roughness the power of the signal varies. Moreover, this power is related to wind speed and direction. However, data can only be used at locations 30 km offshore or more. QuikSCAT data is available for period 1999 to 2009 with a spatial resolution of 0.25° x 0.25° and twice daily.

All these devices (except satellite) must be deployed upon a supporting structure. Moreover, depending on the supporting structure nature, fixed or floating, the measurements would be influenced by several sources of uncertainty (i.e. mast porosity, arms,...). Devices applied to offshore wind energy should face severe environmental conditions, most of them due to corrosion and fast degradation processes. Furthermore, those devices deployed on a floating structure would be moving constantly causing extra measurement uncertainties. Two main designs are being used to support measuring devices:

- **Buoy**

  Buoys are relative small structures joined to the seabed by mooring networks. Several monitoring systems at different scales are deployed along the globe. For instance, REDEXT is the data from the grid of meteorological buoys at deep waters of Puertos del Estado (Spain). These buoys are deployed at more than 200 m of depth. Two types of buoys are used in this measurement grid: i) Wavescan and ii) SeaWatch. Type i) measures waves, atmospheric and ocean parameters, whereas type ii) only measures waves and atmospheric variables. In summary, this kind of device are a multiplatform system where a set of parameters are recorded.

  Several countries have their meteorological buoys grids conceived with different aims. For instance, the National Data Buoy Center (NDBC) from U.S.A. This grid is deployed along the country coastline and it is formed by several types of buoys (http://www.ndbc.noaa.gov/, 2015).

  The sensoring technologies have been tested at onshore sites (Vogt & Thomas (1994)) and their application to offshore sites deployed on fixed structures is also already investigated. However, their development as floating devices requires more research (Jaynes (2009) and Hsuan *et al.* (2014)).

- **Meteorological mast**

Meteorological masts may be fixed to the bottom or floating. Several examples can be found along the globe of fixed met-masts, such as the three FINO masts. In January 2002, the Federal Government of Germany decided to deploy three research platforms (meteorological masts) in the North Sea (2) and the Baltic Sea (1) in the vicinity of great planned offshore wind farms. Each of these research platforms has its own structural design and they are located 45 kilometers to the north of the island Borkum in the North Sea, 40 kilometers to the north-west of the island Rügen in the Baltic Sea and 80 kilometers to the west of Sylt, respectively. It has been a common practice to deploy a fixed met-mast at every offshore wind farm potential site. This is due to the necessity of measurements to justify the great investments required.

Floating met-mast are also under development. In Guanche *et al.* (2011) a floating met-mast designed thanks to the Idermar project is described. Its principal aim is to be applied to offshore energy resource characterization at deep and very deep waters. Idermar floating met-mast is a spar-based structure (figure 4.22), which supports a similar met-mast to those applied at onshore locations to characterize wind resource by measuring different atmospheric variables. From a structural point of view, the system consists of a submerged section which gives stability. It is composed by a floater at the sea surface and a ballast at the deepest part of the structure. The emerged part consists on a cylindrical section on which the met-mast is supported.

2.2.3 From data to wind energy potential

Wind conditions assessment is an essential step in wind energy because it helps determining the technical and economical feasibility of wind farms. It may be characterized at several scales, depending on the phase of the design methodology. Hundreds of kilometers and decades for regional analysis are required from developers.

Figure 2.6: Idermar Meteo III floating met-mast.

The wind resource assessment methodology can be divided into several parts as follows (Rodrigo (2010)):

- Site prospecting
- Measurement campaign
- Long-term extrapolation
- Microscale horizontal extrapolation
- Microscale vertical extrapolation
- Wind farm design
- IEC classification (V_{ref})

The final accuracy of the methodology presented depends on the available data. Landberg *et al.* (2003) presented eight different methods to determine the wind resource. The simplest method is called 'Folklore', which consists of interviewing local people at the studied site. Although it is very cheap and fast, it has a lot of shortcomings. However, more complex methods are used currently when data is available. In this case, the combination of some methods presented by Landberg *et al.* (2003) is used. Site measurements are used for both calibrating micro and mesoscale models and estimating wind conditions. Therefore, mesoscale numerical modeling is used to determine wind conditions at a regional scale

and microscale modeling and instrumental measurements at a local scale.

Wind conditions are influenced by many factors that should be taken into account in the assessment methodology. Consequently, the improvement of wind assessment should be based on the study of the influence of each factor. For instance, coastal topography influences wind patterns in several areas around the globe (i.e. North of Spain), mostly when wind flows from land to sea. Parish (1982) studied barrier winds along the Sierra Nevada Mountains, which consists of low-level, mountain-parallel jet streams. Overland & Bond (1993) analyzed the influence of coastal topography for the Yakutat Storm case. He established that when synoptic-scale flow encounters coastal orography, mesoscale features are formed that have the scale of the half-width of broad coastal mountains. In Overland & Bond (1995) authors investigated the onshore flow for overwater winds near coastal topography. Doyle (1996) studied the interactions of an intense mesoscale precipitation system and strong prefrontal low-level jet with the coastal zone. Alarcón & Alonso (2001) computed atmospheric trajectories for complex orography in western Mediterranean. Yamaguchi & Ishihara (2014) investigated the offshore wind energy potential by means of a mesoscale model and considering technological, social and economic constraints. Carrasco-Díaz *et al.* (2015) assessed wind power along a coastal area in Mexico. They used WAsP model introducing topography and roughness. However, they did not relate the coastal topography with wind behavior. González-Longatt *et al.* (2015) presented a wind resource assessment combining spatial interpolation and orographic correction. Authors explained wind conditions considering the topography characteristics. Torres *et al.* (2015) study the effect of orography and wind variability on flow structures at Baja California. Their research is mostly based on mesoscale model data due to the spatial and temporal resolution required and the lack of offshore instrumental measurements. The inclusion of instrumental data in areas where coastal topography influence is relevant can improve the research.
The natural behavior of wind conditions and the influence of coastal topography can be characterized including a statistical analysis of the wind variability into the wind conditions assessment. Moreover, wind spatial and temporal variability is an important issue for offshore wind energy. Several studies can be found study-

ing it from different points of view. For instance, in Katzenstein & Apt (2012) a cost metric to estimate the variability cost of individual onshore wind plants has been developed. Kubik *et al.* (2013) used reanalysis data and 10 meters high met-mast measurements to investigate the impact of wind variability. Power production from simulations was compared to real onshore wind farms production. In Santos-Alamillos *et al.* (2014) a method for analyzing the potential contribution of wind energy resources to power in a region is proposed. The method consisted of two parts: i) spatial variability of wind resources analysis based on principal component analysis (PCA) and ii) PCA results are used to asses optimal location (onshore and offshore) of wind farms. Gibson & Cullen (2015) investigated linkages between synoptic and sub-synoptic scale atmospheric circulation and temporal wind resource variability, adopting a synoptic weather typing approach. Hirth *et al.* (2015) proposed a method to estimate integration costs taking into account wind and solar variability. Shu *et al.* (2015) studied offshore wind energy potential based on Weibull distribution functions. Although wind has been studied from the atmospheric and environmental point of view, the influence of wind variability over floating wind turbines and offshore wind farms can be studied in more depth.

2.2.4 **Conclusions**

From the state of the art related to the wind conditions assessment carried out in this section some conclusions can be pointed out.

- Future development of offshore wind energy will be based on floating technologies. Therefore, new challenges should be faced, such as the movements suffered by monitoring and sensoring systems. Because of that, analyzing the impact of constant movements in the measurements becomes a key point of wind conditions assessment.

- Floating meteorological masts, as the one presented in Guanche *et al.* (2011), require the development of a movement compensation system to improve

the accuracy of measurements from the anemometers installed.

- In the literature, many efforts have been dedicated to understand the behavior of wind flow in areas where the topography has a great influence. Many of these studies were developed onshore due to the availability of instrumental measurements. Although there are also studies in offshore locations, most of them are based on reanalysis data due to the lack of accurate measurements. However, there is little research focused on areas where coastal topography is important and measurements from meteorological masts are available.

- Wind conditions assessment from the meteorological and atmospheric point of view is an ongoing field of research. Moreover, wind energy has enlarged the importance of this field. Wind variability has been assessed at many locations in order to determine, for instance, the optimal location for wind energy farms. More effort can be put on the estimation of the influence of wind conditions variability on the production, operation and economical assessment of potential offshore wind farms.

2.3 Floating Platform Performance Assessment

As it has been already mentioned in the introduction, offshore wind future is related to deep and very deep water locations. Many efforts from all the agents involved: governments, industry and academy, are being dedicated to the development of specific technologies and design methodologies. One of the key efforts is focused on floating support structures design. Actually, there are guidelines which propose methods in order to enhance the reliability of current and future technologies.

Moreover, several numerical models can be found in the market to simulate the cases proposed by standards. These models should be supported by laboratory tests to reduce as much as possible the uncertainty related to numerical model limitations. Numerical model limitations, mostly due to very complex fluid-structure interaction processes, lead to a great room for improvement of the design methods, for instance, in the floating platform performance under extreme conditions.

2.3.1 Standards review - load cases

During the last years principal offshore wind industry classification societies have made a great effort developing detailed standards. Although their experience in the oil & gas sector contributed to reduce the time needed for their development, they are immersed, constantly, in an improving process.

For instance, some of the most important standards and guidelines are listed in the following:

- American Petroleum Institute (API) - API RP 2A-LFRG/WSD (1993/2000)
- Germanischer Lloyd (GL) - GL Rules and Guidelines (2005)
- International Electrotechnical Commission (IEC) - IEC61400-3 (2009) and IEC61400-1 (2005)
- Det Norske Veritas (DNV) - DNV-OS-J101 (2011) and DNV-RP-C205 (2010)
- Eurocode 1 (1998)
- ISO/DIS 19901-1 (2005)

DNV, IEC and GL stand out from the rest and they are the most commonly used. In these guidelines, the potential met-ocean scenarios are organized separating the different environmental variables (Table 2.2).

Met-ocean loads		
Waves	ESS	Extreme Sea State
	SSS	Severe Sea State
	EWH	Extreme Wave Height
	NSS	Normal Sea State
Wind	NTM	Normal Turbulence Model
	EWM	Extreme Wind Model
	RWM	Reduced Wind Model
Current	NCM	Normal Currents Model
	ECM	Extreme Currents Model
Sea Level	MSL	Mean Sea Level
	NWLR	Normal Water Level Range
	EWLR	Extreme Water Level Range

Table 2.2: Met-Ocean Variable Conditions

Load cases are proposed in the guidelines as a combination of the met-ocean conditions shown in table 2.2. Load cases are distributed in 8 groups, depending on the situation faced by the turbine:

1. Power production
2. Power production plus occurrence of fault
3. Start up
4. Normal shut down
5. Emergency shut down
6. Parked (standing still or idling)
7. Parked and fault conditions
8. Transport, assembly, maintenance and repair

Furthermore, load cases may be spread into service load cases (SLC) or ultimate load cases (ULC). The former are related to normal met-ocean conditions

during the life-time of the platform, whereas the latter is based on extreme conditions in order to analyze the survivability of the platform. Because of that, ultimate load cases are based on extreme and severe conditions. They mainly correspond to load cases 6 and 7. They are summarized in table 2.3.

Case 6.1a includes an Extreme Wind Model (EWM), a turbulent wind model and an Extreme Sea State (ESS). The extreme wind model is represented by the 50 year return level wind speed at the hub height.

The extreme sea state is defined by H_{s50} which is the significant wave height with a recurrence period of 50 years and T_p, as the associated peak period. Guidelines propose to determine this value using appropriate measurements and/or validated/calibrated hindcast data.

Case 6.1c is represented by a Reduced Wind Model (RWM) with steady wind model and Extreme Wave Height (EWH). The reduced wind speed model is represented by a wind speed defined as a fraction of the extreme wind speed:

$$U_{RWM} = \Psi \cdot U_{EWM}(\Psi < 1) \tag{2.3}$$

In this case, the wave height is related to the 50 year recurrence period. The relation between the significant wave height of 50 year return level and the wave height of 50 year return period is:

$$H_{50} = 1.86 H_{s50} \tag{2.4}$$

And the wave period to be taken may be assumed to be within the range given by:

$$11.1\sqrt{H_{s,ESS}(V)/g} \leq T \leq 14.3\sqrt{H_{s,ESS}(V)/g} \tag{2.5}$$

The floating structures described in section 1 must undergo several phases during their lifetime: construction, transportation, service and, at the end, dismantling. Each stage is characterized by its own conditions which should be faced by the structure satisfying the requirements considered from the engineering point

Load Case	Wind Condition	Waves
6.1a	EWM Turbulent wind model $V_{hub} = k_1 V_{ref}$	ESS $H_s = k_2 H_{s50}$
6.1b	EWM Steady wind model $V(z_{hub}) = V_{e50}$	RWH $H = H_{red50}$
6.1c	RWM Steady wind model $V(z_{hub}) = V_{red50}$	EWH $H = H_{50}$
6.2a	EWM Turbulent wind model $V_{hub} = k_1 V_{ref}$	ESS $H_s = k_2 H_{s50}$
6.2b	EWM Steady wind model $V(z_{hub}) = V_{e50}$	RWH $H = H_{red50}$
6.3a	EWM Turbulent wind model $V_{hub} = k_1 V_1$	ESS $H_s = k_2 H_{s1}$
6.3b	EWM Steady wind model $V(z_{hub}) = V_{e1}$	RWH $H = H_{red1}$
6.4	NTM $V_{hub} < 0.7 V_{ref}$	NSS Joint prob. distribution of H_s, T_p, V_{hub}
7.1a	EWM Turbulent wind model $V_{hub} = k_1 V_1$	ESS $H_s = k_2 H_{s1}$
7.1b	EWM Steady wind model $V(z_{hub}) = V_{e1}$	RWH $H = H_{red1}$
7.1c	RWM Steady wind model $V(z_{hub}) = V_{red1}$	EWH $H = H_1$
7.2	NTM $V_{hub} < 0.7 V_1$	NSS Joint prob. distribution of H_s, T_p, V_{hub}

Table 2.3: Load cases wind and wave conditions

of view. Serviceability or operating stop limit conditions depend on mean values of the climate variables, whereas damage and ultimate limit states depend on extremes. The methods to deal with mean values and extreme were, traditionally, different (Castillo (1988), Coles *et al.* (2001)).

In Mínguez *et al.* (2014) authors apply a method which links point-in-time and extreme value distributions to Inverse First Order Reliability Method (IFORM) proposed in IEC61400-3 to determine 50-year return period sea states. In the guidelines, there is no distinction between both distributions, point-in-time and extreme, what may lead to invalid results.

The IFORM method is proposed to extrapolate met-ocean data, producing environmental contour of a specific recurrence period sea-states (combinations of wind speed (mean value) and significant wave height). Rosenblatt (1952) is commonly used to construct the following transformation:

$$\begin{aligned} \phi(z_1) &= F_V(v) \\ \phi(z_2) &= F_{H_s|V}(H_s) \end{aligned} \tag{2.6}$$

where $F_V(v)$ is the marginal distribution of mean wind speed, and $F_{H_s|V}$ is the conditional distribution of significant wave height for given values of mean wind speed.

It is suggested, as good practice, to use instrumental measurements at the site for the analysis. However, when instrumental time series are not long enough, reanalysis data is used in order to be able to evaluate not only the short term but also the long term of the met-ocean variables. Using both measurements and reanalysis data, the quality of the analysis is improved by taking advantage of pros of both databases. Measurements are, commonly, formed by short time series (1-3 years of records) with rare values (as out-layers) and blanks, due to maintenance or breakdown. Besides, they record real data, including extreme-values. Reanalysis data is formed by long time series (>20 years) allowing the long-term analysis, however, as they are obtained from numerical models, they are not able to include

all the processes involved in met-ocean variables behavior. This fact is important in extreme-value distributions due to the mean character of numerical simulations. Combination of both is crucial in order to improve the met-ocean variables analysis.

In Mínguez *et al.* (2013b) authors presented a mixed extreme wave climate model in order to combine instrumental and reanalysis databases. In the literature discrepancies when comparing instrumental and reanalysis data have been pointed out (Caires & Sterl (2005) and Cavaleri & Sclavo (2006)). Several methods to reduce these discrepancies can be found: Caires & Sterl (2005) proposed a non-parametric correction based on analogs, whereas Cavaleri & Sclavo (2006) calibrated decadal time series. When comparing numerical and reanalysis data, for validation or calibration processes, it is important to remove extremes (Mínguez *et al.* (2011)). Due to this, the calibrated reanalysis databases are not able to simulate accurately extreme-values. With the goal to improve the representation of maxima, for instance, Menéndez *et al.* (2009), Izaguirre *et al.* (2010) and Mínguez *et al.* (2010) developed a time dependent model based on GEV distribution. Moreover, this model takes into account the seasonality and interannual variability of extreme. Due to the lack of long records of instrumental measurements, future offshore developments will require new techniques to estimate long-term environmental loads. Increasing the sample of data to fit extreme model distributions will improve the estimation.

2.3.2 **Numerical modeling**

The simulation of offshore floating wind turbines may be divided into four main parts:

- structural dynamics
- aerodynamics
- hydrodynamics
- mooring lines

Different modelling methods are available and each one of them has strengths and weaknesses. As an introductory chapter, it will not include equations describing the various theories for the sake of clarity and brevity.

2.3.2.1 Structural dynamics

In the case of structural analysis, three main methods can be highlighted:

- **Modal approach** - this method uses a low number of degrees of freedom to represent the structure, which reduces the capabilities of the model when simulating floating structures. Its limitation to linear responses means that large deflections of flexible components may not be correctly simulated.
- **Multibody system approach** - the structure is spread in several elements interconnected by joints what enables modelling of systems with large displacements and rotations.
- **Finite element modelling** - the structure is discretized into a mesh of finite elements interconnected at nodes with degrees of freedom. The main advantage is that it allows complex structures to be modelled. Its principal disadvantage is the computational effort required.

2.3.2.2 Aerodynamics

The aerodynamics of the vast majority of commercial wind turbine simulation codes are based on blade element momentum (BEM) theory (Cordie (2010)). This method assumes that the rotor is like an actuator disc assuming axi-symmetric, incompressible, steady flow in a stream tube. Using Bernoulli's theorem the power extracted by the rotor and the thrust force acting on the rotor can be derived. The BEM model is extensively used independently because it does not deal with unsteady nature of a wind turbine rotor. For this reason some corrections are applied in conjunction with the model, such as tip and hub loss (not uniform flow induction over the rotor), dynamic inflow theory (relation between blade loads and rotor wakes) and dynamic stall (the onset of stall may be delayed the static stall angle

undergoing the aerodynamic forces), among others.

The principal advantage of using BEM model is its simplicity, which reduces the computational time. It has been extensively validated (Hansen (2008) and Hansen *et al.* (2006)). The principal limitation of this model is due to its range of application. It is assumed to be applied for steady flow with wind directly approaching the rotor. Furthermore, the corrections explained improve the accuracy but do not fully capture the unsteady effects.

There are also research codes which use free wake lifting line methods, such as the free-vortex based AWSM developed by ECN (Schepers & Van Garrel (2006)). Based on Prandtl's lifting line theory it is able to describe more accurately the shape and strength of time-dependent wake generated. It may be applied when aerodynamic characteristics vary significantly. This methods are slower than BEM.

The alternative to BEM theory and vortex-based methods is computational fluid dynamics codes. These models are based on Navier-Stokes equations. Although the detail they reach is higher, they are complex and have high computer requirements, making them impractical for industry-scale analysis.

2.3.2.3 **Hydrodynamics**

In order to calculate the hydrodynamic behavior of a floating structure the wave particle kinematics must be determined. Potential flow theory is widely used due to its simplicity and speed. The main disadvantage is the assumption of linearity, although it could be taken to be reasonable in deep water. However, for large waves or waves in sallow water non-linearities should be taken into account.

Hydrodynamic loads (figure 2.7) on the structure may be calculated applying Morison's equation from wave particle kinematics. One advantage of Morison's equation is that hydrodynamic loads are calculated in terms of wave particle velocities and accelerations. This means that linear theory and non-linear kinematics

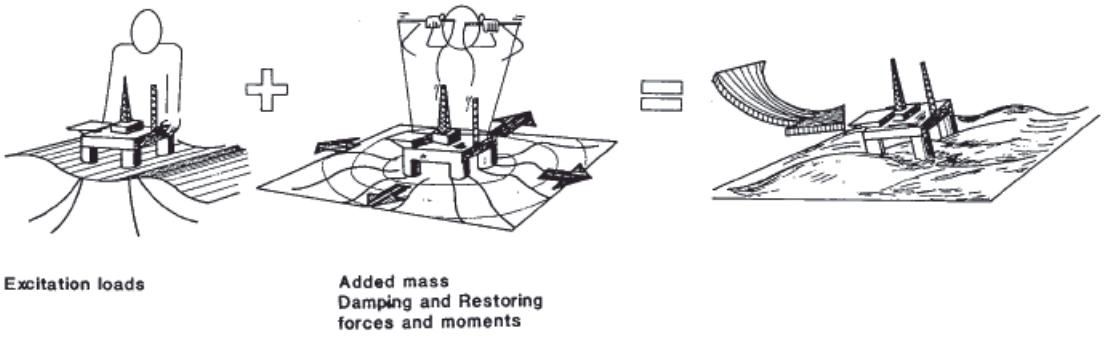

Figure 2.7: Scheme of hydrodynamic forces (Faltinsen (1990)).

models can be used. However, some disadvantages can be pointed out. For support structures with a small relative diameter to the wavelength diffraction effects may be neglected (DNV (2007)). This is commonly the case of floating structures which means that Morison's equation cannot be used. Furthermore, Morison's equation assumes that drag loading is dominated by viscous drag, ignoring wave radiation damping. This may be applied only when the structure motions are very small. Additional terms should be added to Morison's equation to account for hydrostatic restoring forces and non-cylindrical floating platforms.

Slender structures are simulated taking into account that submerged body does not exert any influence on the fluid in terms of diffraction or radiation. However, common floating platform designs are large enough to require including wave diffraction and radiation forces. Numerical methods based on linear wave theory may be used to solve practical cases. Assuming the linearity of the process the problems can be solved individually (Jonkman (2009)):

1. **Radiation**
   Wave radiation loading are loads from the influence of a moving body on the fluid when no incident waves are present. These forces include contribution from both added mass and damping. The added mass contribution is due to the hydrodynamic forces resulting from the outgoing wave pressure field. The damping contribution is described as the free surface memory,

which means, that once a floating body induces an outgoing pressure field it continues as long as the waves radiate away.

2. **Diffraction**
   Wave diffraction loading is due to the influence of the fluid on a stationary body when incident waves are present. The floating body is supposed to be fixed at its mean position and it changes the waves pattern as they pass it. The forces of incoming waves over the body can be computed as the integral of the pressure over the submerged surface of the body.

3. **Hydrostatic restoring**
   Hydrostatic loading are the static loads on the body due to the pressure in the fluid. It is calculated by computing the surface pressure on the submerged part of the structure. The net upward force is equal to the weight of the fluid displaced by the body (Archimede's Principle).

The main advantage of this method to compute hydrodynamic loads is that it takes account of the body influence on the fluid. On the contrary, the main limitation is the assumption of linearity. However, this is not a problem for deep water where wave height is smaller than wavelength. Following the assumption of linearity, this theory cannot be applied for large movements of the body. The nonlinear viscous drag can be included using a quadratic damping based on the velocity of the body or by including Morison elements with relative velocity.

2.3.2.4 **Mooring system**

The mooring system mission is to restrain the movement of the platform. The analysis of its behavior is complex and it is commonly simulated with dedicated codes. It is important to evaluate the interaction between the mooring system and the floating platform. Several ways to simulate this interaction are available:

1. **Force-displacement representation**
   The first model for mooring system analysis is based on an onshore application. Using P-Y springs in the translational and rotational degrees of freedom the relationship between force and displacement can be represented. It can be extended to the analysis of mooring lines for floating platforms by including non-linear spring stiffnesses (for the 6 degrees of freedom) at the fairlead position and force-velocity relationship to account for mooring line drag. The principal advantage is that the model describes in a single stiffness matrix the non-linear geometric restoring properties of the mooring system. However, restoring forces are specified as independent functions of each platform displacement resulting in a limitation for this model. The main advantage of this method is its very low computational cost.

2. **Quasi-static representation**
   Quasi-static methods solve the tension in the mooring lines from the static equilibrium equation for a given platform displacement at every time step. This approach allows introducing the properties of the mooring lines to the system and it also accounts for the non-linear geometric restoration of the mooring system. Like the force-displacement method, the dynamics of the mooring lines are not considered in the quasi-static method. As in the previous case, the main advantage of this method is its very low computational cost.

3. **Full dynamic modelling**
   The dynamics of mooring lines cannot be solved analytically. There are two main approaches to study the dynamic behaviour of the mooring lines: i) Study the motion of the cable submerged in cables by the finite element method (FEM) (Aamo & Fossen (2001) and Palm *et al.* (2013)) ii) discretizing the line into point masses and solving the partial differential equations by using finite difference method (FDM) or FEM (Hall & Goupee (2015)). The principle disadvantage is their significant increase in the computational cost. Besides, the tensions on the lines are better estimated with this model

which takes into account the whole dynamics of the catenary lines.

There are several design tools available to solve all the problems described above. Although codes capable of evaluating all the processes are in the market, it is common to use coupled models to take advantage of the accuracy of each of them. Some of them are enumerated in the following:

- FAST by NREL
- ADAMS by MSC
- Bladed by Garrad Hassan
- SIMO/RIFLEX by MARINTEK
- 3Dfloat by UMB
- SESAM (GeniE, HydroD, DeepC) by DNV

2.3.3 Laboratory testing

Standards and guidelines propose load cases for floating platform design. In order to reduce the uncertainty of numerical models, laboratory testing, where scale prototypes are exposed to the expected sea states that would face during their lifetime, is carried out. Several studies can be found in the literature related to the combination of numerical modelling and laboratory testing.

Philippe *et al.* (2013) tested the Dutch Tri-floater semi-submersible platform equipped with the NREL 5 MW wind turbine (which is commonly considered the reference wind turbine) at the Hydrodynamics and Ocean Engineering Tank (HOET) of École Centrale Nantes. The measurements obtained from the tests were compared to simulations carried out using FAST.

Iijima *et al.* (2013) conducted tank tests at the Ocean Basin of the Institute of Industry Science (University of Tokyo). Hu *et al.* (2013) compared the numerical results (using their own simulation tool) and the tank tests measurements of

their floating platform design. It was supposed to support three wind turbines. They paid attention to the 6 degrees of freedom of the floating body under three different sea states. Chujo *et al.* (2013) studied the behavior of a spar buoy type floater under regular and irregular waves sea states. Shin *et al.* (2013) analyzed the motion of OC4 5MW semi-submersible platform under irregular waves and compared the results with FAST simulations. In López-Pavón *et al.* (2013) authors used SIMO/Riflex models for the numerical simulation of the HiPRWind floater.

2.3.4 **Conclusions**

When designing a floating foundation for wind turbines it must be taken into account the importance of numerical modeling, the methods proposed by guidelines and the statistical tools available to determine the floating platform performance. Floating platform performance assessment becomes crucial due to the investments required to deploy these structures in the ocean.

From the literature review some gaps have been detected and they are presented in the following:

- Inverse First Order Reliability Method (IFORM) proposed in the guidelines to determine the 50-year return period sea states (H_s & W_v) is based on mean distributions. Because of that, the right tail of the distribution (where the sample of extreme is located) is not well fitted. An update of the method was proposed in Mínguez *et al.* (2014) including extreme distributions and improving the results. More validation should be done as authors only applied the method to sea level, which is a well characterized variable.

- The most demanding sea states proposed by standards, from the structural point of view are based on 50-year return level. Furthermore, standards propose to use instrumental data when available or numerical data. There is a lack of methods combining instrumental and numerical data to find synergies between the advantages of both databases.

- The mooring system study is complex and requires more research, not only from a numerical modelling point of view but from a more general perspective. The main factors that influences its behavior are related to the environmental conditions. Due to this, understanding the influence of met-ocean conditions on the mooring system performance may increase the quality of final designs.

2.4 Economical feasibility assessment

Offshore wind farms are very expensive infrastructures with very high rates of CAPEX and OPEX. For instance, Young (2009) presented a base case where CAPEX was around 5M€/MW and OPEX was around 120K€/MW. The investments required and the amount of stakeholders involved draw a very complex scenario. Therefore, the economical feasibility assessment is recommended to be considered from very early stages of development.

Several studies have been carried out to estimate as accurately as possible the real costs of offshore wind farms. Dicorato *et al.* (2011) presented a detailed assessment of investment cost for offshore wind generation. Rademakers & Braam (2002) focused on operation and maintenance of offshore wind turbines strategies optimization. Castro-Santos & Diaz-Casas (2015) analyzed the influence of final location of offshore wind farms in the economic feasibility.

In all cases, detailed information allows authors to estimate the economical feasibility of offshore wind farms, splitting the budget in several parts, such as:

- Wind Turbine
- Foundation (Fixed or Floating)
- Electrical Infrastructure
- Integration System
- Transmission System
- Planning and Development
- Etc.

Depending on the nature of the costs they can be included into CAPEX or OPEX. CAPEX means the capital expenditures and OPEX, the operational expenditures. In CAPEX, construction and financial related costs are included, whereas operational and maintenance costs are included in OPEX. Offshore wind

farm costs are not easily accessible. The sector is so competitive that confidentiality is almost present in every activity. Therefore, it is difficult to find in the literature validated information. Because of that, in this Thesis some reference works are highlighted and used as a base for the economical feasibility assessment.

2.4.1 Costs Assumptions

It is important to notice the difference between the principal kind of costs: construction and O&M. The first one depends on the technologies used at every stage, which includes: turbine, tower, support structure, mooring system, transport vessels, electrical cable, electrical substation, etc. In the case of O&M costs, several authors suggest different models to estimate them during the lifetime of the project. It must be included the financial costs and insurance costs, among others.

CAPEX

In Couñago *et al.* (2010), authors developed the study required for the implementation of an offshore wind farm in the coast of Galicia (Spain). The resources at the location were studied and the floating platform and costs were analyzed in detail. They distributed the costs as follows:

1. Construction of their supporting structure design
2. Transport to the final location
3. Installation of mooring system
4. Electrical system
5. O&M strategies.

The costs assumed in this work can be considered a good reference because authors counted with the collaboration of several professionals from different fields related to offshore wind sector.

The Crown State (BVGA (2010)) published a guide to offshore wind in 2010. This document includes prices of almost every component and activity involved

Cost centre	Cost[k€]	% of Total
Wind Turbine	157,614	49.77
Foundations	77,988	24.62
Collection System	20,454	6.46
Integration System	21,656	6.84
Transmission System	28,220	8.91
Reactive Power Regulation Devices	0	0.00
SCADA/EMS	3,750	1.18
Plant Cost	309,682	97.78
Development Cost	7,020	2.22
Total Invesment	316,702	100.00

Table 2.4: Offshore wind farm costs Dicorato *et al.* (2011)

in the offshore wind farm design, construction and O&M stages. It may be considered a reference guide as it includes almost every potential cost.

In Castro-Santos & Diaz-Casas (2015), authors proposed a methodology for economical feasibility assessment of offshore floating wind farms based on generic equations dependent on local variables, such as significant wave height, peak period, water depth, etc. Dicorato *et al.* (2011) proposed guidelines for the estimation of costs of offshore wind generation. In table 2.4, the results of the cost model proposed are shown.

OPEX

Offshore wind operation and maintenance costs are expected to be substantially higher than those for onshore turbines. Rademakers & Braam (2002) assumed 0.003 to 0.006 €/kWh for preventive maintenance and 0.005 to 0.010 €/kWh for corrective maintenance. In general, the O&M costs are assumed to be 20-30% of the CAPEX for offshore wind turbines, whereas for onshore wind turbines would be 10 to 15%.

In the Report *Renewable Energy Technologies: Cost Analysis Series: Wind*

Power (IRENA (2012)) sub-assembly and component cost structure for long term averages and for O&M specifically are included, explaining also where O&M fixed and variable costs come from and the potential areas of cost reduction.

In de Prada Gil *et al.* (2014) authors proposed a complete model for cost estimation. In particular, O&M costs are expressed as:

$$C_{O\&M} = \sum_{k=1}^{LS} \frac{E_{O\_L}^{Ci} P_e}{(1 + \frac{R_r}{100})^k} \tag{2.7}$$

where LS is the life span of the offshore wind power plant, P_e is the price of energy, R_r is the real interest rate, E_{O_L} is the total losses.

2.4.2 Uncertainty assessment

Some research has been carried out related to the uncertainty of economical feasibility assessment. There are several variables that may influence the final results of the assessment. Dicorato *et al.* (2011) analyzed the investment cost when varying the distance to shore, sea depth, the existence of an onshore substation, the collection scheme and the voltage levels and proposed an economical model based on a review of expressions for estimating the cost of several components such as the turbine, the foundation and the electric system.

In Castro-Santos & Diaz-Casas (2015), authors studied the influence of the location in floating offshore wind farms. Authors included a factor in all the terms of the CAPEX and OPEX where authors considered location would be important. They followed a costs structure similar to Dicorato *et al.* (2011)

More research has been carried out related to O&M costs due to its relation with met-ocean conditions. Furthermore, met-ocean conditions are an important source of uncertainty for O&M activities. Due to this, there are several models in the literature. O&M research may be decomposed in three main topics: i) failure rate data, ii) failure modes and iii) cost estimation.

Failure rate data can be found, for instance, in Van Bussel & Schöntag (1997), Van Bussel & Zaaijer (2001) and Faulstich *et al.* (2009). Rademakers & Braam (2002) focused on the study of NL7 wind farm. Failure modes represent the description of the cause of failures and the activity required to fix them. In this case, Alewine (2011) explained in detail the failure modes of wind turbine generators. Alewine & Zeglinski (2013) explained the step by step processes of specific repairs for specific components in wind turbines. Wiggelinkhuizen *et al.* (2007) identified failure modes of offshore wind turbines and which conditions are monitored. The report also described the benefits of monitoring the life-long behaviors of wind turbines and of condition-based maintenance over unscheduled maintenance. In the case of Blanco (2009) the component breakdown and market breakdown are included.

However, cost estimation is not always treated at the same time as failure rate and mode information due to the complexity and the amount of elements involved. Braam *et al.* (2011), in their estimating process, clearly pointed out what parameters to include in the operation and maintenance cost per component per failure.

In order to evaluate the feasibility of an investment some financial indicators are estimated. They help decision makers by summarizing the information in a clear way. Moreover, the use of these parameters allows comparing different investments by comparing their profitability (Heptonstall *et al.* (2012)). In Guanche *et al.* (2014b) authors studied the uncertainty of financial indicators applied to wave energy farms. They selected four principal parameters: i) net present value (NPV), ii) internal rate of return (IRR), iii) payback period (PBP) and iv) levelized cost of energy (LCOE).

LCOE seeks to capture the lifetime costs in terms of the present value, applying the discount rate considered in the project. Due to this, this parameter provides a straightforward method to give a per MWh cost that summarized the full costs of the energy plant. Moreover, it is used to compare, even, different technologies.

Makridis (2013) analyzed at global scale the offshore wind power resource

availability and prospects. In his analysis, the LCOE is one of the relevant parameters for implementing the linear programming model, among others such as the rate of learning and the discount rate. Moreover, he assigns the value suggested by EIA (2010) of $243.2 MWh taking into account a regional variation that results in a maximum of $349.5 MWh (for US).

Barturen *et al.* (2010) assumed a price of energy of 140€/MWh. The IRR of their study is 6.6% and a PBP of about 9 years. Furthermore, an interesting point analyzed in their work is the sensitivity of the project in relation to the energy price. Results are summarized in table 2.5.

€/KWh	IRR	PBP
0.18	9.7%	9
0.16	8.8%	9
0.14	6%	10
0.12	3.7%	11
0.10	0.9%	12

Table 2.5: Price of Energy, IRR and PBP from Barturen *et al.* (2010)

In the literature, the most common approach used to analyze the economic performance of offshore wind farms has been based on isolated farms. This means, that the economical feasibility assessment was applied to a single wind farm. Consequently, more complex studies, including energy production, failure rate simulation, O&M realistic strategies, etc., will allow relating met-ocean variables behavior and main financial estimators response.

2.4.3 Conclusions

The economic feasibility assessment is important to improve the information for investors and it must be based on realistic costs of construction and operation and maintenance. This is difficult as data related to costs is commonly private. Furthermore, economic assessment is very sensitive to climate variability. Therefore, it is important to assess as accurately as possible the variability related to wind, waves, currents, among other important variables to estimate the financial

requirements of an offshore wind farm. From the literature review carried out a main conclusion can be highlighted.

- Economic feasibility assessment has been commonly carried out for specific developments by private agents with high accuracy. When a more generic point of view is required, for instance when a more wider area is analyzed, more homogeneous costs may be used to allow the comparison of the main economic estimators performance along the area. Therefore, it is recommended to analyze wind variability and its influence on the feasibility assessment based on representative costs when general assessments are carried out.

CHAPTER

3

Scope and work structure

From the literature review carried out in chapter 2 it can be concluded that the future of offshore wind will be based on floating technologies in order to exploit wind resource at deep and very deep waters. However, the current developments are very limited. There are still major several knowledge and technological gaps as it has been highlighted by agencies like EWEA and evidenced in previous chapters. Therefore, the design methodology should be adapted to face new challenges in deep and very deep waters.

The present chapter introduces the general objective of the present work. Its specific objectives are also addressed. The methodology to overcome the shortcomings and gaps identified is explained next.

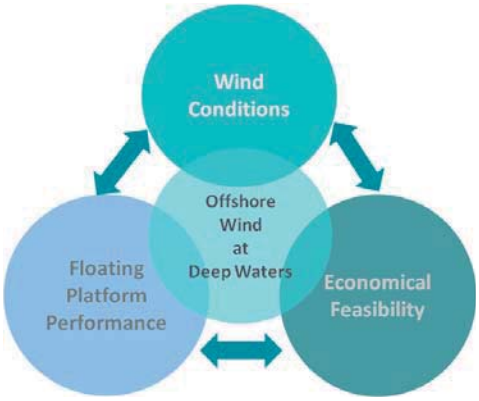

Figure 3.1: Methodology general scheme

3.1 Scope and goals

The main objective of the present study is:

To characterize the influence of met-ocean conditions spatial and temporal variability on offshore wind technology and economic feasibility.

It has been observed that met-ocean conditions show short and long-term variability and its influence on offshore wind farms long-term uncertainty has not been investigated yet. Loads estimation as well as power production variability, as a consequence of met-ocean conditions will be investigated. In order to achieve the primarily objective, the following secondary objectives need to be addressed. They are grouped into the next topics (see figure 3.1):

1. Offshore wind conditions assessment
2. Floating wind performance assessment
3. Economic feasibility assessment

3.1.1 Offshore Wind Conditions

Almost every stage of design methodology depends on wind, e.g.: site selection due to the direct relation between wind and energy production or; wind loads

assessment. Consequently, wind analysis and characterization is crucial for an accurate design of offshore wind farms. The specific objectives of this section can be summarized as follows:

- **Analysis of wind measurements uncertainty at deep waters.**

  New technologies for measuring met-ocean variables at deep and very deep locations are conceived as floating structures. Hence, they will introduce new sources of uncertainty on wind measurements due to the relative movement between them and the wind yield.

  An analysis of those sources of uncertainty is required to evaluate the accuracy and applicability of floating systems for this purpose.

- **Evaluation of wind conditions spatial variability and the influence of coastal topography.**

  Some deep and very deep feasible areas for offshore wind farms are close to the coast. In these areas, coastal topography may influence wind patterns.

  Consequently, the spatial variability analysis becomes crucial to estimate accurately the most promising locations for the deployment of offshore wind farms.

- **Characterization of wind conditions variability.**

  The need for wind reanalysis numerical databases validation, as well as the lack of instrumental measurements at deep and very deep waters reduces the accuracy of wind conditions long-term analysis.

  The combination of high resolution reanalysis databases and floating met-mast data will improve the quality of long-term wind variability analysis. For this purpose, numerical tools from climate prediction field may be applied.

3.1.2 Floating Platform Performance Assessment

Offshore wind designs are subjected to strict rules and standards written by different certification bodies. They propose methodologies, design load cases and procedures to be followed during the design process. It has been noticed in chapter 2 that these standards are an adaptation of Oil&Gas guidelines. Because of that, they do not capture some of the offshore wind singularities. Specific objectives are proposed and explained in the following:

- **Review of the IFORM method proposed by the standards.**

  The application of the IFORM method as proposed in standards leads to imprecise results (Mínguez *et al.* (2014)). However, the updated method proposed in Mínguez *et al.* (2014) was applied only to sea level, which seems to be a negligible variable for deep and very deep water locations.

  The IFORM method, including corrections, should be applied to wind and wave variables to estimate more precisely the 50-yr return level sea states.

- **Updating extreme methods to deep and very deep waters.**

  The inconvenient of working in offshore and far-offshore locations is the lack of field measurements. Although reanalysis databases simulate correctly mean values of met-ocean variables, they may not characterize accurately extreme events. By contrast, instrumental measurements are able to register extreme values related to storms. However, most likely times series are too short or they are not even available.

  Because of that, mixed extreme models, considering instrumental and reanalysis data, will be proposed in order to obtain an accurate characterization of the extreme met-ocean variables distribution.

3.1.3 Economic Feasibility Assessment

Offshore wind initiatives entail great investments. Because of that, stable economic frameworks favor those investments and the characterization of the potential risk helps decision makers and developers.

- **Analyze wind conditions variability influence over principal financial estimators.**

  Whereas private agents develop detailed analysis of wind conditions focused on local scale, public agencies use wind atlas to locate the most promising sites for offshore wind development from a regional point of view. Consequently, detailed environmental risk associated to long-term wind conditions spatial and temporal variability analysis is not carried out at a regional scale.

  The analysis of main financial estimators from a regional point of view, considering the variability of met-ocean conditions, is proposed to assess accurately the offshore wind farm long-term performance.

3.2 Methodology

In this section, the methodology to address the objectives outlined is presented following the same scheme used for the state of the art and the objectives. Then, the methodology presentation is divided in three main topics (figure 3.2).

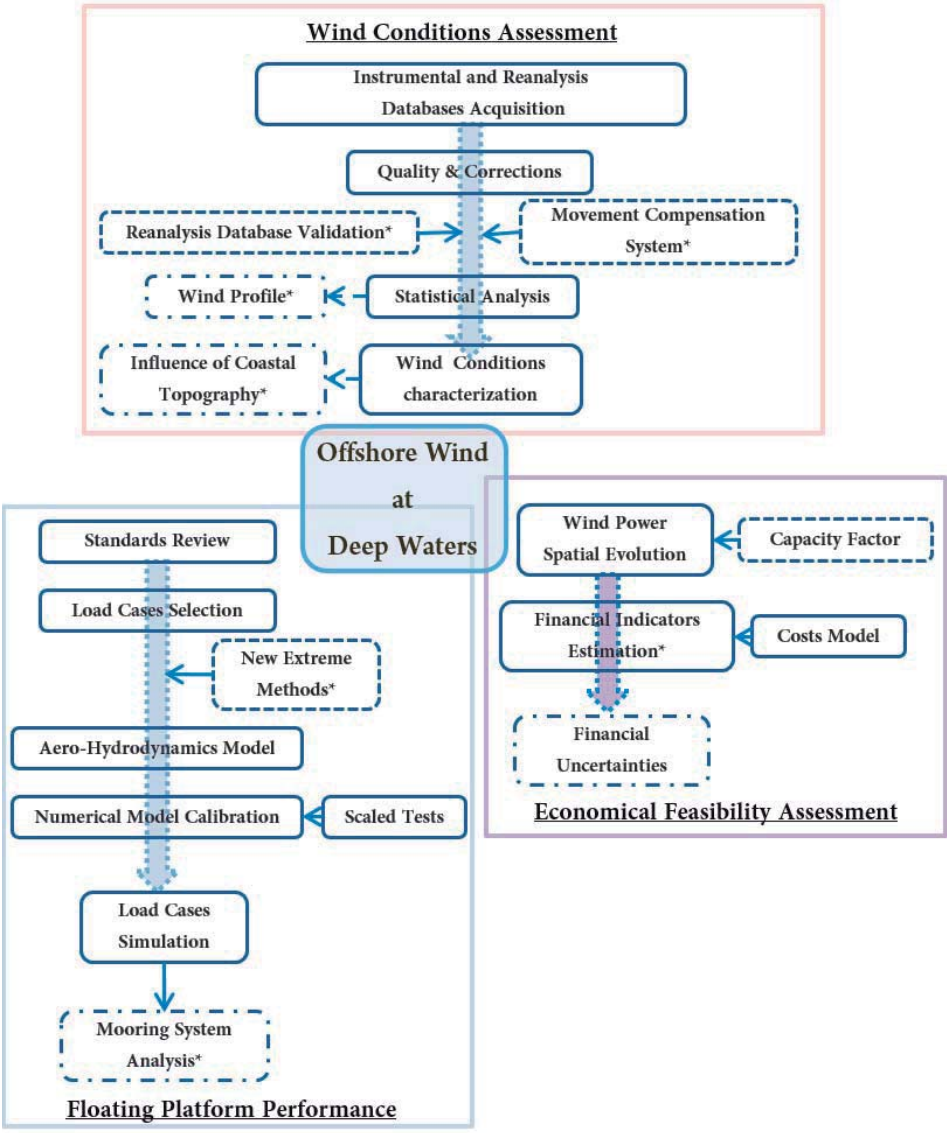

Figure 3.2: Methodology detailed scheme

3.2.1 Wind Conditions Assessment

The analysis of wind conditions at deep and very deep waters has been highlighted as one of the key points for future offshore wind development. This thesis will try to address some challenges related to the analysis of wind conditions, focusing on three main topics that are presented in the following.

- **Analysis of wind measurements uncertainty at deep waters.**

  The lack of field measurements at these locations reduces the accuracy of the assessment, whereas the development of floating technologies for measuring met-ocean conditions introduces new sources of uncertainty that need to be studied.

  The main source of uncertainty is related to the movement of the device. Because of that, it is proposed, as a first step, to develop a numerical analysis of the influence of the movement in the wind speed measurements. Based on the representative sea-states selected for the design of the met-mast presented in Guanche *et al.* (2011), the movement time series of the cup anemometers are computed. The error on wind speed measurement is obtained for each sea-state and reconstructed for the long-term analysis following the methodology outlined in Guanche *et al.* (2014c). This process will allow estimating the long-term error on wind speed measurements from cup anemometers mounted on floating met-masts.

- **Evaluation of wind conditions spatial variability and the influence of coastal topography.**

  The costs related to deep and very deep water locations increase the significance of the distance to shore. Consequently, it must be taken into account the influence of coastal topography on wind conditions.

  In order to analyze how coastal topography influences wind conditions in feasible areas for offshore wind applications, reanalysis databases as well as instrumental measurements are gathered. The North of Spain is chosen as the study area due to its characteristics. The spatial analysis of wind conditions separating southerly winds will allow evaluating the disturbance

of coastal topography, not only in wind speed but also in the capacity factor of commercial wind turbines or the wind profile shape.

- **Characterization of wind conditions variability.**

  The implementation of offshore wind at deep and very deep waters requires higher investments. Because of that, it is needed to assess wind conditions more precisely.

  In this thesis, numerical tools from climate analysis and prediction are applied. The selection of the most important synoptic patterns helps understanding the temporal variability of wind conditions. The study of wind conditions at regional scale will increase the accuracy of optimal location selection for future offshore wind farms.

3.2.2 Floating Platform Performance Assessment

Standards and guidelines for offshore wind platform design are based on oil&gas background. Therefore, there is place to the improvement of the methodologies proposed.

- **Review of the IFORM method proposed by the standards.**

  The IFORM method proposed in the standards leads to inaccurate results, and Mínguez *et al.* (2014) proposed the use of extreme value distributions for the estimation of high recurrence period sea-states (wind speed and wave height) for design purposes.

  This reviewed method is applied to calculate the design parameters of floating platforms for offshore wind turbines. Afterwards, using the numerical model FAST (Jonkman (2009)) the response of a reference floating platform is simulated. This model allows simulating the structural, hydrodynamic and aerodynamic performance of the structure, including the mooring system. Therefore, the changes on the mooring system loads will be calculated and their spatial variability analyzed.

- **Updating extreme methods to deep and very deep waters.**

  In Mínguez *et al.* (2013b) authors presented a method to combine numerical and instrumental data to estimate long recurrence period design parameters based on annual maxima. Taking into account the lack of field measurements at deep and very deep water locations, annual maxima samples that may be available do not allow the direct application of that method.

  In this thesis it is proposed to use the Generalized Pareto Distribution (GPD), based on peaks over threshold, that will allow using shorter time series to estimate the long recurrence period design parameters. As well as it will be done in the case of IFORM method, the numerical model FAST will be used to evaluate the spatial variability of mooring system loads taking into account the modifications on the mixed extreme value method.

3.2.3 Economic Feasibility Assessment

Offshore wind is commonly analyzed at a regional scale to locate optimal locations for offshore wind farms. Normally, the analysis is focused on the wind resource energy potential. Because of that, the first look does not include the economic feasibility point of view.

- **Analyze wind conditions variability influence on principal financial estimators.**

  Deep and very deep water locations were not studied in detail due to the lack of interest. However, nowadays the interest is growing as new technologies for offshore wind exploitation are being developed. In order to reduce the uncertainty of site selection it is recommended to include the economic aspects in the evaluation.

  The wind conditions influence on the economic feasibility assessment of offshore wind farms will be estimated. The analysis of the main financial estimators variability will be carried out by developing a random life-cycle simulator based on a realistic offshore wind farm costs model.

3.3 Work structure

On account of the work structure, the contents are organized in chapters as follows:

- Chapter 0: Resumen en Español

  Summary of the document in Spanish.

- Chapter 1: Introduction

  Brief summary standing out the motivation and interest of the Thesis.

- Chapter 2: State of the Art on Offshore Wind Energy

  Analysis of the background related to offshore wind energy. The aim of the chapter is to find potential gaps and improvements to be done.

- Chapter 3: Scope and Work Structure

  This chapter includes the objectives of the Thesis and the methodology to fulfill them.

- Chapter 4: Wind Conditions Assessment

  The first part of the Thesis, related to wind conditions spatial and temporal variability, is presented.

- Chapter 5: Floating Platform Performance Assessment

  The numerical tools for the analysis of the mooring system loads are described, as well as the performance of a specific case study. It is also analyzed the spatial and temporal variability of mooring system loads related to met-ocean variables.

- Chapter 6: Economic Feasibility Assessment

  In this chapter the regional economic feasibility at the North coast of Spain is carried out, considering realistic costs model and the random simulation of life-cycles.

- Chapter 7: Conclusions

  The main conclusions of the Thesis are presented in this chapter.

- Chapter 8: Future Research Lines

  Based on the work developed in this thesis, future research lines are proposed.

- Chapter 9: References

  The bibliography used in this Thesis is included in this chapter.

CHAPTER

4

Deep Waters Wind Conditions Assessment

In this chapter, the base for the rest of the work, which is related to wind conditions, is developed. The analysis of the error in the measurements from floating devices as well as the statistical analysis of offshore wind conditions and the influence of coastal topography will be presented. Hence, the structure of the chapter will be as follows:

- Introduction
- Deep waters measurement error analysis
- Offshore wind spatial and temporal variability evaluation
- Conclusions

4.1 Introduction

4.1.1 Motivation

Wind assessment is required to identify feasible locations for the implementation of wind farms. The seeking of more energetic wind conditions led to the deployment of wind turbines offshore. The main challenge faced in these cases is the lack of instrumental measurements.

The lack of instrumental measurements is due to the novelty of the offshore wind (short time series) as well as the financial requirements to deploy devices in deep and very deep waters. In this context, floating met-masts may be considered a competitive alternative.

This study takes advantage of the several sources of data available in the coast of Cantabria. Hourly high resolution numerical databases of wind speed, three floating met-masts and two meteorological buoys.

The analysis developed in this chapter will be the base for the wind power production estimation needed for the economic feasibility assessment presented in chapter 6, as well as for the load cases characterization of chapter 5.

4.1.2 Scope of the chapter

- Evaluation of the error of floating met-mast measurements.
- Wind conditions spatial and temporal variability analysis at local and regional scale.

4.1.3 Chapter structure

The chapter follows the scheme set by the objectives. Therefore, in a first section the wind measurement error will be analyzed and in a second section, the analysis of wind conditions variability will be carried out, paying special attention to the coastal topography influence.

4.2 Wind measurement error analysis at deep waters

Floating technologies for offshore wind applications presented in the state of the art has pros and cons. In this section, the floating met-mast presented in Guanche *et al.* (2014a) is used as the reference technology. On one hand, it has an advantage: it can reduce the cost compared to fixed technologies in deep waters. On the other hand, new sources of error will appear, mainly due to the constant movement of the floating body.

The movement of the floating met-mast introduces a deviation between real wind speed and met-mast wind measurements. In this section, the deviation between real and measured wind speed will be analyzed to determine the error introduced by the movement of the floating met-mast.

The proposed methodology is based on a calibrated numerical model used to simulate the combined effect of waves, wind and currents on the met-mast movements (displacements and rotations). The methodology for the short (1h) and long-term (years) error analysis can be summarized as follows:

- Applying the technique outlined in Guanche *et al.* (2014a), the most representative sea and wind states are selected from long enough hourly reanalysis time series (>20 years of data).
- For each selected sea-wind state, a synthetic time series is generated for wind and waves.
- A numerical simulation of the floating met-mast dynamic behavior for each selected sea-wind state based on a laboratory calibrated numerical model is carried out to obtain a six degree of freedom time series.
- For each selected sea state, the wind speed measurement error due to the floating met-mast movements is computed.
- The long-term sea state wind speed measurement error time series using the technique outlined in Guanche *et al.* (2014a) is reconstructed.

- Finally, the long-term analysis of the wind speed error due to the floating met-mast movements is carried out.

This methodology is based on the following assumptions:

- Synthetic wind time series generated are considered as the reference wind speed at each height. In the following, they are treated as the wind time series recorded by conventional anemometry mounted on a fixed met-mast.
- The wind field is supposed to be horizontal, which means that no vertical wind speed component is considered in this research. This assumption, in the open sea, is not a difficult assumption because there are no topographical or abrupt surface changes that may induce vertical wind components.
- For the sake of simplicity, it is assumed that the wind and waves are collinear. The test case used has a clear predominant direction from NW for waves and wind. However, there are several sites with a higher directional variability. The proposed methodology can be implemented in those cases as well.

4.2.1 **Sea-wind state selection**

Generating a long-term time series of wind speed error requires an efficient use of databases. With this aim, the methodology begins with the selection of a representative sea-wind state subset (500) at the location of the meteorological mast from the long-term sea-wind states database. The database used was generated according to the methodology outlined in Camus *et al.* (2011b). In this case, the MAX-DISS algorithm (MDA, Snarey *et al.* (1997)) has been used to select five hundred sea-states that, as reported by Guanche *et al.* (2011), are enough for a representative sea state subset.

The sea-wind state parameters chosen for the MAX-DISS selection of sea states are the significant wave height, H_S, the peak wave period, T_P and the mean wind speed at z = 10 m high, U_{10}.

4.2.2 Numerical modeling of the floating met-mast dynamics

The one-hour sea and wind states selected are used to simulate the behavior of the floating met-mast. The numerical model used in this work is SESAM-DeepC software developed by DNV (www.dnv.com (2013)). The model was previously calibrated using laboratory tests (Guanche *et al.* (2011)). As simulations run in the time domain, random time series of wave and wind variables were produced based on representative case parameters. The model returns, among other factors, the movements of the device.

4.2.3 Wind speed error estimation

The hourly average wind speed at ten meters high, U_{10}, is used. Moreover, a neutral boundary layer logarithm profile is assumed. Consequently, the mean velocity at any height, U_H, can be calculated. By means of a random phase method and using random initial seeds, hourly time series of instantaneous wind speed every 5 m high have been generated to include the instantaneous wind speed variability along the wind profile. The Frøya wind speed spectrum has been considered (Andersen & Løvseth (2006)). It should be highlighted that the same U_{10} time series has been used in the numerical model simulation and in the wind error assessment. Then, given the wind speed and the met mast movement time series, the wind speed error is calculated as shown below.

Taking into account the main assumptions considered in this research, only surge, V_S, heave, V_H and pitch, ω_P, velocities and heave, Z_H, and pitch, α_P, displacements will be taken into account. Figure 4.1 shows the nomenclature for wind and anemometer motions that will be used in the following.

It must be noted that cup anemometers only measure wind velocity in their plane. The floating met-mast tilt motion disturbs that plane, thereby affecting the wind speed observed by the cup anemometer.

- Surge velocity at the anemometer: $V_{AS} = V_S * cos\alpha_P$

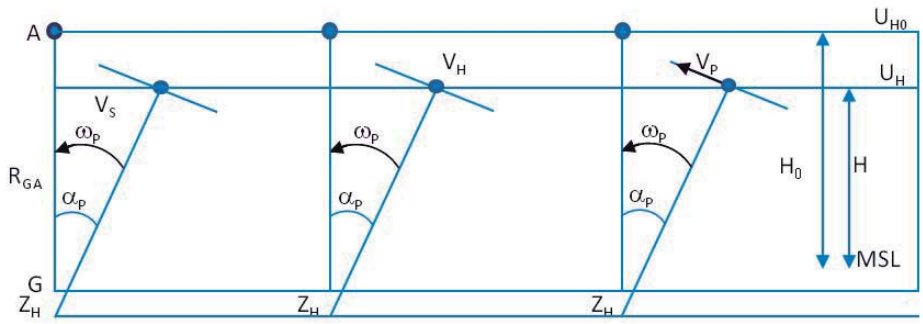

Figure 4.1: Nomenclature for the position and displacement of the anemometer

- Heave motion velocity at the anemometer: $V_{AH} = V_H * sin\alpha_P$
- Pitch-induced velocity at the anemometer: $V_{AP} = \omega_P * R_{GA}$

where R_{GA} is the distance from the floater center of gravity and the anemometer position. The time series of the surge velocity, $V_S(t)$, pitch angle, $\alpha_P(t)$, and pitch angular velocity, $\omega_P(t)$ are obtained from the numerical model. In the following, the observed wind speed estimation error is explained considering the different sources of error.

4.2.3.1 **Error associated with changes in the elevation**

The anemometer height changes due to floating met-mast movements (figure 4.2). The final height is given by the combination of the heave and pitch met-mast movements. Hence, the instantaneous height of the anemometer, $H(t)$, is given by the following expression:

$$H(t) = H_0 + Z_H(t) + R_{GA}[1 - cos\alpha_p(t)] \tag{4.1}$$

where H_0 is the anemometer theoretical height, $Z_H(t)$ is the time series of heave displacements, $\alpha_p(t)$ is the time series of pitch displacements and R_{GA} the distance from the met-mast gravity center to the anemometer.

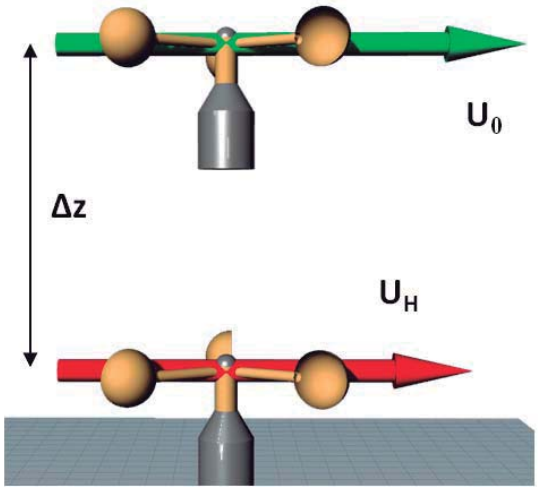

Figure 4.2: Height error scheme

The observed horizontal mean wind velocity at its instantaneous location (height) has been obtained by interpolating from the synthetic wind speed time series.

$$U_{mH}(H(t)) = f(U_1(H_1, t), U_2(H_2, t)) \tag{4.2}$$

where the U_1 is the mean horizontal wind velocity at height H_1 and U_2 is the mean horizontal wind velocity at height H_2.

The wind speed at the objective height can be obtained by applying a theoretical expression of the wind profile. In the case of low motions the potential wind profile may be applied.

If changes in the anemometer height due to the met mast movements are not taken into account and the horizontal instantaneous wind velocity $U_{H0}(t)$ is computed at the anemometer theoretical height H_0, a measurement error will be produced. To correct that error, the factor $f_H(t)$ given by equation 4.3 should be applied to the wind speed time series at the anemometer still elevation, $U_{H0}(t)$.

$$f_H(t) = \frac{U_{mH}(t)}{U_{H_0}(t)} \tag{4.3}$$

where $U_{mH}(t)$ represents the wind speed measurements considering the anemometer height variation.

4.2.3.2 **Error associated with anemometer tilt**

The met-mast tilt due to pitch motion affects the observed wind velocity (Figure 4.3, right panel). As shown in the cup anemometer calibration curve, figure 4.3 (left panel), if the anemometer pitch is less than $20°$, the relation between the measured wind speed and the true wind velocity may be approximated by the cosine of the pitch angle. Therefore, the following factor f_T given in equation 4.4 should be applied to correct the anemometer measurement.

$$f_T(t) = \frac{U_{mT}(t)}{U_{HO}} = cos\alpha_p(t) \tag{4.4}$$

where U_{mT} is the tilted measurement.

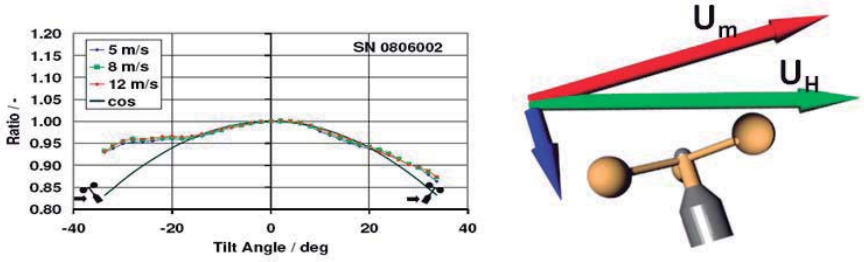

Figure 4.3: Tilt error scheme

4.2.3.3 Error associated to the anemometer motion

Anemometers oscillate due to the movement of the met-mast. Vector equation 4.5 gives the velocity vector of the anemometer.

$$V_A = V_G + \Omega \times R_{GA} \tag{4.5}$$

where V_G is the velocity at the floating mast gravity center, Ω is the vector of rotation around the gravity center, $\times$ is the symbol for cross-product and R_{GA} is the position vector of the anemometer. If only three degrees of freedom are considered: heave, surge and pitch; these vectors are $V_G \equiv (V_S, 0, V_{Heave})$;$\Omega \equiv (0, \alpha_p, 0)$ and $R_{GA} \equiv R_{GA}(cos\alpha_P, 0, sin\alpha_P)$. The two-dimensional V_A vector components are:

$$V_A(t) = [V_S(t) + \omega_p(t)R_{GA}cos(\alpha_p(t)); V_H(t) - \omega_p(t)R_{GA}sin(\alpha_p(t))] \tag{4.6}$$

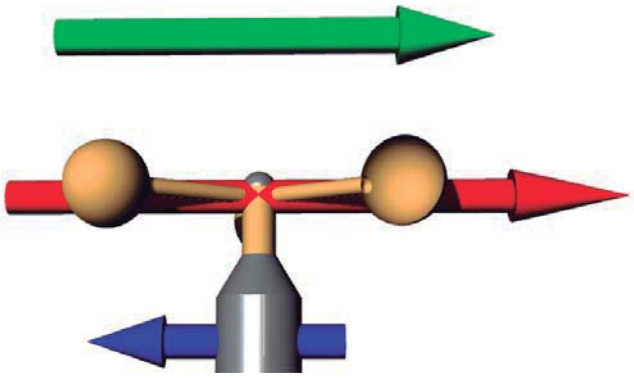

Figure 4.4: Relative speed error scheme

The observed wind velocity due to the anemometer motion (Figure 4.4), $U_{mA}(t)$, will be the projection of $V_A(t)$ over the anemometer plane (considering that cup anemometers do not react to the vertical component). This measured velocity due to motion is shown in equation 4.7:

$$U_{mA}(t) = \omega_p(t)R_{GA} + V_S cos\alpha_p(t) - V_H sin\alpha_p(t) \tag{4.7}$$

For small pitch angles, the sine component of 4.7 is very small and can be neglected, so the motion measured velocity could be expressed by equation 4.8:

$$U_{mA}(t) \approx V_S cos\alpha(t) + \omega_p(t) R_{GA} \tag{4.8}$$

4.2.4 Error of measured wind speed - Long term analysis

Taking into account the errors produced by the anemometer varying height, tilt and velocity, the observed wind velocity would be defined as in equation 4.9.

$$U_m(t) = U_{mA}(t) + U_{mHT}(t) = V_S cos\alpha_p(t) + \omega_p(t) R_{GA} + U_{H0}(t) f_H(t) f_T(t) \tag{4.9}$$

where $U_{mHT}(t)$ is the observed wind velocity by the anemometer for a still met mast after the surge, heave and pitch displacements have occurred.

The instantaneous absolute error is given by the difference between the measured velocity, $U_m(t)$ and the theoretical wind speed at the anemometer's theoretical position, $U_{H_0}(t)$ (eq. 4.10).

$$E_A(t) = U_m(t) - U_{H_0}(t) = V_S cos\alpha_p(t) + \omega_p(t) R_{GA} + U_{H_0} f_H(t) f_T(t) - U_{H_0}(t) \tag{4.10}$$

and the relative instantaneous error is the relation between the absolute error and the computed velocity at the theoretical still height, as in expression 4.11.

$$E_R(t) = \frac{E_A(t)}{U_{H_0}(t)} = \frac{V_S cos\alpha_p(t) + \omega_p(t) R_{GA}}{U_{H_0}(t)} + f_H(t) f_T(t) - 1 \tag{4.11}$$

In order to simplify the analysis, the relative errors for each movement considered are given in the next expressions:

Elevation error, $E_{RH}(t)$:

$$E_{RH}(t) = \frac{U_{mH}(t) - U_{H0}(t)}{U_{H0}(t)} = f_H(t) - 1 \tag{4.12}$$

Tilt angle error, $E_{RT}(t)$:

$$E_{RT}(t) = \frac{U_{mT}(t) - U_{H0}(t)}{U_{H0}(t)} = f_T(t) - 1 \tag{4.13}$$

Motion error, $E_{RM}(t)$:

$$E_{RM}(t) = \frac{U_{mA}(t)}{U_{H0}(t)} = \frac{V_S cos\alpha_p(t) + \omega_p(t) R_{GA}}{U_{H_0}(t)} \tag{4.14}$$

If these three errors are summed, the relative error given by equation 4.11 is an approximation to the relative error equation 4.15.

$$E_R(t) \cong E_{RH}(t) + E_{RT}(t) + E_{RM}(t) = \frac{V_S cos\alpha_p(t) + \omega_p(t) R_{GA}}{U_{H_0}(t)} + f_H(t) + f_T(t) - 2 \tag{4.15}$$

4.2.5 Error Calculation

From the relative wind error time series (eq. 4.15), the 10-minute and hourly mean relative errors (10MRE and HMRE, respectively) can be calculated as shown below.

Hourly mean relative error

The hourly mean relative error (HMRE) is calculated from the 1-hour sea state time series error (eq. 4.15) composed of N samples using expression 4.16.

$$\overline{E}_{RH} = \frac{1}{N} \sum_{i=1}^{N} E_{Ri} \tag{4.16}$$

10-minute mean relative error

The 10-minute mean relative error (10MRE) is calculated as described by equation 4.15 but for consecutive N/6 samples of 10 minutes. Therefore, six ten-minute errors for each simulated sea state are obtained. To be on the safe side, it is assumed that the maximum 10-minute error in the sea state represents the 10-minute error of the sea state.

4.2.6 **Long-term time series reconstruction of the mean relative error (MRE)**

In this work, the SeaWind and Global Ocean Waves databases have been used. SeaWind is a daily re-forecast for the Mediterranean and Euro-Atlantic region at 15 km resolution, providing wind-related variables with hourly frequency (Menéndez *et al.* (2014)). This product is produced by a mesoscale limited-area atmospheric model (WRF, Skamarock & Klemp (2008)) nested into ERA-Interim reanalysis data for the period 1989-2010. The focus is on the accurate representation of hourly variability and, thus, a scheme with daily restarts from global reanalysis data was adopted to keep the model as close to the observed marine wind as possible.

The wave data were taken from Global Ocean Waves 1.0 (GOW 1.0), an hourly wave reanalysis database for the period 1948-2009, with a spatial resolution of 1^ox1.5^o, from IH Cantabria (Reguero *et al.* (2012)). GOW 1.0 is generated using the Wave Watch III model (WW3) and forced by winds from the NCEP/NCAR 40-year reanalysis project (Kalnay *et al.* (1996).

With this information, 60-year (1948 - 2009) long-term time series of the MRE are built using the nonlinear interpolation technique of the radial basis function (RBF) (Camus *et al.* (2011a), Guanche *et al.* (2014a)).

4.2.7 **Results**

To analyze the influence of each source of error independently, a representative location in the Atlantic Ocean near Santander (43.3°N, 3.8°W) was selected from the database (figure 4.5). It corresponds to the location of the met-mast. It was deployed around 3 km offshore Santander city, in the North of Spain.

Figure 4.6 (left panel) shows in red the selected H_s - T_p points against the total database points (shown in grey), and figure 4.6 (right panel) shows the same selected points in the plane H_s - U_{10}. In figure 4.6, it can be seen that extreme

Figure 4.5: Representative location.

sea states reach a significant wave height of 9 m, and extreme wind states are no greater than 30 m/s. Thanks to the MDA algorithm, the sea state variability observed is well represented by the selected sea states (red dots in left panel and blue dots in right panel).

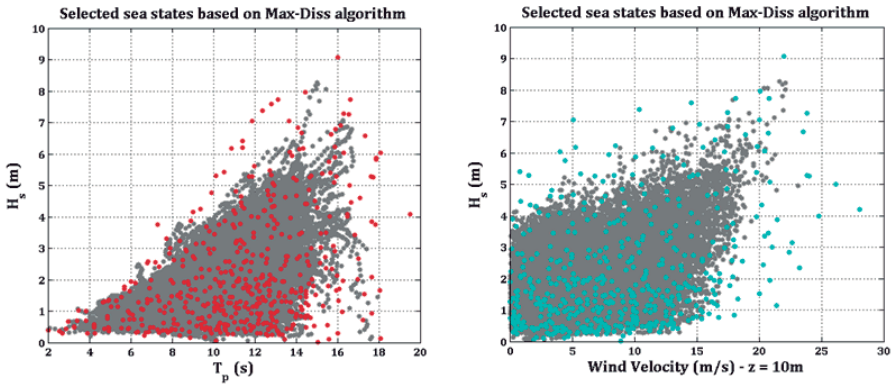

Figure 4.6: Max-Diss 500 selected H_s vs. T_p points (left) and U_{10} vs. H_s (right) at the met-mast location.

Figure 4.7 is shown as an example. The wind speed time series for a sea-wind state described by H_s =4.2 m, T_p =12.47 s and U_{10} =28.06 m/s is represented.

In this case, the mean value of the wind speed corresponds to the 50 year return period. The blue and red lines show the computed fixed and floating mast velocities, respectively. The measurement height considered is 90 m in both masts.

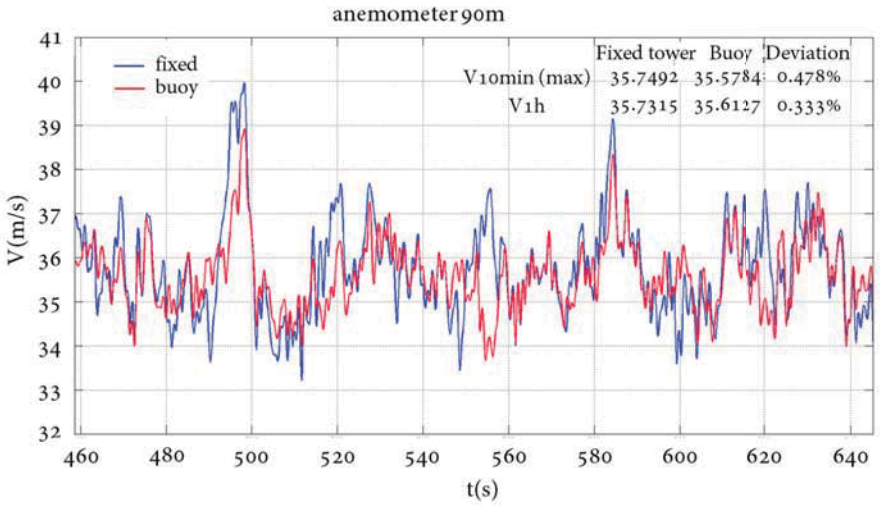

Figure 4.7: Time series of instantaneous computed wind speed for a sea-wind state having H_s=4.2 m, T_p=12.47 s and U_{10}=28.06 m/s. In blue color, fixed met mast; and in red color, floating met mast. The U_{10} wind state has a return period of 50 years. Anemometer height: 90 m.

The 10-minute (maximum for the six 10-minute averages, which is called 10MW in advance) and hourly averaged wind velocities (HMW) computed for the fixed mast are 35.75 m/s and 35.73 m/s, respectively. The same figures for the floating mast are 35.58 m/s and 35.61 m/s, respectively. Those values imply 10MRE and HMRE of 0.48% and 0.33%, respectively.

Tables 4.1, 4.2 and 4.3 show the elevation, tilt and motion mean relative errors results, equations 4.12, 4.13, 4.14, 4.15 and 4.16. Both the errors for the hourly and 10-minute means are presented for several anemometer heights. Each table corresponds to a different sea-wind state. Table 4.1 corresponds to a sea-wind state with 50 years U_{10} return period and the corresponding H_S and T_P. Table

4.2 corresponds to a sea-wind state with 2 year U_{10} return period and the corresponding H_S and T_P. Finally, Table 4.3 corresponds to a sea-wind state having the mean U_{10} and the corresponding H_s and T_p.

		Hourly mean				10min mean	
Tilt(°)		-11.21				-11.83	
Heave(m)		-0.99				-1.11	
Error(%)	Time Period	Z=45m	Z=55m	Z=75m	Z=85m	Z=90m	Mean
Height	10min	-0.43	-0.41	-0.45	-0.46	-0.47	-0.44
	1hour	-0.49	-0.47	-0.37	-0.39	-0.33	-0.41
Tilt	10min	-2.15	-2.15	-2.19	-2.32	-2.49	-2.26
	1hour	-2.28	-2.29	-2.16	-2.17	-2.12	-2.20
Motion	10min	-0.01	0.003	0.03	-0.05	-0.004	0.001
	1hour	-0.004	-.0.04	-0.005	-0.005	-0.005	0.01
Total	10min	-2.6	-2.54	-2.61	-2.83	-2.97	-2.71
	1hour	-2.78	-2.73	-2.53	-2.57	-2.45	-2.61

Table 4.1: Tilt, heave and motion means and relative errors for different anemometer heights for a 50-years return period wind (U_{10m} = 28.06m/s) and the corresponding sea state (H_s = 4.2m, T_p = 12.47s).

In the case of the 50-year return period wind speed ($U_{10} = 28.06$ m/s, $H_s = 4.2$ m and $T_p = 12.47$ s) the tilt is the movement most relevant to the mean relative error (MRE) for both 10-min and hourly averages. In this case, a mean tilt of 11° is obtained and around 85% of the total MRE is due to the tilting (2.2% of MRE). This error is consistent with the cosine function, see figure 4.3, which predicts MREs between 2% and 3% ($0.97-0.98$ reduction factor). Heave is less relevant, with a mean heave of around 1 m producing around the 15% of the total MRE. The motion error is practically irrelevant due to the meteorological mast slow motions (max upper tip horizontal lower than 2 m/s) and the relative movement symmetry, that average near zero error, being the damping produced by the wind drag the unique source of asymmetry.

In the case of the 2-year return period storm, ($U_{10} = 22.4$ m/s, $H_s = 2.8$ m and $T_p = 9.8$ s) see table 2, tilt (more than 7° in average) is again the most relevant to the MRE (around 1% of error, corresponding to more than 85% of the total MRE) followed by far by the heave motion (0.5 m in average and less than 15% of the total MRE). The heave error is higher for the lower anemometers (around 0.2 % compared to 0.13 to 0.18 %) because the wind vertical gradient is higher at lower heights. Again the mast motion is irrelevant to the MRE.

		Hourly mean				10min mean	
Tilt(°)		-7.251				-7.64	
Heave(m)		-0.5				-0.53	
Error(%)	Time Period	Z=45m	Z=55m	Z=75m	Z=85m	Z=90m	Mean
Height	10min	-0.21	-0.22	-0.15	-0.13	-0.17	-0.18
	1hour	-0.21	-0.22	-0.17	-0.15	-0.18	-0.19
Tilt	10min	-1.00	-1.01	-0.88	-0.95	-0.96	-0.96
	1hour	-1.05	-1.04	-1.00	-0.98	-1.01	-1.02
Motion	10min	0.003	0.003	0.015	0.023	0.004	0.01
	1hour	0.003	0.003	0.003	0.004	0.001	0.003
Total	10min	-1.21	-1.24	-1.03	-1.11	-1.13	-1.14
	1hour	-1.27	-1.26	-1.17	-1.12	-1.18	-1.2

Table 4.2: Tilt, heave and motion means and relative errors for different anemometer heights for a 2-years return period wind ($U_{10} = 22.4$m/s) and the corresponding sea state ($H_s = 2.8$m, $T_p = 9.8$s).

Among the 500 cases analyzed there is a sea state with similar wind velocity but much higher and longer waves ($U_{10} = 21.98$ m/s, $H_s = 9.1$ m and $T_p = 16$ s). In this case, the mean tilt is $6.94°$, very similar to the case presented in table 4.2 and the mean 10-min tilt measurement shows an error about -1.12% (-1.14% in the Table 4.2 case). For the hourly mean, the corresponding MREs are -1.07%, for this case and -1.2% for table 4.2. These results indicate that the most relevant parameter for the MRE is wind velocity because it is responsible of the met-mast permanent tilt.

The third case analyzed is a sea state having the annual mean wind velocity and the corresponding wave characteristics ($U_{10} = 5.01$ m/s, $H_s = 1.0$ m and $T_p = 6.6$ s). In this case, the mean tilt is very low (around $0.3°$) and the mean heave is nearly zero, see table 4.3. As can be seen in table 4.3, even in nearly calm conditions, tilt is the main source of MRE (although very low).

		Hourly mean				10min mean	
Tilt(°)		-0.3				-0.32	
Heave(m)		-0.01				-0.01	
Error(%)	Time Period	Z=45m	Z=55m	Z=75m	Z=85m	Z=90m	Mean
Height	10min	-0.003	-0.001	-0.002	-0.001	-0.001	-0.002
	1hour	-0.003	-0.002	-0.001	-0.001	-0.001	-0.002
Tilt	10min	-0.19	-0.19	-0.19	-0.19	-0.19	-0.19
	1hour	-0.19	-0.19	-0.19	-0.19	-0.19	-0.19
Motion	10min	0.002	0.002	0.009	0.003	0.009	0.005
	1hour	0.001	0.001	0.002	0.002	0.002	0.002
Total	10min	-0.19	-0.19	-0.19	-0.19	-0.19	-0.19
	1hour	-0.19	-0.19	-0.19	-0.19	-0.19	-0.19

Table 4.3: Tilt, heave and motion means and relative errors for different anemometer heights for yearly mean wind velocity ($U_{10} = 5.01$m/s) and the corresponding sea state ($H_s = 1.0$m, $T_p = 6.6$s).

4.2.7.1 **Long-term measurement error analysis**

Following the proposed methodology, the total MRE long term time series can be computed. Thus, the error related to the use of a floating spar for measuring the wind speed to support further wind developments can be determined. Figure 4.8 shows the 1948-2009 HMRE time series. As can be seen in the figure, the maximum relative errors are always below 2.5% and only two sea-wind states exceed 1.5%. Most of the time, the total HMRE is below 0.5%.

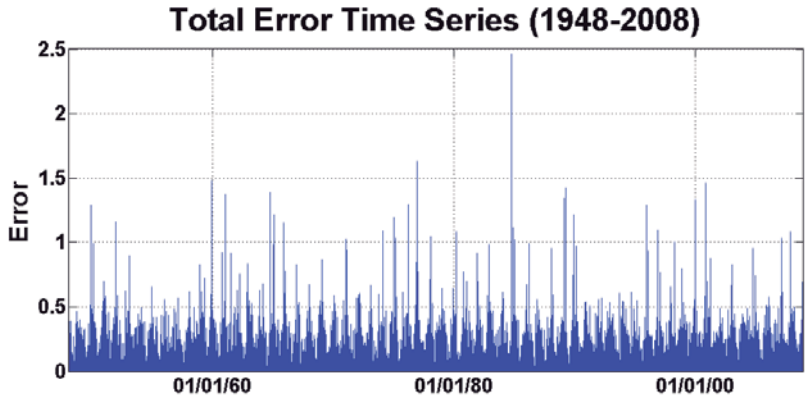

Figure 4.8: Error time series.

A better form to visualize the error is by plotting the scatter diagram (fixed mast versus floating mast wind measurements) (see figure 4.9). Besides, the analysis of the error functions allows the calculation of the probability thresholds in which the measurements could be considered correct without the application of any movement compensation system.

As can be seen in figure 4.9 (left), the HMRE is very low (lower than 0.25%) for hourly mean wind velocities (HMW) below 20 m/s. The HMRE exceeds 1% when the HMW exceeds 27 m/s. As can be seen in the right panel of figure 4.9, the 10MRE exceeds 0.5% when the 10-minute mean wind velocity (10MW) exceeds 22 m/s. In this case, large errors appear for the lowest wind velocities because small deviations produce large relative errors. However, these values are beyond the common threshold to take into account the cup anemometer measurements (2 m/s).

Figure 4.10 shows the HMRE for the anemometer located at 90 m in terms of the HMW. As it can be seen in the figure, the error shows a parabolic shape for hourly mean speeds higher than 12 m/s. Taking into account that most wind turbines enter into survival mode for HMW higher than 25 m/s, it can be said that the HMRE is below the acceptable limits at the full operational range. When the

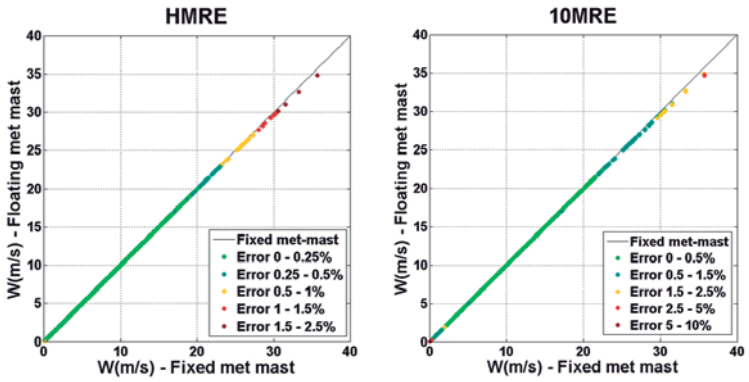

Figure 4.9: Scatter plot of (left) hourly error and (right) 10-min error .

error exceeds 1% the wind velocity is higher than the survival mode threshold of most of current commercial wind turbines.

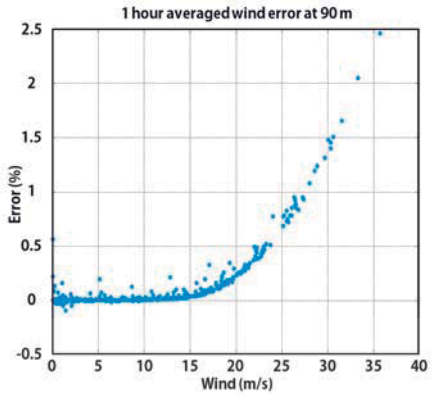

Figure 4.10: Hourly mean wind speed measurement error at 90 m

The HMW cumulative distribution function (CDF) (see figure 4.11) allows calculating the time percentage that the HMW is below a given value. As shown in figure 4.10, the HMRE exceeds 0.5% for HMW higher than 23 m/s. Using the CDF of figure 4.11, it can be seen that the HMRE exceeds 0.5% the 0.1% of the time (less than 9 h per year). Therefore, in terms of the hourly mean error, the

maximum expected error is limited.

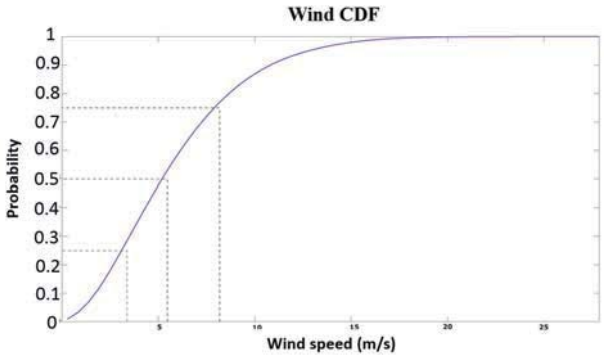

Figure 4.11: Wind speed cumulative distribution function

Figure 4.12 shows the CDFs of the 10MRE (left) and HMRE (right). From these figures it can be derived that the 50% percentile corresponds to a 10MRE of 0.05% and a HMRE of 0.07%. The corresponding 95% percentiles are 0.57% for the 10MRE and 0.35% for the HMRE. It can also be seen that the increase in the averaging time increases the kurtosis of the probability distribution function (the error is distributed narrower around the average in the HMRE than in the 10MRE).

From figure 4.12, it can be concluded that in terms of the 10MRE and HMRE, the uncertainty of the wind measurement is limited in the test site studied. In both cases, an error of 0.5% is achieved for less than 7.5% of the time in the absence of any motion compensation system.

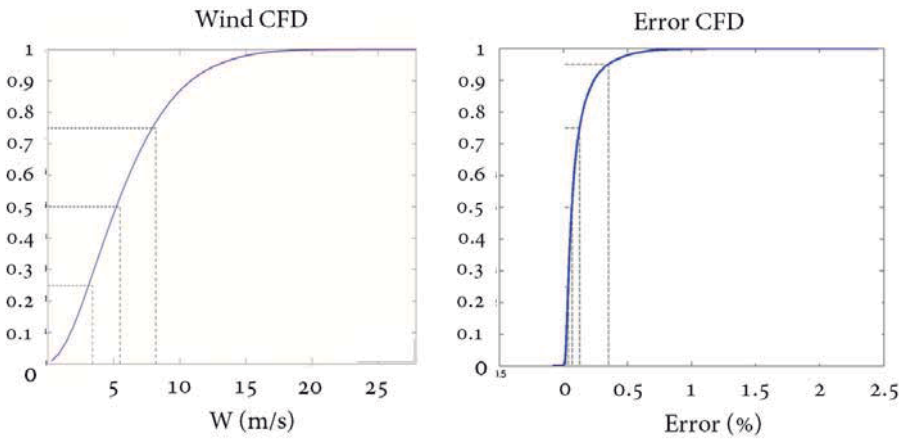

Figure 4.12: (Left) Hourly mean error and (right) 10-min error cumulative distribution functions.

4.3 Wind conditions spatial and temporal variability evaluation

4.3.1 Area of Study

The Cantabrian coast (North of Spain, figure 4.13) is the area of study for offshore wind assessment. The area analyzed goes from longitude -4.51 to -3.15 and from latitude 43.35 to 44.15, including the first 80 km offshore, which may be considered the transitional area from earth to sea, where the wind is influenced by coastal topography.

Cantabria is a region characterized by a high mountain range parallel to the coast at relative short distance ($<$ 60km) with peaks higher than 2000m. Furthermore, a series of mountain ranges an valleys, perpendicular to the coast, result in a specific shape of the flow, mainly for southerly winds. This geographic structure (see figure 4.14) concentrates the wind flux, increasing wind speed, at the valleys and diverges wind at the top of the mountain ridges decreasing the wind speed. Because of that, this region seems to be a good area to study the effects of coastal topography on wind conditions.

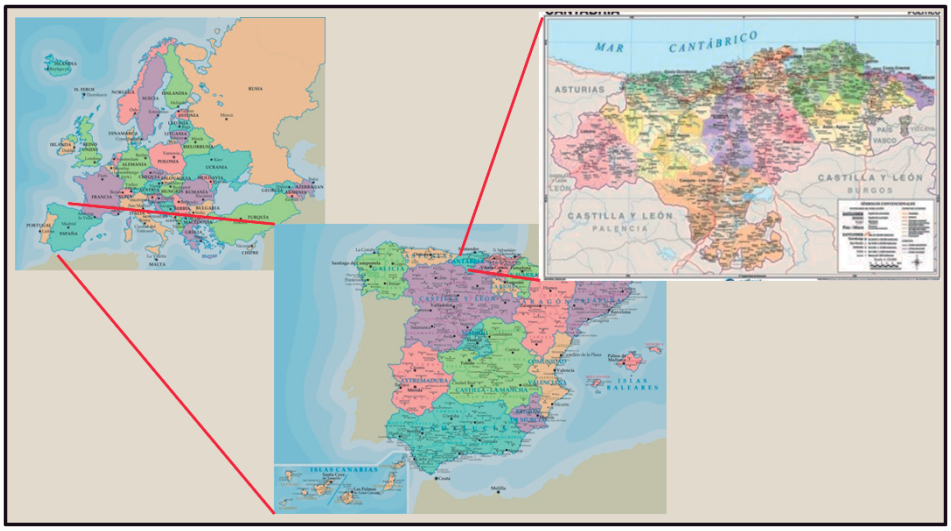

Figure 4.13: Location of the area of study.

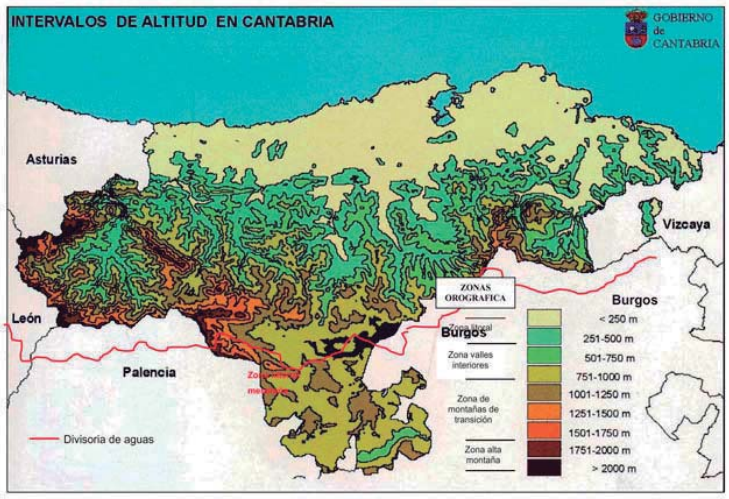

Figure 4.14: topography of the area of the study.

Furthermore, it is important to highlight that the Cantabrian coast bathymetry

reaches deep waters ($>$ 50m) few kilometers offshore ($<$ 5km). Depending on the specific area around 15 km offshore depths of more than 100m can be found. Consequently, any future development of wind energy in this region will be based on floating foundations.

4.3.2 Databases Description

In last years it has been an increasing interest in homogeneous high resolution wind databases at offshore sites. On one hand, instrumental measurements and observations, from ships, buoys or meteorological masts may be applied for local analysis due to their coarse spatial resolution. On the other hand, satellite data may be an alternative to *in situ* measurements, although their records are short and irregular in time and space.

Reanalysis databases (e.g. ERA-Interim or NCEP/NCAR) become a complement for measurements. They have been considered quasi-observations in some research. They are produced, commonly, using a global atmospheric model and long time series with a spatial resolution of degrees are obtained. Reanalysis databases are calibrated taking into account the available observations.

Summarizing, instrumental measurements add value to the wind resource assessment due to their accuracy by measuring *in situ* wind variables, even under extreme conditions. However, their principal disadvantage is their common short length. This is solved by introducing numerical databases in the analysis.

4.3.2.1 Reanalysis databases

SEAWIND

This hourly wind database was produced by historical numerical simulation of the atmosphere at a regional scale using WRF (Skamarock & Klemp (2008)) with ERA-Interim (Dee & co authors (2011)) as boundary conditions. It includes the Mediterranean and the European Atlantic basins (figure 4.15). Its spatial resolution is 15 km.

SEAWIND HR

SeaWind HR (-High Resolution-) database consists on an update of SeaWind database to provide a greater spatial resolution (1 MN $\sim$ 1.8 km) in the coastal area. 1.8 km hourly reanalysis requires great computational cost. Consequently, SeaWind HR is a hybrid downscaling, which combines a dynamic downscaling

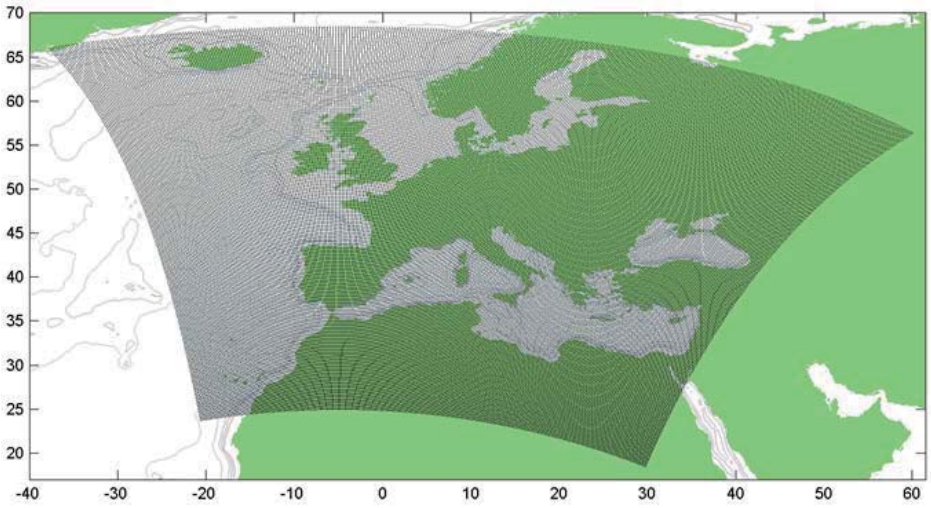

Figure 4.15: SeaWind Grid.

(WRF model) and a statistical downscaling (weather type classification and analogous method for reconstruction). This methodology is formed, basically, by three stages: i) representative cases selection; ii) numerical simulation (dynamic downscaling); and iii) application of analogous method for the hourly reconstruction of high resolution wind field time series.

4.3.2.2 **Instrumental measurements**

Several instrumental sources of data were available for the study. Two meteorological buoys and three meteorological floating masts have been used to validate the behavior of the reanalysis database. In figure 4.16, the locations of the five devices are shown.

Meteorological buoy (Red Vigía)

The Integral Water Watch Grid (Red Vigía) was conceived to control in real time the environmental quality parameters in Cantabria.

Two buoys were deployed offshore La Virgen del Mar (longitude: -3.88; lat-

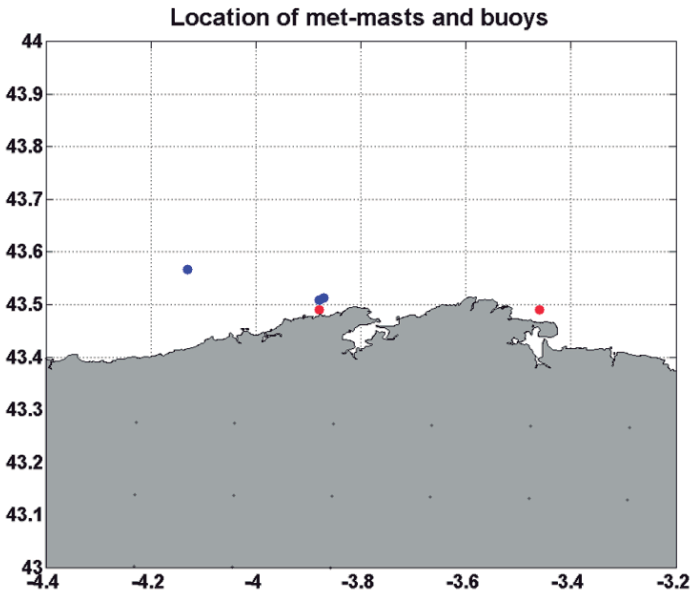

Figure 4.16: Location of measuring devices: In red dots: buoys; in blue dots: met-masts.

itude: 43.49) and Berria (longitude: -3.46; latitude: 43.49) in December 2009. They are installed at 32 and 28 meters deep, respectively. Both buoys are adapted to ocean conditions treated against biofouling and corrosion.

The system records parameters related to waves, such as: wave height, period and direction; currents at several depths including speed and direction; wind speed and wind direction, humidity, atmospheric pressure, air and water temperature and solar radiation. Moreover, related to water quality, instruments installed on the buoys measure indicators such as: green-blue bacteria level, chlorophyl, oxygen concentration, salinity, pH, turbidity, among others.

Wind speed measurements are recorded at 3 meters above sea level. Then, applying an internal algorithm the wind speed is extrapolated to 10 meters above sea level.

Figure 4.17: Red Vigía meteorological buoy (Source: $www.redvigia.es$).

Floating Meteorological Mast (IDERMAR METEO)

Idermar floating met-mast is a structure, based on SPAR type, which supports a similar met-mast to those applied at onshore locations to characterize wind resource by measuring different atmospheric variables.

From a structural point of view, the system consists of a submerged section which gives stability formed by a floater at the sea surface and a ballast at the deepest part of the structure. The emerged part consists of a cylindrical section supporting the met-mast.

IDERMAR developed three floating met-masts. The first two were deployed as prototypes to understand the behavior of these type of devices. The third one was conceived as a pre-commercial device.

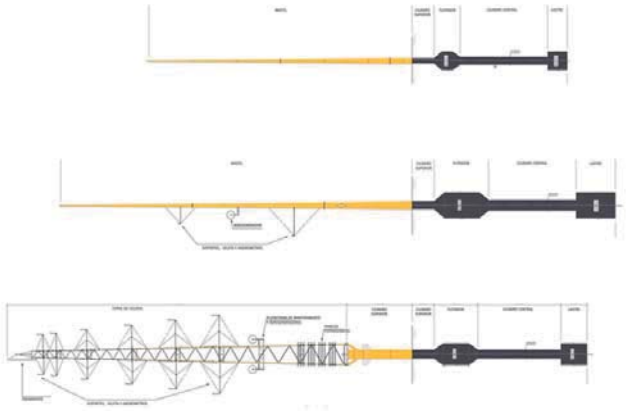

Figure 4.18: Floating meteorological masts from Idermar

Idermar Meteo I

This first prototype (figure 4.19) was deployed in June 2009 at La Virgen del Mar. The total length of the structure is 95.7 m, from which 60 m are emerged. The mast structure is tubular reducing the diameter of the section to the top. The anemometers are located at 20, 40 and 60 m above sea level.

Figure 4.19: Floating meteorological mast Idermar I

Idermar Meteo II

This met-mast (figure 4.20) is located 16 km offshore (longitude: 4°7'48.00"O; latitude: 43°34'12.00"). It follows the same design of the first prototype with a tubular tower but its total length is 80 m. In this case, the anemometers are located at 26, 53 and 80m.

Figure 4.20: Floating meteorological mast Idermar II

Idermar Meteo III

The third one is located at La Virgen del Mar (figure 4.21). The structure has a total length of 134 meters, from which 44 m are submerged. The 90 meters above sea level are formed by different sections. It is tubular in the first meters supporting a lattice structure where the sensors are deployed. The design of this mast solves a problem that was found in the others masts: the shadow due to the tubular mast reduces the quality of measurements. The effect is reduced, not only using a lattice mast but also using supporting arms for the anemometers in order to maintain the measuring devices as far as possible of the mast. Moreover, two anemometers are deployed at each height allowing one of them to measure 'clean' air.

The anemometers are deployed at 5 different heights: 45, 55, 75, 85 and 90 meters. In addition, wind vanes are located at 2 different heights: 65 and 82 meters. More measuring devices are located at the mast in order to characterize

Figure 4.21: Idermar Meteo III floating met-mast during transport in 2011

the atmospheric variables behavior. In figure 4.22 the location of the most important instruments is shown.

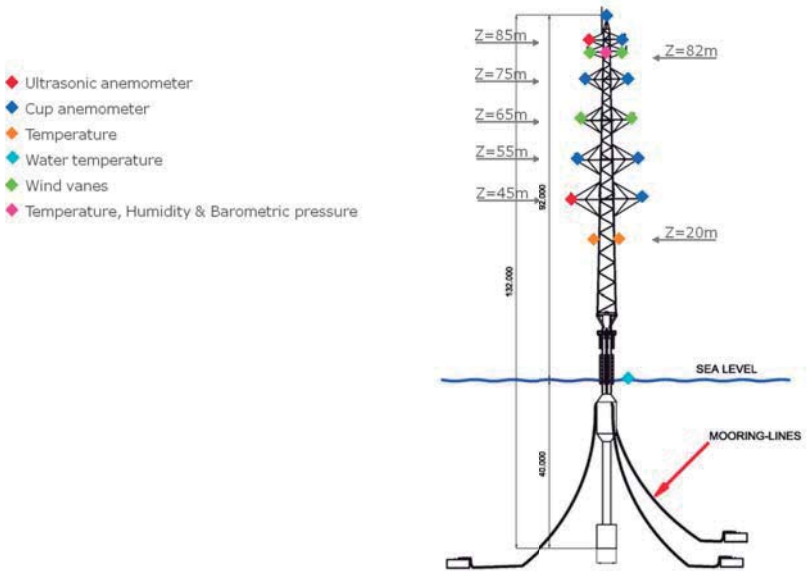

Figure 4.22: Idermar Meteo III floating met-mast

4.3.3 Instrumental and Numerical databases analysis

In this section, instrumental and numerical databases available for the analysis are analyzed in order to determine their applicability for the evaluation of offshore wind conditions assessment.

Firstly, the length of the time series and the height of the measurements will be analyzed in order to determine the best way to carry out the analysis. Afterwards, a direct comparison of the time series when possible will be done, using scatters to estimate the correlation between the sources of data. Finally, in those cases where no common period exists, the wind intensity rose will be used as a statistical approximation.

4.3.3.1 Analysis of time series length and measurement height

Time series cannot be always directly compared due to the lack of common time periods or the differences in height. In figure 4.23, the length of the time series is shown. As it can be seen, the SeaWind HR time series can be compared to Idermar Meteo I, whereas SeaWind is comparable to data recorded by Red Vigía and Idermar Meteo I and II.

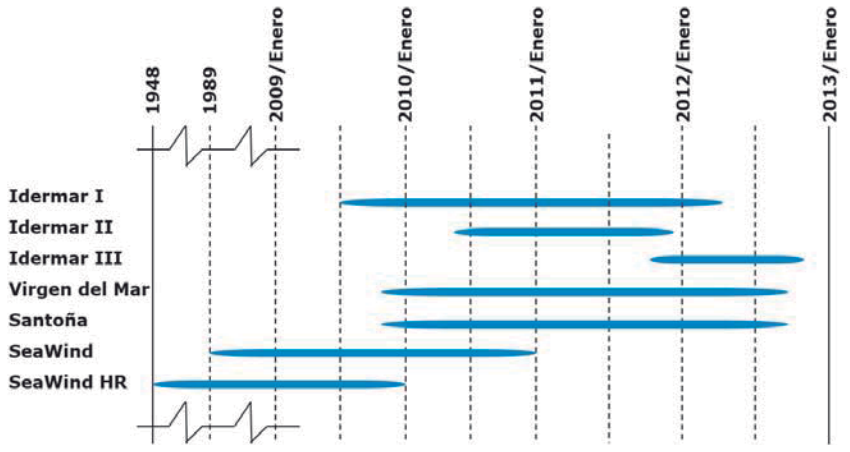

Figure 4.23: Length of the measurements.

The time series of wind speed records have different heights depending on the database. In figure 4.24, the height where measurements are registered is shown.

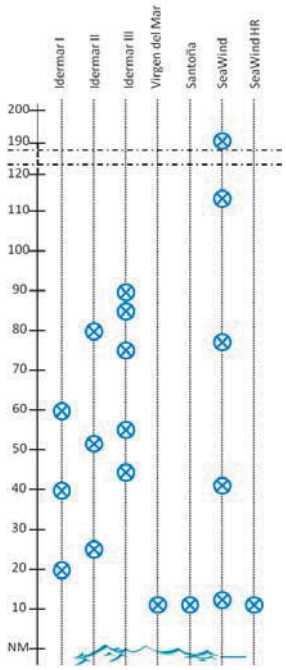

Figure 4.24: Height of the measurements.

4.3.3.2 **Comparison of time series - Scatters**

Firstly, the Red Vigía wind speed measurements are compared to numerical databases (figure 4.25). SeaWind II has a great deviation from instrumental measurements at both locations. For values higher than 5 m/s the reanalysis database overestimates wind speed. However, SeaWind HR reduces this overestimation improving the performance of the numerical database.

In figure 4.26, the scatter plots of Idermar I are shown. In this case, Idermar I wind speed measurements are compared to SeaWind 2, SeaWind HR and Virgen del Mar buoy. In the first case, SeaWind 2 overestimates wind speed as well as

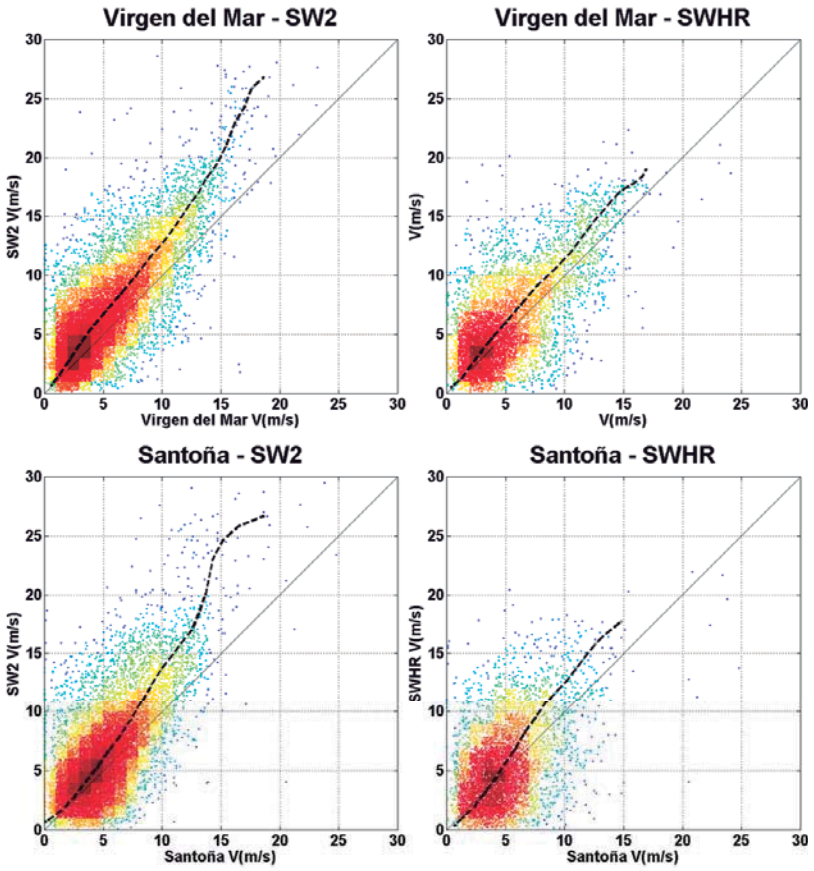

Figure 4.25: Scatter plot of Red Vigía, SeaWind and SeaWind HR

in the previous analysis. However, SeaWind HR has negligible deviation in mean terms as the Q-Q line shows. Last plot, related to Idermar I and Virgen del Mar buoy, shows that Idermar I overestimates wind speed. This can be a consequence of the internal algorithm of the buoy (to extrapolate wind speed from 3 meters to 10 meters), the shadow of the waves influence over the buoy measurements during several sea-states or the theoretical wind profile used to extrapolate wind speed from the met-mast, among other possibilities.

In figure 4.27, the comparison between Idermar II and SeaWind is shown. In

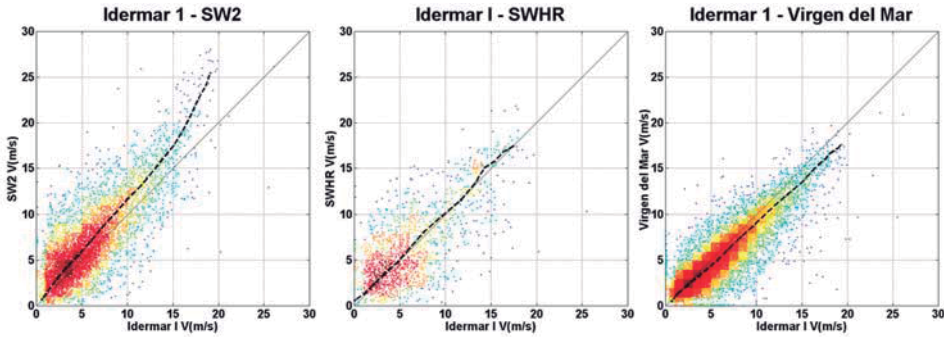

Figure 4.26: Scatter of Idermar I, SeaWind and SeaWind HR

this case, SeaWind overestimates wind speed, as well as in the other comparisons. One difference can be highlighted: below 15 m/s the wind speed deviation is lower than in the other comparisons. This can be explained as the met-mast is deployed 15 km offshore, where the influence of coastal topography is lower.

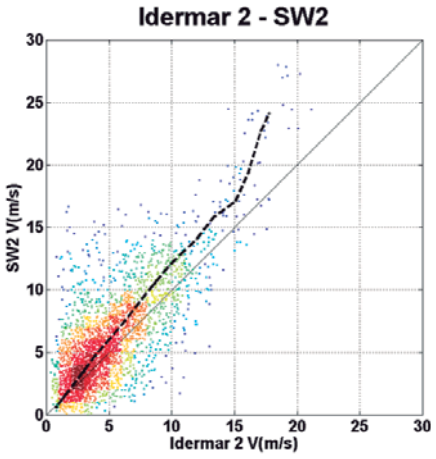

Figure 4.27: Scatter of Idermar II and SeaWind

Idermar III met-mast can be compared to Idermar I and Virgen del Mar buoy (4.28). It can be seen in the first case that measurements have low deviations and the QQ line has a good performance. However, Idermar III and Virgen del Mar

buoy scatter has the same behavior as Idermar I and Virgen del Mar buoy as can be seen in figure 4.26.

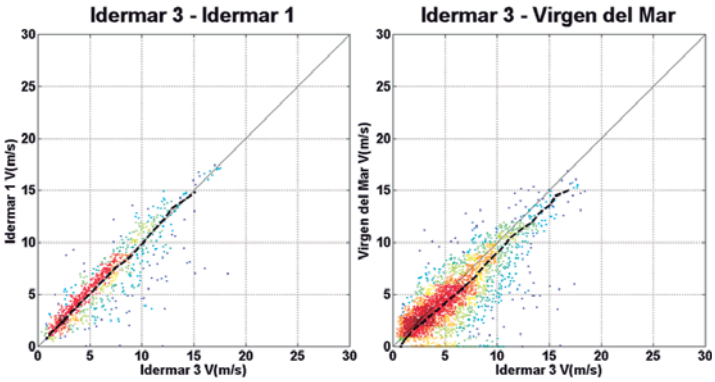

Figure 4.28: Scatter of Idermar 3, Idermar 1 and Virgen del Mar buoy.

4.3.3.3 Comparison of time series - Wind intensity roses

The validation process not only includes the comparison of wind velocity but also wind direction. Taking into account the different length of records, the common periods are chosen to be compared. The principal directions (4.29) are West and East appearing in both wind intensity roses, Idermar Meteo I and SeaWind. Southerly winds, related to 200° also appear at both databases.

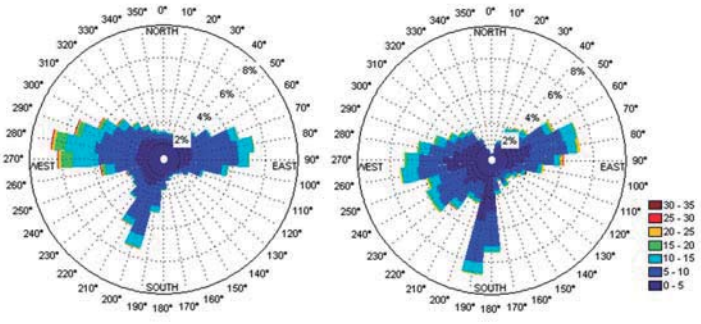

Figure 4.29: Wind intensity roses from (right) Idermar Meteo I and (left) SeaWind

The floating meteorological mast Idermar Meteo III and SeaWind reanalysis database provide similarities in both intensity maxima and principal directions (figure 4.30). Southerly winds do not seem to follow a similar correlation as well as in the comparison with Idermar Meteo I.

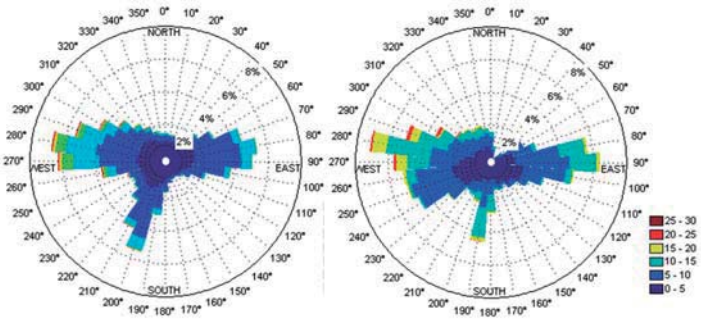

Figure 4.30: Wind intensity roses from (right) Idermar Meteo III and (left) SeaWind

In the further offshore location, where Idermar Meteo II is located, the southerly winds disappear from the wind rose (4.31). This fact may be due to the influence of the European Peaks, that creates a shadow decreasing the southerly wind speed.

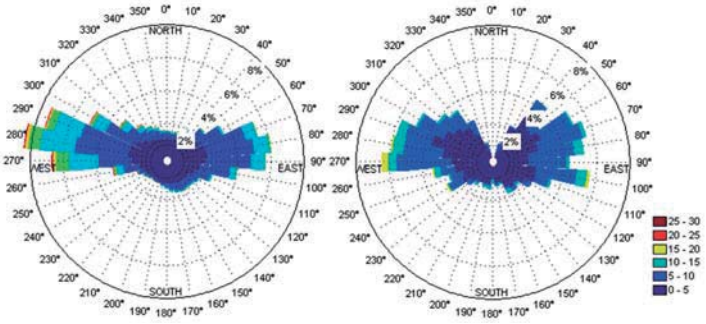

Figure 4.31: Wind intensity roses from (right) Idermar Meteo II and (left) SeaWind

As it can be seen, the numerical databases simulate correctly the characteristics of wind conditions in terms of mean wind speed and behavior. Consequently, the reanalysis databases can be used to analyze the wind conditions, the influence of coastal topography and the time and spatial variability.

4.3.4 **Wind conditions spatial variability - Influence of Coastal Topography**

In section 4.3.1, the area of study was described. The topographical structure of Cantabria is characterized by a succession of valleys and ranges, perpendicular to the coast. Wind converges and diverges due to this structure, with areas of high and low speeds. Consequently, southerly winds are directly affected by coastal topography. Therefore, the first step is understanding the wind field pattern due to southerly wind events. For this purpose, this section is focused on the analysis of the influence of coastal topography on three different issues:

- Wind profile
- Wind power

- Capacity factor

4.3.4.1 **Wind profile**

The wind profile is analyzed at several locations along the coast, corresponding to those locations where instrumental data are available. The analysis of some parameters of the wind profile theoretical expressions allows emphasizing the influence of coastal topography. For instance, the alpha parameter of the potential wind profile (expression 4.17).

$$\frac{U(z_1)}{U(z_2)} = (\frac{z_1}{z_2})^{\alpha} \tag{4.17}$$

where $U(z_1)$ and $U(z_2)$ are the wind speed at heights z_1 and z_2, respectively; and α is an exponent between 0.1 and 0.14 (for offshore conditions) summarizing all the atmospheric effects. Normally, z_2 is known as z_0 or z_{ref}, which is the reference height, assumed to be 10 meters.

In Virgen del Mar, SeaWind 2 (which has information to rebuild the wind profile) the α-parameter follows the pattern shown in figure 4.32. It is noticed that when α increases wind speed increases with height more rapidly. α is higher for southerly winds, which means that the influence of coastal topography is important and is contributing to decrease wind speed in the first meters of the air column.

A potential wind profile is fitted to SeaWind 2 data also at Ubiarco, where Idermar Meteo II met-mast is located. In figure 4.33 the α-parameter rose is shown. This location is about 16 km offshore. In this case, the α-parameter reaches the maximum values when wind comes from South-West, which is related to the influence of European Peaks.

Instrumental data from Idermar Meteo III and Idermar Meteo II are also used to obtain the α-parameter rose. In figure 4.34, the Idermar Meteo II α-parameter is shown. It can be seen that southerly winds, as well as more energetic directions (storms from North-East and North-West) are reaching the highest values. It could

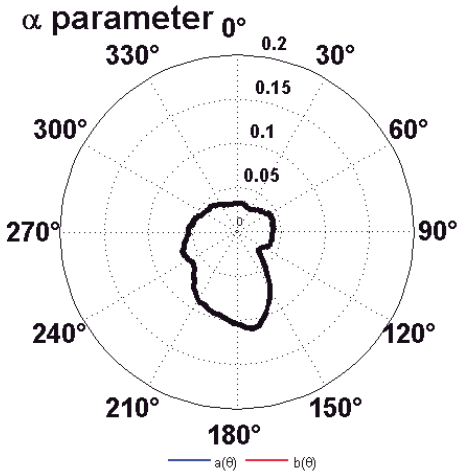

Figure 4.32: α-parameter from SeaWind 2 at Virgen del Mar

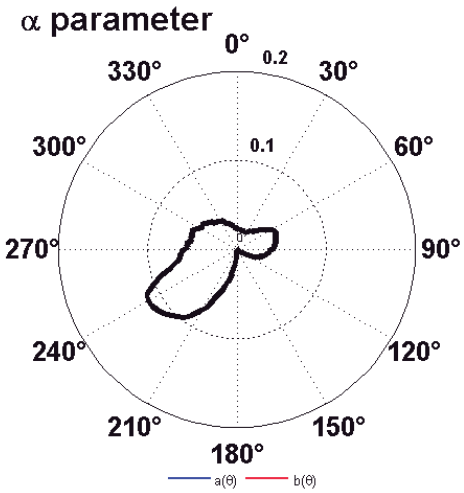

Figure 4.33: α-parameter from SeaWind 2 at Ubiarco

be related to the wind speed which is commonly higher from these directions.

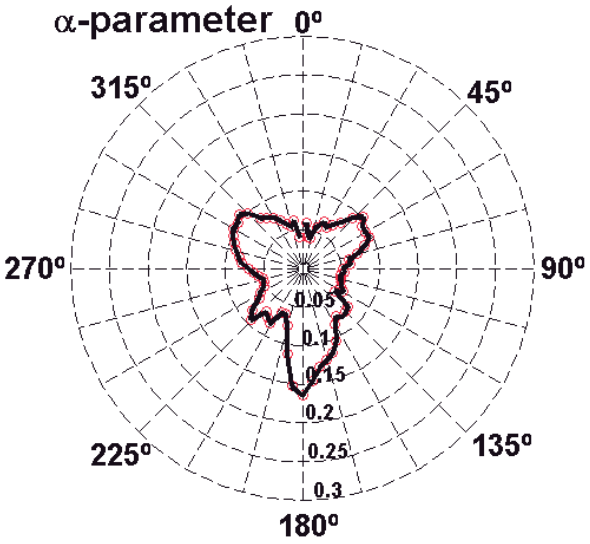

Figure 4.34: α-parameter from Idermar Meteo II at Ubiarco

In figure 4.35 the α rose for Idermar Meteo III met-mast is shown. In this case, the lack of data explains the shape of the rose (lack of storms from North-East and North-West directions). The impact of coastal topography can be seen due to the tail which corresponds to southerly winds.

The logarithmic wind profile (eq. 4.18) expression introduces the roughness length parameter which is directly related to the type of terrain that wind flow crosses over.

$$\frac{U}{u_*} = (\frac{1}{k})log(\frac{z}{z_0}) \tag{4.18}$$

where the parameter z_0 represents the surface roughness and u_* the friction velocity.

At Ubiarco, SeaWind 2 and Idermar Meteo II data are used to fit the logarithmic profile. As the objective of this section is to analyzing coastal topography influence, attention is paid to surface roughness. In figure 4.36, the surface rough-

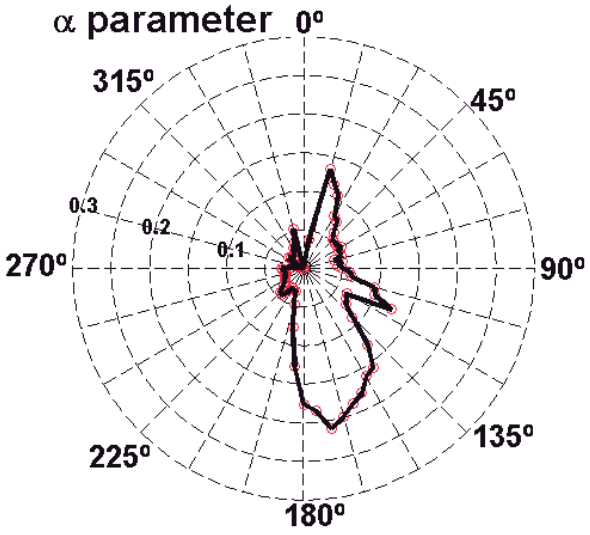

Figure 4.35: α parameter from Idermar Meteo III at Virgen del Mar

ness obtained from Idermar Meteo II is shown, whereas in figure 4.37, surface roughness from SeaWind 2 is shown.

It can be noticed in figure 4.36 that surface roughness is high when wind flows from onshore. Moreover, it is high in the directions related to storms. This may be seen as a consequence of high wave height sea states which influence the low part of the air column.

In the case of SeaWind 2 (figure 4.37) the influence of coastal topography can be noticed at 280° (approximately the European Peaks direction).

The Idermar Meteo III and SeaWind 2 data is fitted to the logarithmic profile at La Virgen del Mar. In figure 4.38 the Idermar Meteo III roughness length is shown. In this case, the lack of data only allows detecting one high peak in the graph. This peak is related to southerly winds, directly affected by coastal topography.

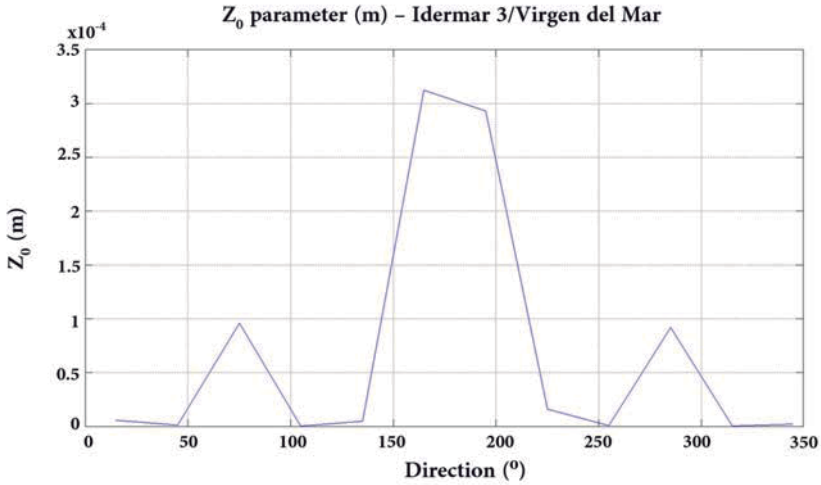

Figure 4.36: z_0 parameter from Idermar Meteo II at Ubiarco

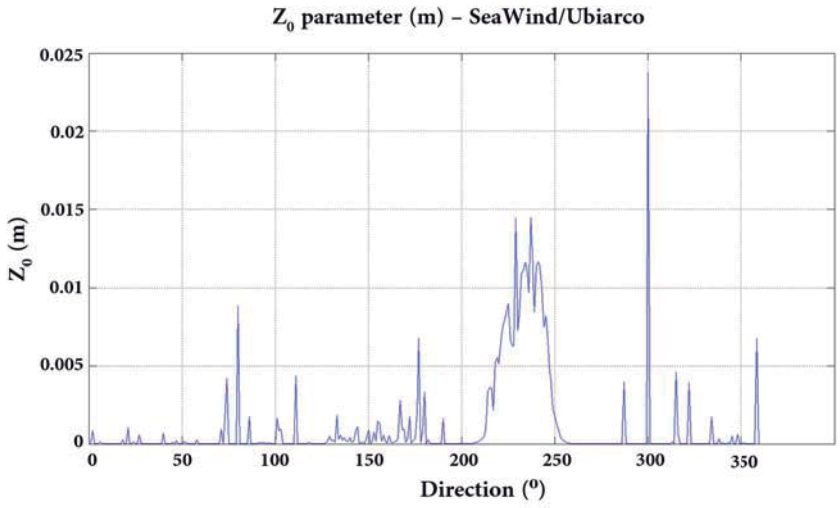

Figure 4.37: z_0 parameter from SeaWind 2 at Ubiarco

In figure 4.39 the roughness length of SeaWind 2 data at La Virgen del Mar is

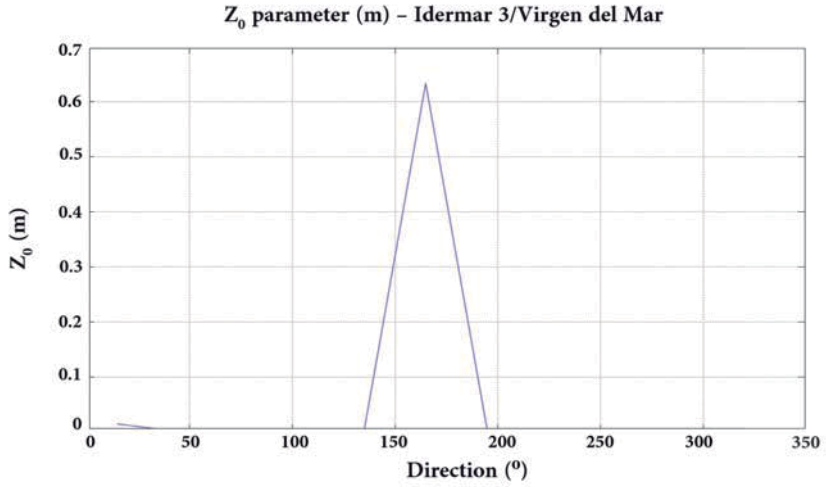

Figure 4.38: z_0 parameter from Idermar Meteo III at Virgen del Mar

shown. In this case, the sector where roughness length is higher corresponds also to southerly winds. As more data is available, some other peaks appear.

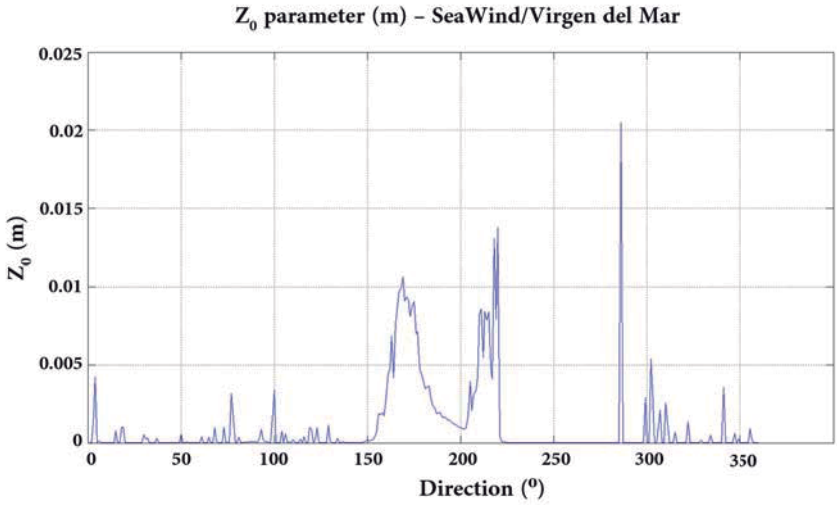

Figure 4.39: z_0 parameter from SeaWind 2 at Virgen del Mar

4.3.4.2 Wind power

On the upper panel of figure 4.40 the mean wind energy potential for southerly winds is shown. On the lower panel of the same figure, the mean wind energy potential is also shown but considering the full set of wind data. The power scale is completely different in both figures because southern winds in this area are associated to higher speeds. It can be noticed how at the west part of the area of study wind energy potential is lower than 100 w/m^2. However, at the eastern part of the region, due to a mild coastal topography, higher rates of wind power are found. In some cases, more than twice the power of western locations at the same distance from the shore.

4.3.4.3 Capacity factor

The influence of coastal topography on wind turbine performance can be noticed. It has been previously described that wind conditions along the coast are different and some areas are more affected than others. Figure 4.41 shows the five wind turbine power curves considered. The annual energy produced was calculated for

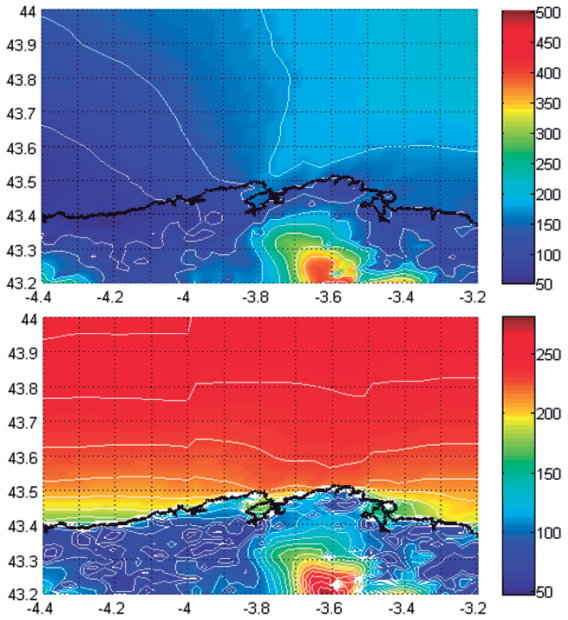

Figure 4.40: Southerly wind mean energy potential in W/m2 (above) and Mean wind energy potential in W/m2 (beyond)

all of them in five points in order to compare results of the capacity factor (Table 4.4). These five points are located along the North coast of Spain (4.42).

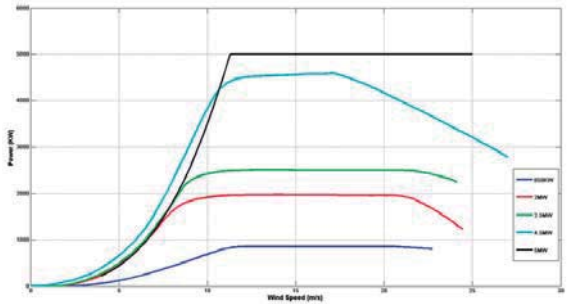

Figure 4.41: Power curves selected.

The wind energy potential of the selected nodes presents a high variability

(point 1: 402.3 w/m^2; point 2: 279.5 w/m^2 ; point 3: 201.7 w/m^2 ; point 4: 222.6 w/m^2 ; point 5: 193.1 w/m^2).

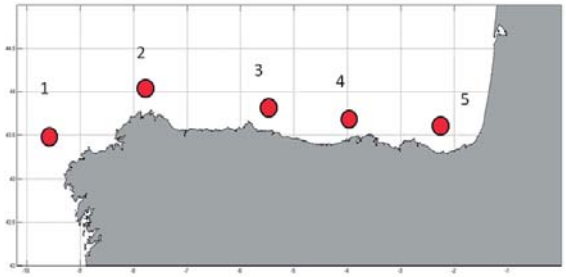

Figure 4.42: Location of points to evaluate capacity factor

In order to achieve high rates of economic efficiency, the power curve has to reach its maximum as soon as possible. Therefore, depending on wind velocity and installed capacity, the capacity factor may vary. From Table 4.4 the largest capacity factor has been obtained with a 2 MW wind turbine at every site. As it can be seen in figure 11, its maximum is almost reached at 8 m/s, while 5 MW turbine reaches its maximum at 11 m/s. Moreover, lower wind speed increases the capacity factor of turbines with lower installed capacity, because they reach their rated power production more frequency than turbines with larger capacity.

CF	Point 1	Point 2	Point 3	Point 4	Point 5
5 MW	0.41	0.31	0.22	0.24	0.22
4,5 MW	0.48	0.38	0.28	0.29	0.28
2,5 MW	0.56	0.46	0.34	0.35	0.35
2 MW	0.58	0.48	0.36	0.37	0.37
850 KW	0.47	0.38	0.27	0.29	0.28

Table 4.4: Capacity factor

The most energetic node (point 1) is also the node where wind turbines reach their maximum capacity factors. The lowest capacity factors are reached at point

3. This node is the most affected by coastal topography. It is located in Asturias, where the Cantabrian range is wider and higher, increasing its capacity to affect the wind flow.

4.3.5 Wind conditions time variability

Synoptic patterns or weather types are proposed as an atmospheric classification to determine the specific weight of winds coming from earth. In order to obtain a correct classification the following methodology has been applied:

1. Thirty years (from 1980 to 2009) of wind fields, defined by the u and v components with a time resolution of three hours and a spatial resolution of 7 km, are selected for the regional scale analysis.

2. In order to be able to work with this amount of data a method to reduce its dimension is applied. It is known as PCA (principal components analysis) and it reduces the database by selecting the PC's (principal components) that explain 95% of the variability of data. In this case, 5 PC's are selected.

3. The K-means technique is applied next. This technique consists of finding the most representative case of a group as mean of that group. To start this iterative method the cases selected by the application of Max-Diss are used.

4. Results are shown in a figure were the similitude between cases is taken into account.

5. Different number of weather types was studied and 25 was considered the best option to summarize the information.

Southerly winds, which come from onshore in this area, are represented by the panels at the top right part of figure 4.43. The strong influence of coastal topography on wind flowing patterns can be observed. In the cases with the highest wind intensity, which are at the first row and the three columns from the right in the figure 4.43, it can be seen that the highest values of wind speed are found on the top of the mountains.

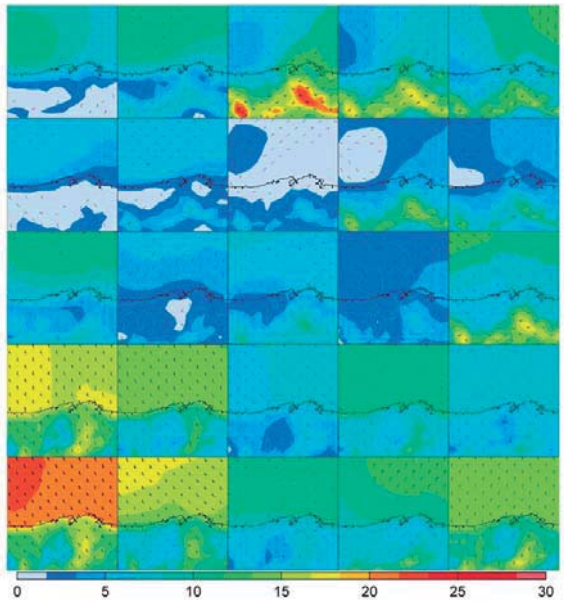

Figure 4.43: The 25 most probable synoptic patterns.

Moreover, at the west of Santander a large shadow area caused by the European Peaks is to be seen and, in some cases, this shadow extends over some kilometers far offshore (figure 4.44).

The most relevant weather types show that, in addition to the shadow created by the European Peaks, a more powerful zone can be found between the Santander Bay and the Santoña Bay, which means that the influence of coastal topography is lower and, consequently, wind speed is higher. This is due to the confluence of winds caused by the topography of the region. The probability of each weather type is shown in figure 4.45.

It can be observed that the most probable wind weather types are spread across the four principal quadrants, however the fourth quadrant has more weight. The weather types occurrence probability by seasons is shown in figure 4.46. A very different seasonal behavior is found, with two main patterns: i) Autumn and

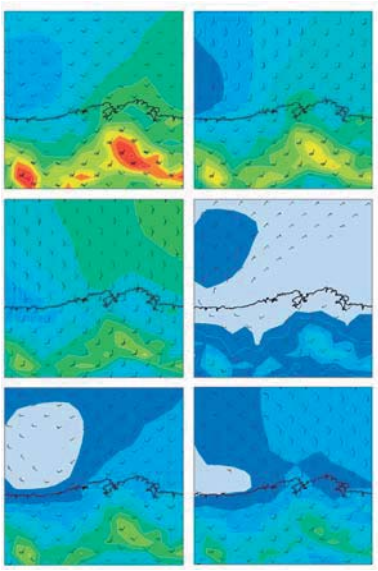

Figure 4.44: Most relevant situations for southerly winds.

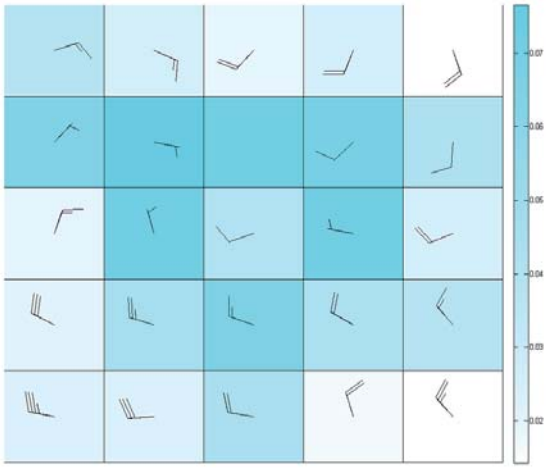

Figure 4.45: Occurrence probability, wind direction and wind speed of the principal 25 synoptic patterns.

Winter and ii) Spring and Summer. In Autumn and Winter wind from South-

West have the highest probability of occurrence, followed by North-West winds, both related to the extreme storms in this area. In Spring and Summer the direction variability is higher, although, North-East and Southerly winds are common.

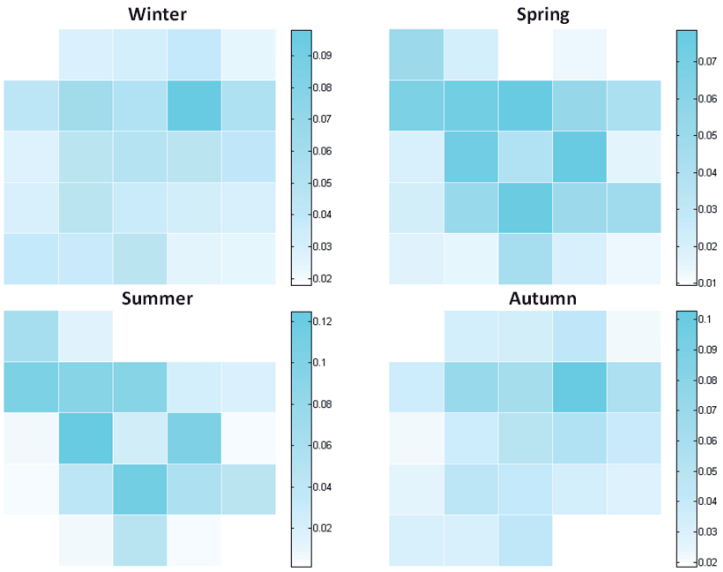

Figure 4.46: Seasonal occurrence probability of the synoptic patterns.

It is important to analyze the temporal variability associated with wind conditions. In order to show the variability in a simple way, four locations are selected (figure 4.47) spread along the coast of the area of interest. In this case, as local comparison is carried out, 60 years are used (from 1948 to 2009).

The behavior of the mean wind energy power is shown in figure 4.48. It shows a high inter-annual variability with peaks of mean power greater than $600 w/m^2$ and minima around $350 w/m^2$. Furthermore, it can be noticed that the spatial variability along the coast is not relevant because the mean wind power time series is similar in the four locations. The largest difference is in 2002 achieving an 18%. The difference is lower than 10% in the rest of the time series.

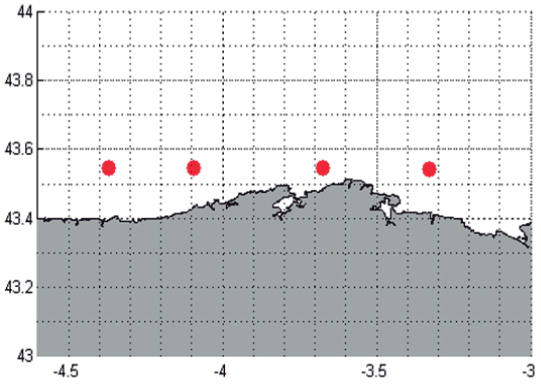

Figure 4.47: Selected points.

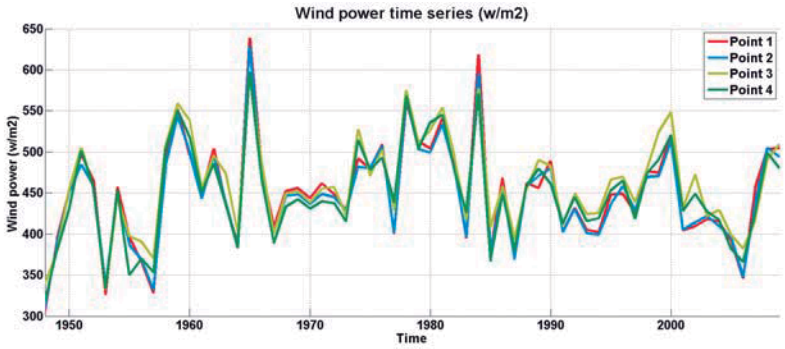

Figure 4.48: Mean wind power time series at the selected points.

The behavior of wind power along the year is analyzed by using the monthly mean wind energy (figure 4.49). In this figure, the monthly means over 60 years is printed. Large differences between summer and winter months can be observed. In fact, the mean wind power in winter is twice the amount in summer.

The seasonal behavior analysis is done by representing in figure 4.50 the histograms for each season. It is confirmed that the wind power behavior is similar in autumn and winter with a higher probability of occurrence at the right tail of the distribution, which means higher wind velocities. In the case of spring and

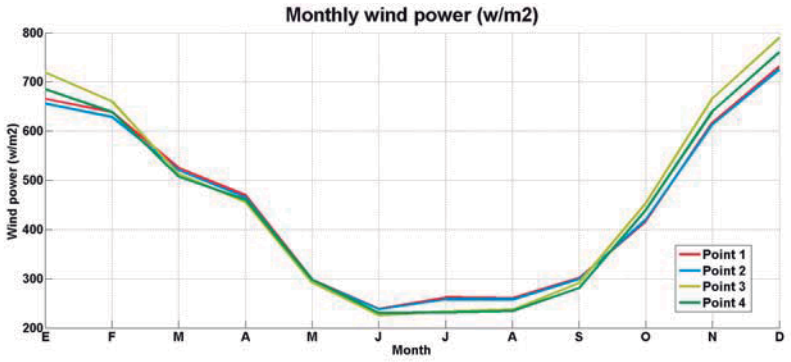

Figure 4.49: Monthly mean wind power time series at the selected points.

summer the left tail, related to low wind speeds, increases its probability of occurrence. The histograms for the autumn and winter are almost overlapped. Summer has a peak at the left tail of the distribution that is not found in spring.

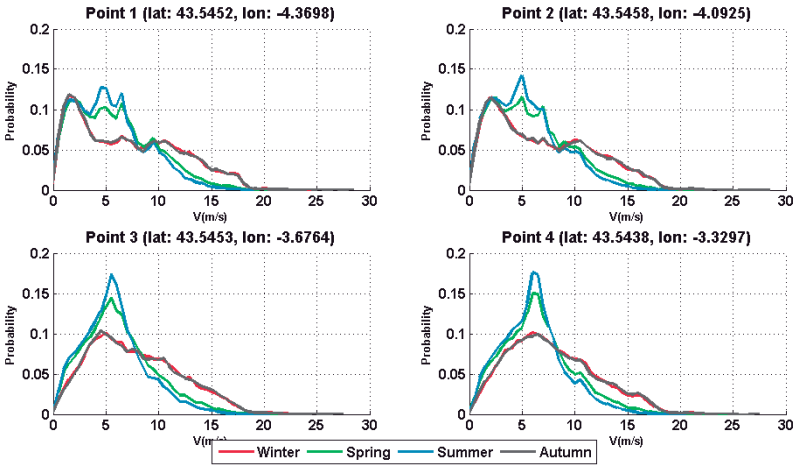

Figure 4.50: Seasonal PDF for the selected points.

Points 3 and 4 present a quite similar behavior, whereas in point 1, which is located in the shadow of European Peaks, the lower wind speed probability is higher when southerly winds flow. This behavior can be also noticed in point 2

but mitigated.

The analysis of these four points show differences on offshore wind behavior. To the West of the area, the wind variability is higher due to the influence of coastal topography, whereas, at the East the influence is lower and wind speed achieves higher values with higher occurrence probability.

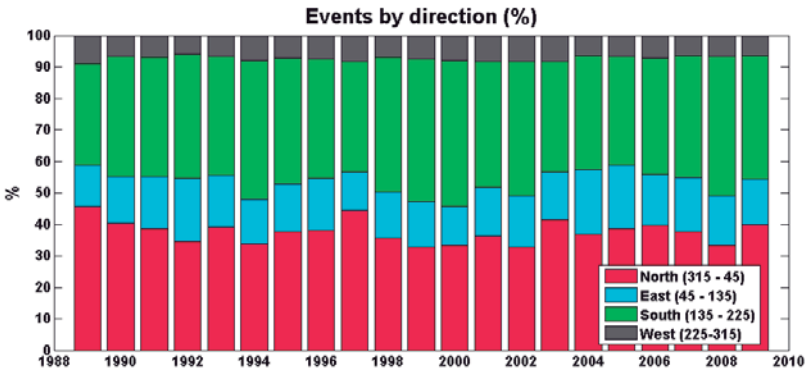

Figure 4.51: Percentage of occurrence for each quadrant: (red) North, (blue) East, (green) South and (Grey) West.

In figure 4.51, the distribution of wind direction by sectors for thirty years of data is shown (the time series corresponding to the regional scale analysis). Its behavior is quite homogeneous along the 30 years considered. For instance, winds from the west never reach the 10% of occurrence. Large storms in this area come from this direction. The most probable winds are, during the whole time series, the Northerly and Southerly winds, for almost 75% of the time.

4.4 Conclusions

In this last section of the chapter, the main conclusions are presented.

- The analysis carried out in the first part of the chapter related to the potential long-term error of floating met-mast measurements concludes that the

floating technology considered introduces low deviations. Moreover, in the common operational range of wind turbines the maximum error expected is around 0.5%.

- Wind resource assessment may require different sources of data. The best option is to combine numerical and instrumental data from reanalysis databases and field measurements, respectively. The numerical data can contribute to the long-term analysis due to the length of the time series. Field measurements are commonly short time series. However, they are characterized by high quality data, including extreme data which is the kind of data that is worst simulated by numerical models. Extremes are required to determine design parameters. Because of that, it is recommended to always count of instrumental data.

- The influence of coastal topography is to be crucial for wind understanding behavior. In the case analyzed, the Cantabrian range influences wind behavior even far offshore. Furthermore, southerly winds can affect over more than 80 km offshore. The coastal topography influence is observed on both the spatial variability of wind conditions and the wind profile at specific sites.

- The methodology applied to analyze the spatial variability of wind conditions (based on synoptical situations) contributes improving wind conditions assessment. The data mining approach by highlighting only the most important features clarifies the final result and reduces the amount of data processed.

CHAPTER

5

Floating Platform Performance Assessment

In the review of the state of the art a gap was detected in relation to the methods proposed to estimate extreme and severe conditions. In this chapter, an update of these methods is proposed in order to improve the characterization of load cases for floating platform performance assessment. The structure of the chapter is:

- Introduction
- New extreme model for load cases definition
- Offshore wind floating platform performance: spatial variability
- Mixed extreme model and IFORM method
- Conclusions

5.1 Introduction

5.1.1 Motivation

Floating platform performance assessment is already treated by design standards and guidelines. These reference documents were, in the beginning, adaptations of standards and guidelines from other fields. In the case of floating offshore wind, the majority of knowledge comes from oil and gas. Because of that, there is a chance to implement new methods to improve the quality of floating platform performance assessment.

In the case of design load cases, in the state of the art, two methods to estimate the design parameters for floating platforms were highlighted to be subject to potential of improvement: IFORM and MEV. In the first case, the guidelines propose a methodology to determine the 50-year return level of H_S and V pairs. It was noticed in Mínguez *et al.* (2014) that extreme distributions improves the final results. In this thesis, this improved method is applied to the met-ocean variables used in the design of floating platforms. In the second case, a mixed extreme value method to combine instrumental and reanalysis data to improve the estimation of occurrence periods is proposed. This method has been developed considering that offshore locations are not commonly monitored and instrumental time series are not long enough for long-term conditions estimation.

5.1.2 Scope of the chapter

In this chapter, two main objectives are proposed:

- Compare the updated IFORM method and the IFORM method proposed by the standards.
- Updating extreme methods to deep and very deep waters.

5.1.3 Chapter structure

In the first section, the updated IFORM method is applied to met-ocean conditions and evaluated at some locations in the North of Spain. In the second section, the

updated mixed extreme value model is presented and applied to evaluate the impact of met-ocean conditions variability. Finally, some conclusions are presented.

5.2 Updated IFORM Method Analysis

In the state of the art, some discrepancies to calculate the 50-yr return level load parameters related to the IFORM method proposed in DNV-RP-C205 have been outlined. Therefore, in this section the differences between results of the application of the IFORM method from the guideline and the updated IFORM method proposed in Mínguez *et al.* (2014) are analyzed at four locations. The locations selected are shown in table 5.1.

The IFORM method is applied at four locations (Estaca de Bares, Cabo de Peñas, Virgen del Mar and Bilbao, see table 5.1) along the Cantabrian Sea in order to analyze the application of the model to several sea states (Figure 5.1).

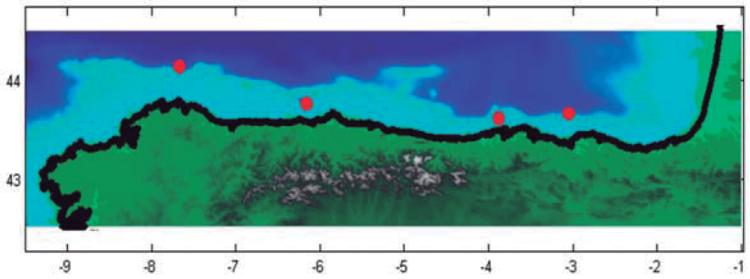

Figure 5.1: Locations selected for the application of RMEV model.

The locations are named with the same name given by administration in charge (Table 5.1).

Time periods available for the application of this method are shown in table 5.2 for the locations chosen.

Furthermore, time series of significant wave height are also shown in order to allow detecting the blanks in the instrumental data (Figure 5.2). In red dots, instrumental data is shown; and in black line reanalysis data is shown.

Buoy-Location	Latitude(°)	Longitude(°)
Estaca de Bares	44.13	-7.67
Cabo de Peñas	43.75	-6.16
Virgen del Mar	43.49	-3.88
Bilbao	43.65	-3.05

Table 5.1: Coordinates of the locations where RMEV model is applied.

Buoy-Location	Initial Date (dd/mm/yyyy)	Final Date (dd/mm/yyyy)
Estaca de Bares	19/07/1990	13/04/2014
Cabo de Peñas	09/06/1997	13/04/2014
Virgen del Mar	13/02/2012	03/12/2014
Bilbao	07/11/1990	13/04/2014

Table 5.2: Time periods of instrumental data available.

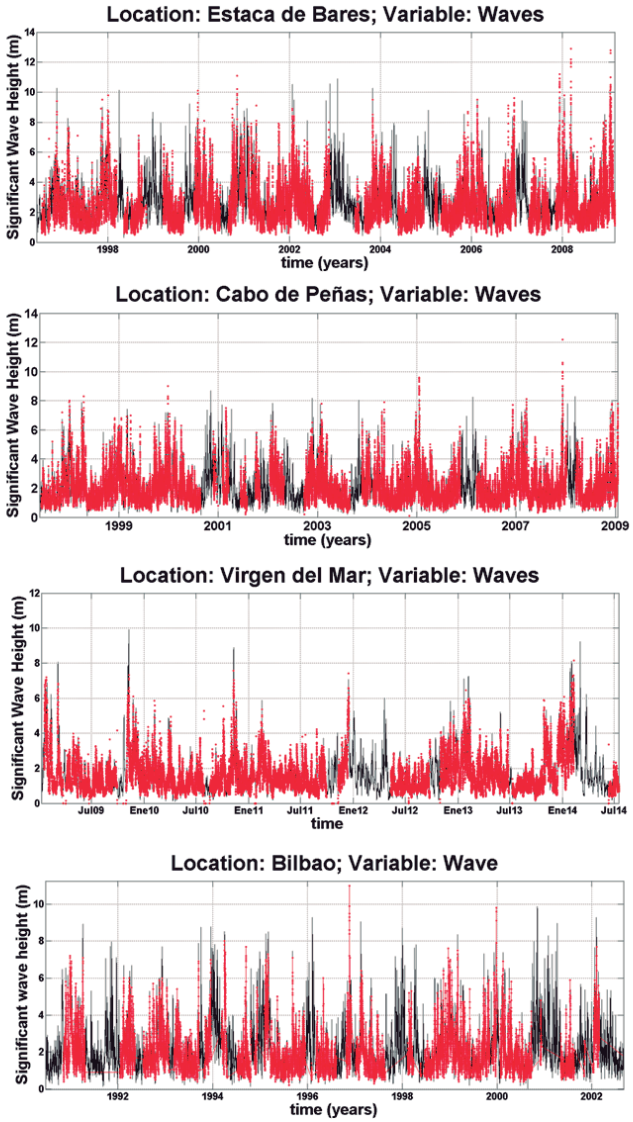

Figure 5.2: Wave height time series at the four locations selected.

In figure 5.3 and 5.4, the results for Estaca de Bares are presented. As it can be seen in figure 5.3, the mid part of the sea states ($5 \leq V \leq 20$) are not correctly fitted resulting in 50-yr return level sea states out of the reality of the case. Besides, the application of the corrected method (figure 5.4) explains more precisely

the behavior of the met-ocean extreme conditions in this locations. Therefore, the strategy followed in Mínguez *et al.* (2014), paying attention to the right tail of the distribution by using Pareto distribution, improves the sea state return level estimation.

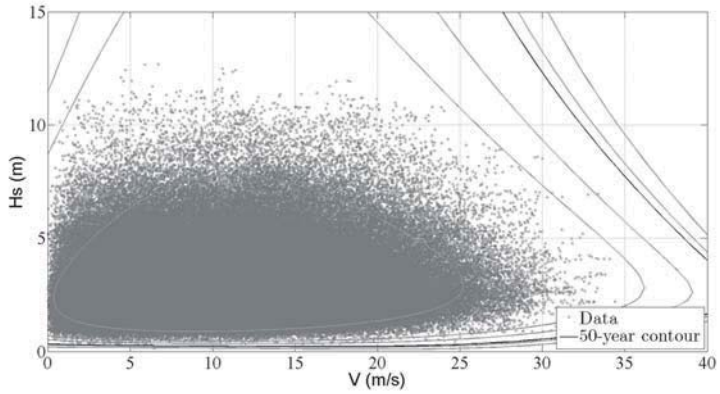

Figure 5.3: IFORM application - occurrence level at Estaca de Bares.

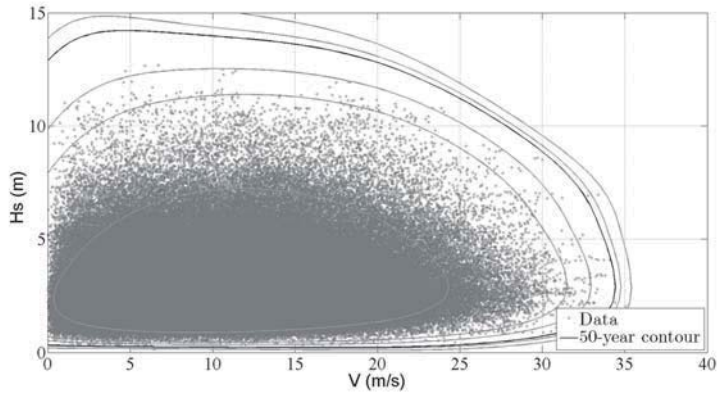

Figure 5.4: Updated IFORM application - occurrence level at Estaca de Bares.

In the case of Bilbao, the behavior of the 50-yr return level fitted by the IFORM non-updated method (figure 5.5) is not explaining correctly the low and

high tails of the distribution ($V \leq 20$ and $V \geq 25$). In figure 5.6, the curves related to the return levels are better fitted and their shape follows a more realistic behavior.

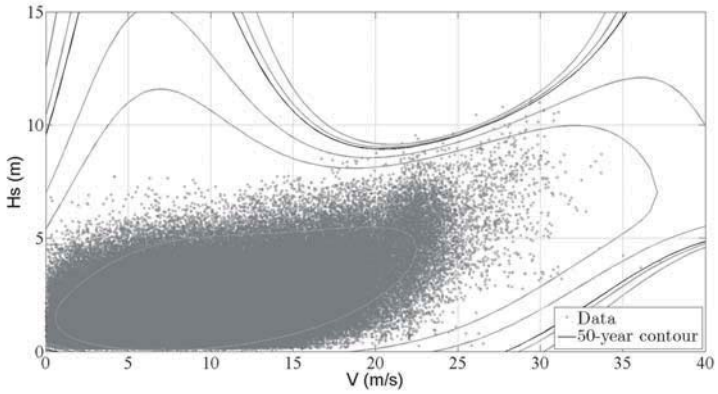

Figure 5.5: IFORM application - occurrence level at Bilbao.

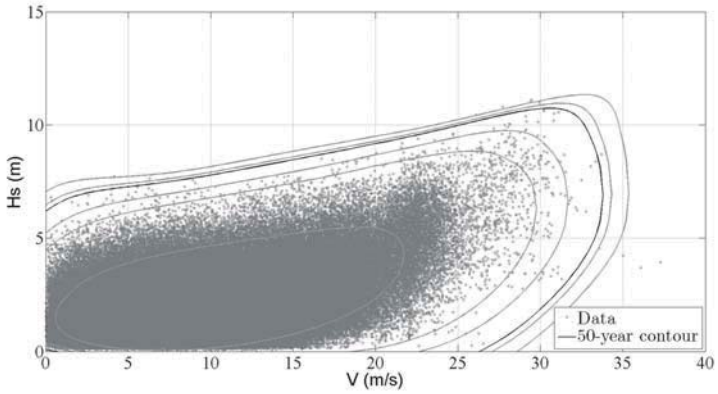

Figure 5.6: Corrected IFORM application - occurrence level at Estaca de Bares.

The third location evaluated is Cabo de Peñas. The results at this location are similar to the ones from Bilbao. It can be noticed in figure 5.7 how the low and high part of the distribution are not well simulated ($V \leq 20$ and $V \geq 30$). In

figure 5.8, the occurrence level curves are better fitted to reanalysis sea states.

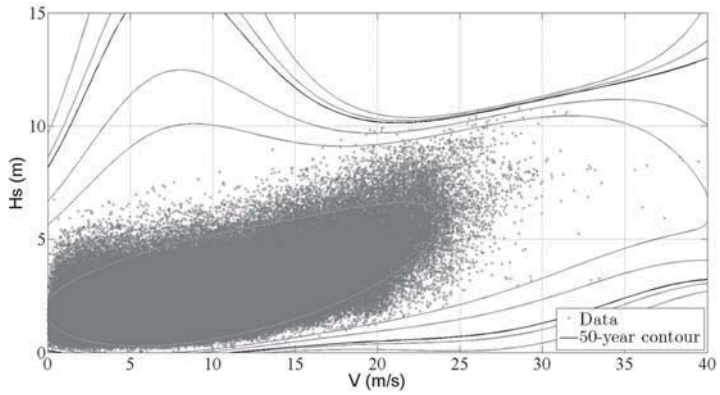

Figure 5.7: IFORM application - occurrence level at Cabo de Peñas.

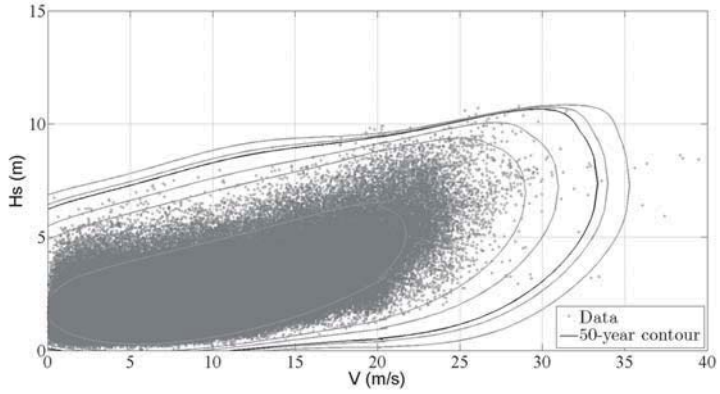

Figure 5.8: Corrected IFORM application - occurrence level at Cabo de Peñas.

The last case is located at La Virgen del Mar. As it can be seen in figure 5.9, in this case the right tail of the sea states is wider, which means that the sea states related to high wind speeds have a great range of significant wave height. The low part of the distribution is not well fitted as well. However, in figure 5.10 the shape of the 50-year return level curve fits better to data.

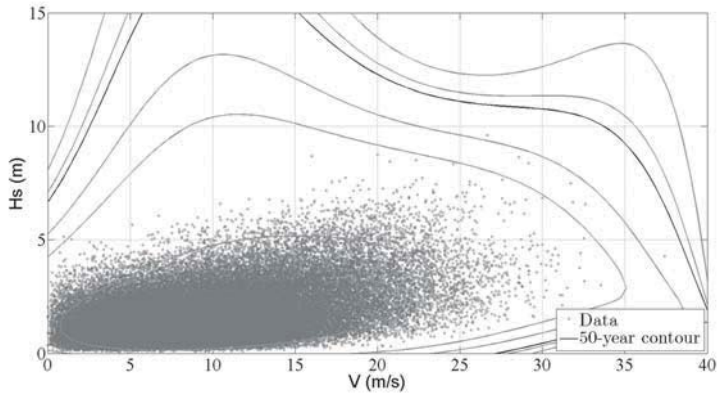

Figure 5.9: IFORM application - occurrence level at Virgen del Mar.

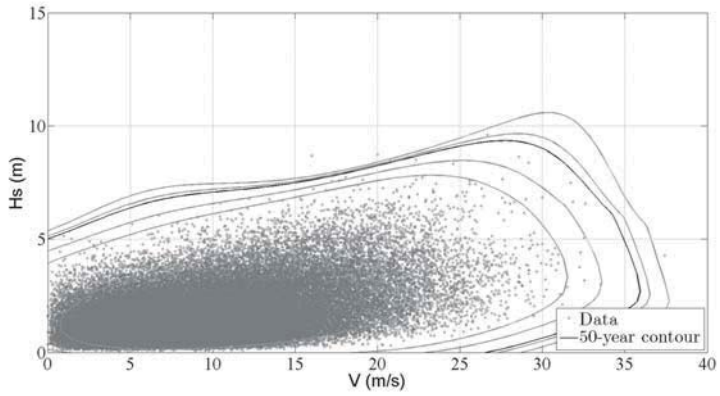

Figure 5.10: Corrected IFORM application - occurrence level at Virgen del Mar.

5.2.1 Spatial variability of 50-yr return level sea states

As it has been seen in the previous section, IFORM method application results in return level curves for specific numbers of years. In this section, only the 50-yr return level curve is considered.

Firstly, in figures 5.11 and 5.12, the significant wave height related to the more energetic sea state in the 50-year return level curve for the original IFORM method and the updated IFORM method, respectively, are shown.

In figure 5.11, it is noted that the highest values are reached offshore the coast of Asturias and Cantabria with peak values around 13 meters near Santander.

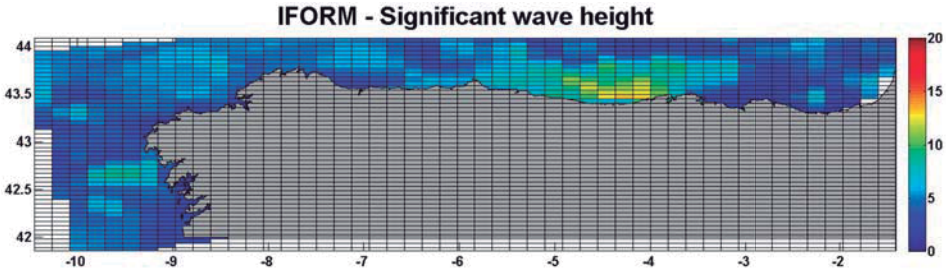

Figure 5.11: IFORM significant wave height 3^{rd} criteria.

In figure 5.12, the corrected IFORM results are shown. In this case, the area with higher values in figure 5.11 reaches lower values with accordance to the observations.

The wind speed related to the same sea state is shown in figures 5.13 and 5.14. In figure 5.13, the wind speed related to the IFORM method is shown and the same pattern highlighted for significant wave height can be seen in wind speed behavior. The area close to the coast between Gijón and Santander is characterized by wind speeds higher than 60 m/s, which is too high and far away of observations. However, the rest of the region, mainly in the area of Galicia, seems to follow a realistic pattern.

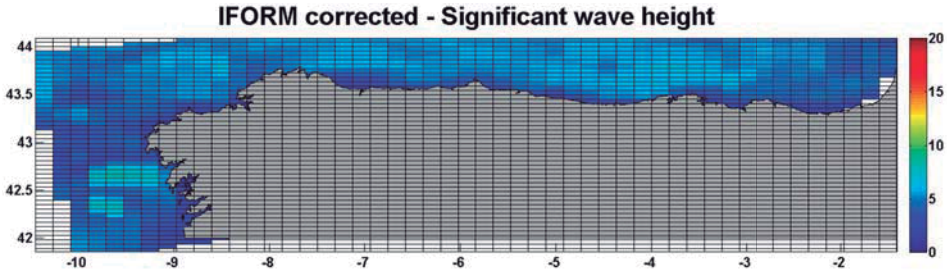

Figure 5.12: Corrected IFORM significant wave height 3^{rd} criteria.

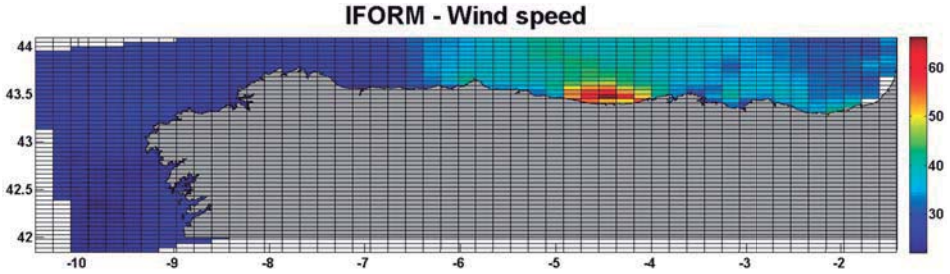

Figure 5.13: IFORM wind speed 3^{rd} criteria.

In figure 5.14, the corrected IFORM method results are shown. In this case, the range of values is not as wide as it was for classic IFORM. The wind speed behavior, in this case, is in accordance with the analysis of wind resource presented in chapter 4. Therefore, the maximum value is around 28 m/s and it is reached offshore Galicia. Moreover, the center part of the North coast of Spain reaches higher values due to the confluence of wind flux caused by the influence of the European peaks. Lower values are reached close to the coast line and in the Basque Country.

The wind speed related to the 50-yr return level sea state described by the maximum wind speed from IFORM is shown in figure 5.15. It can be seen that the same pattern where the maximum values are reached between Asturias and Cantabria, is occurring.

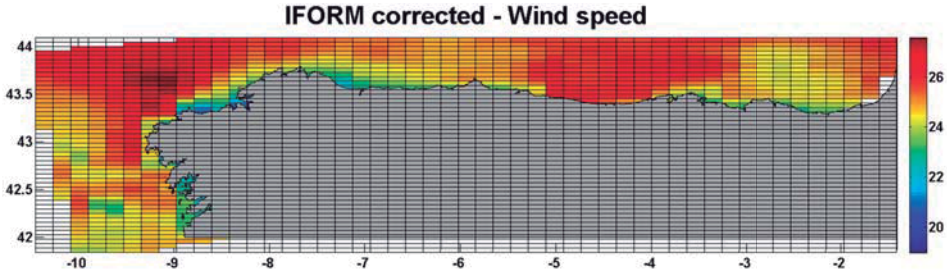

Figure 5.14: Corrected IFORM wind speed 3^{rd} criteria.

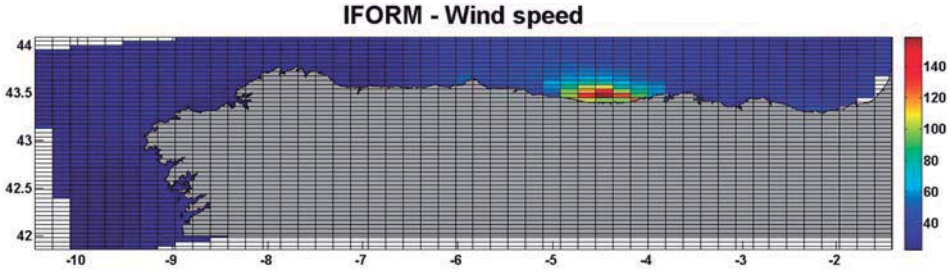

Figure 5.15: IFORM wind speed 1^{rd} criteria.

In the case of the corrected IFORM (figure 5.16), the wind speed related to the 50-yr return level sea state with maximum wind speed follows a similar pattern than the mean wind speed. The highest values are located offshore Galicia, North-West of the studied area. A second area with high values is found in the North, between Asturias and Cantabria.

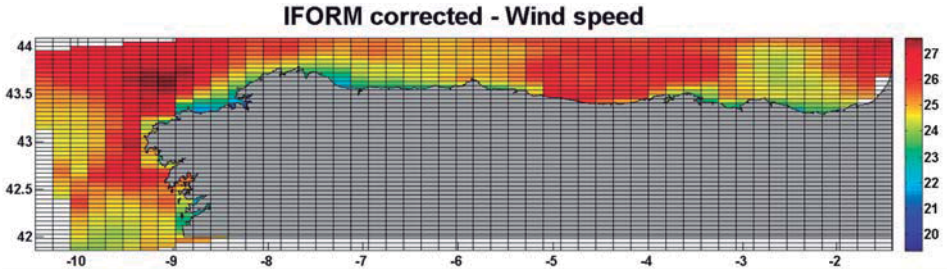

Figure 5.16: Corrected IFORM wind speed 1^{rd} criteria.

5.3 Mixed Extreme Value Model

The mixed extreme value (MEV) model developed by Mínguez *et al.* (2013b) has proven to be an appropriate tool for dealing with wave maxima because it takes full advantage of both i) reanalysis and ii) instrumental measurements. However, this model only uses information about annual maxima.

The MEV model proposed in Mínguez *et al.* (2013b) relies on the following assumptions:

1. The annual maximum reanalysis random variable X follows a distribution with probability density and cumulative distribution functions $f_X(x, \theta_X)$ and $F_X(x, \theta_X)$, respectively. The distribution functions may correspond to any kind of distribution for maxima, such as, GEV, Pareto-Poisson, Peaks-over-threshold (POT), Gumbel, among others, but the final distribution is always expressed in terms of the annual maximum.

2. The random variable Y corresponding the difference between instrumental and reanalysis data conditioned to the annual reanalysis maximum data (X) follows a normal distribution, i.e. $f_{Y|X}(y)\ N(\mu_{Y|X}, \theta^2_{Y|X})$. Note that $\mu_{Y|X}$ and $\theta_{Y|X}$ correspond to the conditional mean and standard deviation parameters, which ca be obtained using an heterocedastic regression model.

According to these assumptions, the MEV extreme value model can only use annual maxima information to characterize the difference between instrumental

and reanalysis data, and in the case of working with Peak Over Threshold methods, this constraint does not allow to use all differences available between reanalysis storm peaks and their corresponding instrumental records. Alternatively, the Revisited Mixed Extreme Value (RMEV) model is based on the following alternative assumptions:

1. The number of independent storm peaks N exceeding a given threshold u in any one year follows a Poisson distribution with parameter λ.

2. The random variable X associated with independent reanalysis storm peaks follows a distribution with probability density and cumulative functions $f_X(x, \theta_X)$ and $F_X(x, \theta_X)$, respectively. According to Davidson and Smith (1990) this distribution function may correspond to Pareto. This distribution is used in this thesis, however the fapplication of the proposed method is not limited to this distribution.

3. The random variable Y corresponding to the difference between instrumental and reanalysis data conditioned to the reanalysis storm peak (X) follows a normal distribution, i.e. $f_{Y|X}(y)\ N(\mu_{Y|X}, \theta^2_{Y|X})$. Note that $\mu_{Y|X}$ and $\theta_{Y|X}$ correspond to the conditional mean and standard deviation parameters, which can be obtained using an heterocedastic regression model.

The random variable related to storm peaks is equal to $Z = X + Y$, and their corresponding cumulative distribution function is equal to:

$$F_Z(z) = Prob(Z \leq z) = \int_{x+y \leq z} f_{X,Y}(x, y) dy dx \tag{5.1}$$

where $f_{X,Y}(x, y)$ is the joint probability density function of the random variables X and Y. Considering assumptions (2) and (3), expression 5.1 becomes:

$$F_Z(z) = \int_{-\infty}^{\infty} f_X(x, \theta_X) \left[\int_{-\infty}^{z-x} f_{Y|X}(y) dy \right] dx \tag{5.2}$$

and since the distribution of Y conditioned to X is assumed to be normally distributed, expression 5.2 results in:

$$F_Z(z) = \int_{-\infty}^{\infty} f_X(x, \theta_X)\phi\left[\frac{z - x - \mu_{Y|X}}{\sigma_{Y|X}}\right] dx \tag{5.3}$$

where $\phi(\cdot)$ is the cumulative distribution of the standard normal random variable.

The corresponding probability density function is obtained by deriving 5.3 with respect to z:

$$f_Z(z) = \int_{-\infty}^{\infty} f_X(x, \theta_X)\phi\left[\frac{z - x - \mu_{Y|X}}{\sigma_{Y|X}}\right] \frac{1}{\theta_{Y|X}} dx \tag{5.4}$$

where $\phi(\cdot)$ is the probability density function of the standard normal random variable. Note that the integration limits range is from u to ∞ since we are assuming the use of Pareto. However, these limits may change depending on the type of probability density function used for X.

The structure of the RMEV model is the same as the MEV, but the data used in the analysis are different. Regarding the numerical solution of the integrals in 5.3 and 5.4, the same recommendations given for the MEV method still apply, i.e., the adaptive Gauss-Konrod quadrature method (Shampine (2008)) is the most appropriate, since it supports infinite intervals and can handle moderate singularities at the endpoints.

However, the distribution function given by 5.3 and 5.4 does not correspond to annual maxima, which is usually the information required for engineering design. Considering assumptions (1)-(3), the probability of the annual maximum of the process to be lower than or equal to z is:

$$\begin{aligned} &Prob\left(max_{1\leq i\leq N} Z_i \leq z\right) = \\ &Prob(N=0) + \sum_{n=1}^{\infty} Prob(N=n) F_Z(z)^n = \\ &e^{-\lambda}\left[\sum_{n=1}^{\infty} \frac{e^{-\lambda}\lambda^n}{n!} F_Z(z)^n\right] = e^{-\lambda(1-F_Z(z))} \end{aligned} \tag{5.5}$$

Note that expression 5.5 allows calculating the annual maxima probability distribution function as a function of: i) the Poisson parameter associated with the annual occurrence of storm peaks, and ii) the storm peak magnitude distribution $F_Z(z)$. Considering the asymptotic relationship between return period (T) and annual maxima given by Beran & Nozdryn-Plotnicki (1977):

$$T = -\frac{1}{log\left(Prob\left[max_{1\leq i\leq N} Z_i \leq z\right]\right)}, \tag{5.6}$$

which improves estimates associated with returns periods lower than 10 years, and using (5.5), the following relationship is derived:

$$T = \frac{1}{\lambda(1 - F_Z(z_T))} \tag{5.7}$$

Equation 5.7 allows using the RMEV model for annual return period estimation. Conversely, quantile z_T associated with given return period T is obtained by solving the following implicit equation:

$$F_Z(z_T) = 1 - \frac{1}{\lambda T}, \tag{5.8}$$

which can be transformed into the problem of finding the root of the function $g(z_T) = 1 - \frac{1}{\lambda T} - F_Z(z_T)$. Analogously to the MEV approach, numerical tests indicate that the algorithm proposed by Forsythe *et al.* (1977), which uses a combination of bisection, secant, and inverse quadratic interpolation methods, is robust and efficient.

An important issue associated with the Poisson parameter is its estimation. Note that threshold selection is performed using reanalysis data and any of the methods proposed in the literature for this task, such as the mean residual life plot. However, instrumental data might be even below that threshold due to the discrepancies among both type of data. This fact might result in differences among Poisson parameter estimates using instrumental and reanalysis data, respectively,

which could affect the return level estimates in 5.7. Our advice is to use the estimate given by instrumental data because this data is more reliable, however, we also recommend to use the estimate given by reanalysis data for comparative purposes, especially if the instrumental record length is below 5 years.

5.3.0.1 Extreme model applied to mooring system

For the application of the extreme model the same four sites in table 5.1 are chosen. These sites are chosen because numerical and instrumental data are available and they are located at energetic areas of the Cantabrian Sea which allows seeing greater differences between RMEV application cases and direct reanalysis cases.

Currents and wind speed time series are also shown in figures 5.17 and 5.18, but in this case only for Cabo de Peñas locations for the sake of simplicity. In the case of currents, it can be seen that the common period is shorter than in the case of waves, however almost ten years of data are available.

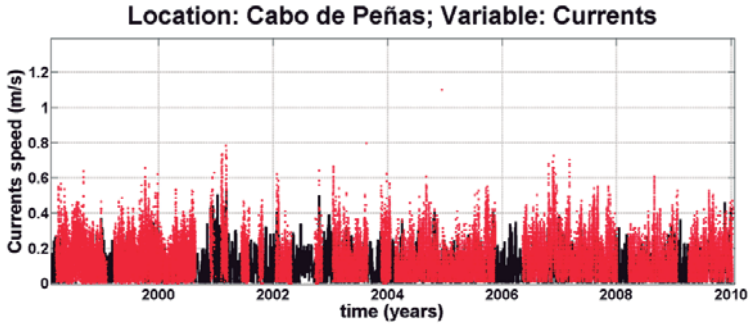

Figure 5.17: Currents intensity time series at Cabo de Peñas.

Both, currents and wind speed started to be measured at the same time, consequently, the time series length is similar and the blanks are quite similar too. In figure 5.18, wind speed time series for reanalysis data and instrumental data are shown for the common period.

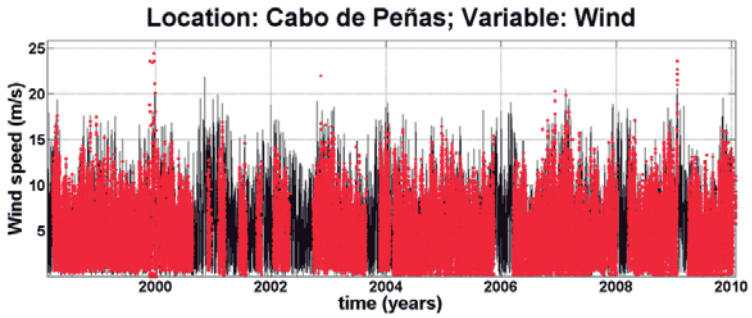

Figure 5.18: Wind intensity time series at Cabo de Peñas

The application of RMEV model to data turns out in an improved return period estimation. Three different cases can be faced after the application of the method: i) the 50-yr return period value increases, which means that reanalysis data is underestimating extreme values; ii) 50-yr return period value does not change considerably or reanalysis data is accurate; and iii) the 50-yr return period value decreases. In the last case, the security factor used during the design process is overestimated and it can be reduced, because the loads due to extreme would be lower than expected.

In figures 5.19, 5.20, 5.21 and 5.22 the results of the application to wave data are shown as an example. It can be seen how the return period curve changes and the values corresponding to key return periods increase in Estaca de Bares (figure 5.19), Cabo de Peñas (figure 5.20) and Bilbao (figure 5.22). In the case of Virgen del Mar (figure 5.21), all principal return periods decrease.

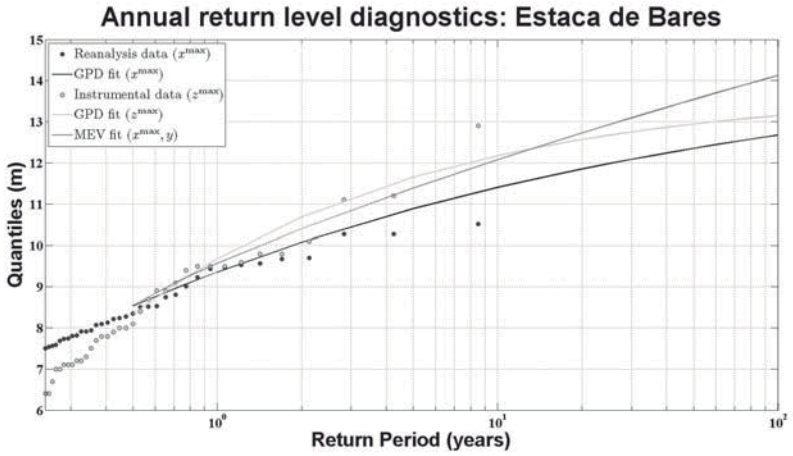

Figure 5.19: Results of RMEV application at Estaca de Bares.

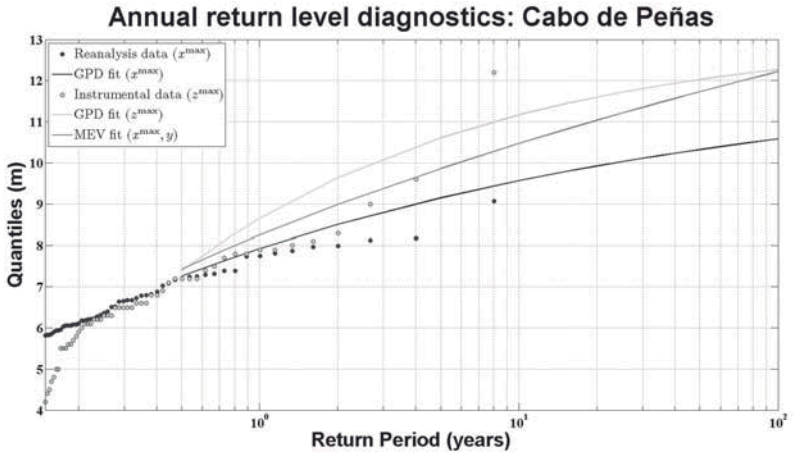

Figure 5.20: Results of RMEV application at Cabo de Peñas.

This method is applied not only to wave data, but also to wind and currents. The 50-yr return period values are summarized in table 5.3, where hindcast (H) and RMEV values are separated in columns for each one of the variables and locations.

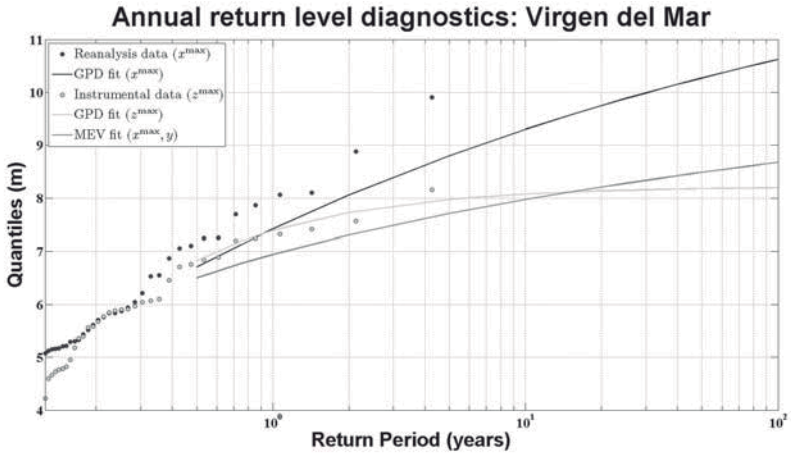

Figure 5.21: Results of RMEV application at Virgen del Mar.

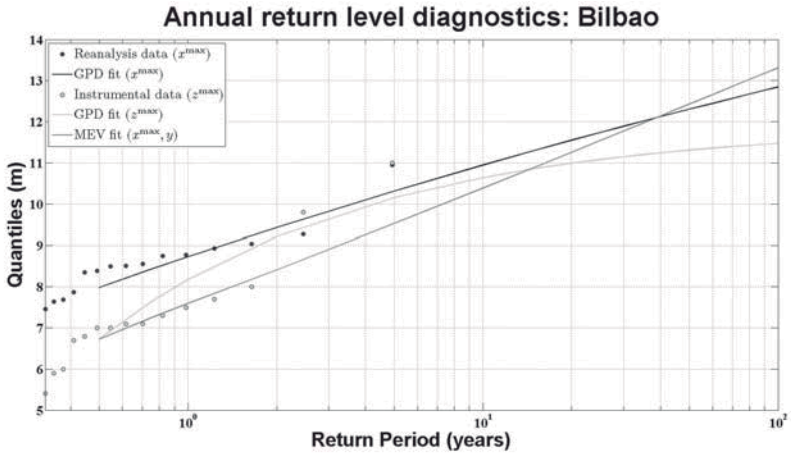

Figure 5.22: Results of RMEV application at Bilbao.

In table 5.3, it can be seen how return level values change due to the implementation of the mixed extreme model. Normally, the values increase. This fact may be due to the lack of accuracy of reanalysis databases in the right tail of the distribution (extreme). Then, the combination of both databases: reanalysis and instrumental, is supposed to improve the estimation of return period values.

	Wind (m/s)		Waves (m)		Currents (m/s)	
Location	H	RMEV	H	RMEV	H	RMEV
Estaca de Bares	25.29	23.01	12.58	13.59	0.33	0.49
Cabo de Peñas	24.25	26.33	10.41	11.72	0.62	0.76
Virgen del Mar	26.4	35.2	10.3	8.5	0.825	1.25
Bilbao	24.72	29.67	12.2	12.4	0.57	0.69

Table 5.3: 50-yr return level values for wind, waves and currents.

5.4 Offshore Wind Platform Performance: Spatial Variability Assessment

In this section, the mooring system response of a floating platform is analyzed. The met-ocean loads temporal and spatial variability impact on the performance of the floating platform will be evaluated. The steps of this analysis are:

1. Selection of a reference floating platform and mooring system
2. Selection of numerical models
3. Numerical model calibration
4. Mooring system loads variability analysis

5.4.1 Floating Platform Description

The floating platform used in this work is based on the semi-submersible concept (figure 5.23). Moreover, it is a tri-floater (cylinders) with heave plates (horizontal plates installed at the base of the floaters) and an asymmetric mooring system. It is designed to support a great capacity wind turbine in an eccentric position.

The three cylinders give the required buoyancy to support not only the wind turbine but also the weight of the structure. Furthermore, they give the inertia required at the flotation surface in order to achieve the stability of the system. These columns layout is an equilateral triangle. The columns are joined by a lattice of cylindrical bars with a diameter of 1200 mm.

Heave plates at the base of the columns are included to increase the added mass of the structure, increasing its natural period of pitch and heave degrees of freedom, which means that both natural periods are far from waves natural period.

The two columns that do not support directly the wind turbine have a concrete ballast in their lower sections to compensate the overturn moment due to the position of the wind turbine. Moreover, the three columns can be filled with water as

Figure 5.23: Semi-submersible floating platform.

Semi-submersible platform general characteristics	
Turbine	NREL 5 MW
Draft (m)	22.9
Design depth (m)	50
Displacement (m^3)	6217
Buoyancy center[1] (m)	11.14
Length (m)	67.08
Total weight (tn)	6372
Gravity center[1,2] (m)	20.77
Fairleads (m)	0

Table 5.4: Principal characteristics of the semi-submersible platform. [1] Gravity center and buoyancy center heights are considered with respect to the base of the structure. [2] Gravity center height takes into account the support structure, rotor, nacelle, tower and wind turbine.

ballast to achieve the required draft, and compensate the momentum due to wind and waves direction in order to keep the nacelle plane as horizontal as possible.

Semi-submersible platform geometry	
Columns diameter (m)	10.7
Structure airgap (m)	14.7
Heave plate diameter (m)	12.34
Distance between columns centers (m)	56.4
Bracings diameter (m)	1.2

Table 5.5: Geometry of the semi-submersible platform.

The mooring system is formed by four asymmetric lines. Two of them joined to the wind turbine supporting column and one more joined to each one of the other two columns (figure 5.24). The characteristics of the line for the design depth (50 m) are shown in table 5.6.

Semi-submersible mooring system	
Line length (m)	233
Diameter (m)	0.105
Weight/Length (kg/m)	221
Stiffness (kN)	8.62E+05
Horizontal projected length (m)	140
Shy length (m)	180

Table 5.6: Geometry of the semi-submersible platform mooring system.

5.4.2 Numerical Models and Methodology

The numerical models are commonly used in floating platform design because they allow reducing the total period of design. They are part of a general methodology that combines laboratory testing and numerical modeling. The first is used to validate and calibrate the numerical models. Once they are calibrated and they are simulating correctly the behavior of the floating platform they are used to

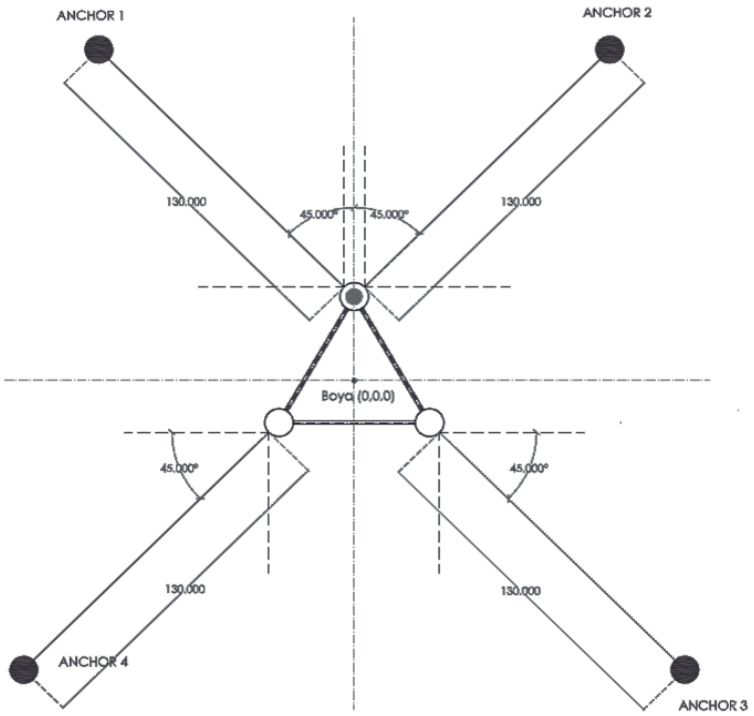

Figure 5.24: Semi-submersible floating platform mooring system scheme.

evaluate the response of the structure under several sea states. In this work, two numerical models were used SESAM and FAST.

5.4.2.1 **SESAM**

This software is developed by DNV (Det Norske Veritas). It includes three different independent modules:

- Sesam GeniE: structural design and analysis
- Sesam HydroD: frequency domain analysis
- Sesam DeepC: time domain analysis (movements and structural analysis)

The methodology to simulate the response of a floating platform using this software is shown in figure 5.25.

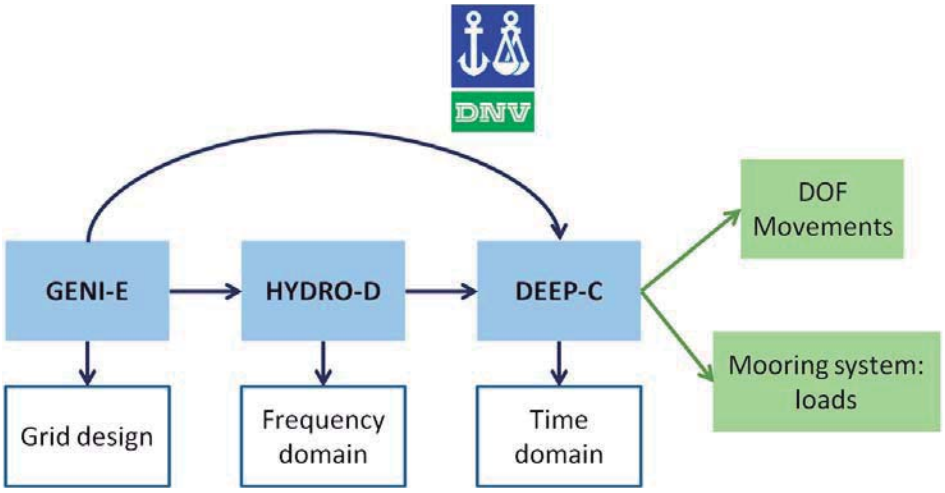

Figure 5.25: Numerical model methodology description.

5.4.2.2 **FAST**

The FAST (Fatigue-Aerodynamics-Structures-Turbulence) code (Jonkman (2009)) is a comprehensive aeroelastic simulator. It is applied to predict the extreme and fatigue loads of two or three bladed wind turbines. The wind turbine may be configured in order to take into account the rotor-furling, tail-furling and tail aerodynamics. It employs a combined modal and multibody dynamics formulation. The model works with a variable number of degrees of freedom, reaching 24 for three-bladed horizontal axis wind turbines deployed on a floating platform.

5.4.2.3 **Methodology**

In this first section, the methodology followed along the section is explained. The scheme summarizing this methodology is shown in figure 5.26.

It is required to define the project bases and assumptions. In this case they concern to: on one hand, the floating platform, the wind turbine, and the mooring system; on the other hand, to a reference scenario characterized by a specific depth, atmospheric stability, among other environmental characteristics.

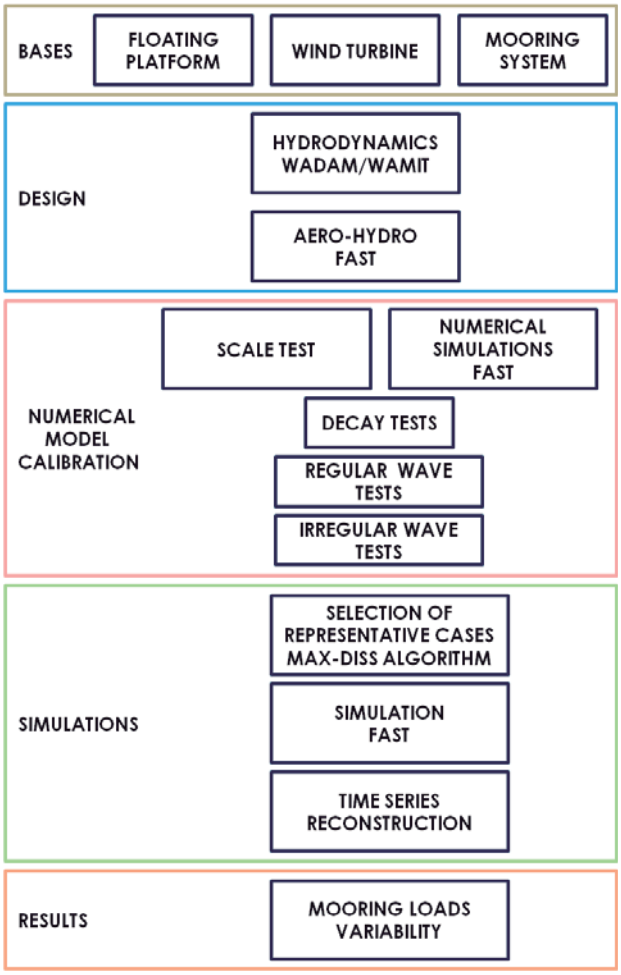

Figure 5.26: Descriptive scheme of the methodology.

The design step based on the characterization of the floating platform is carried out next. For this purpose, WAMIT is used to determine the hydrodynamics of the floating platform and FAST to couple hydrodynamics and aerodynamics.

The model defined on FAST must be calibrated. The calibration process requires the laboratory testing of the platform in order to estimate the value of the calibration parameters. Firstly, decay tests are used to calibrate the natural fre-

quencies of the structure. Secondly, regular wave cases are used to fit other parameters, such as the pretension of the mooring lines. Lastly, irregular wave cases are used to validate the calibrated model.

Simulation stage starts by selecting the most representative cases of the met-ocean conditions in the area of study using the MAX-DISS algorithm (Camus *et al.* (2011b)). Next, the sea states selected are introduced as input in FAST to simulate the response of the floating system. Then, the response at every sea state simulated is used to reconstruct the time series of any variable using the Radial Basis Functions (RBF) method (Camus *et al.* (2011a)).

Finally, a statistical analysis is applied to the time series in order to obtain results that can summarize and explain the influence of the met-ocean variables variability on the mooring system loads.

5.4.3 Numerical Model Calibration

It is mandatory to calibrate the numerical model in order to improve the estimation of the real behavior of the floating system during its lifetime. The calibration methodology follows several steps, where the first one is the decay tests. These tests are carried out in order to estimate the natural periods of some degrees of freedom of the structure.

The first decay test results shown in this work are related to surge degree of freedom (figure 5.27). It must be noticed that the only way to carry out this test is by taking into account the mooring system lines.

5.4.3.1 Decay Tests

As it can be seen the numerical model is simulating correctly the first seconds of the platform response for surge movement. The behavior of the numerical model with respect to the laboratory tests is smoother.

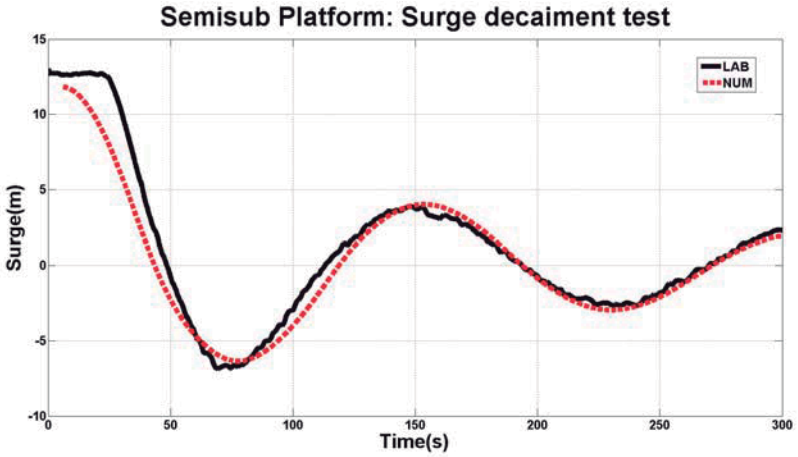

Figure 5.27: Surge decay-test time series.

In the case of heave movement (figure 5.28), it can be seen that the numerical model and the scale test have a similar natural period. The response of the numerical simulations has larger amplitudes than the scale test. However, these small difference are considered to be acceptable.

The last decay test that is shown in this work is related to the pitch movement (5.29). In this case, the numerical model is simulating closely the response recorded during the laboratory test. Moreover, it is following the trend at the first oscillations with a small larger response, whereas a good agreement is reached during the last ones.

5.4.3.2 **Regular waves**

The next step is to compare the results of regular wave case. In this case, wave characteristics are a significant wave height of 2 meters and a peak period of 16 seconds.

The oscillations simulated are larger than the ones registered in the laboratory

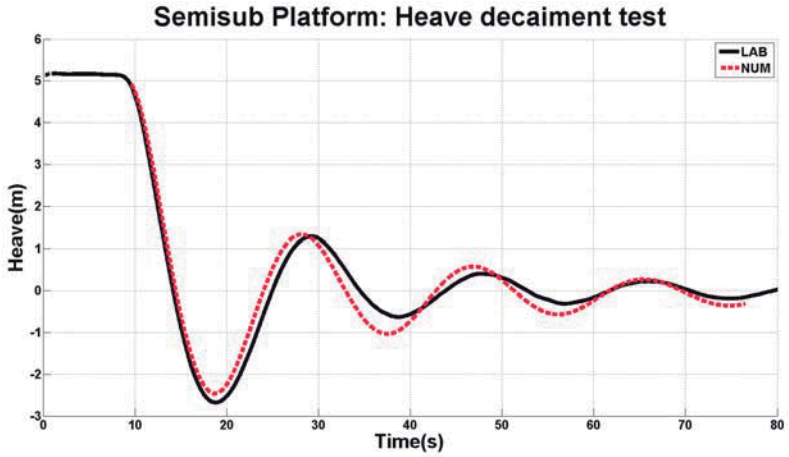

Figure 5.28: Heave decay-test time series.

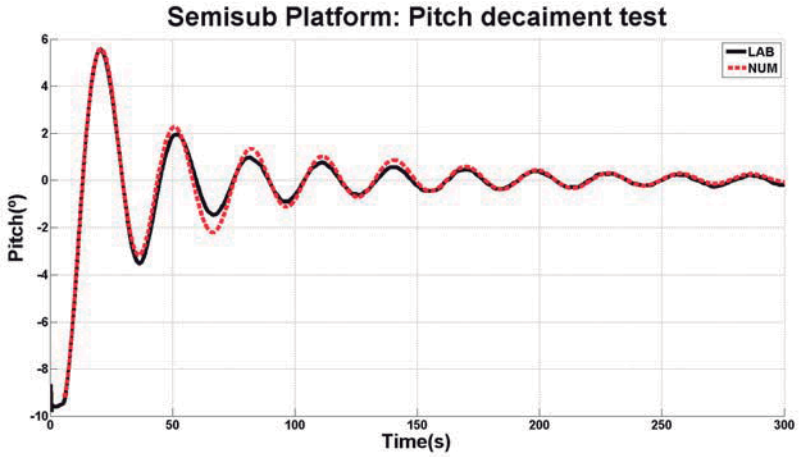

Figure 5.29: Pitch decay-test time series.

for surge and heave movements. However, the pitch angle is quite similar in both cases.

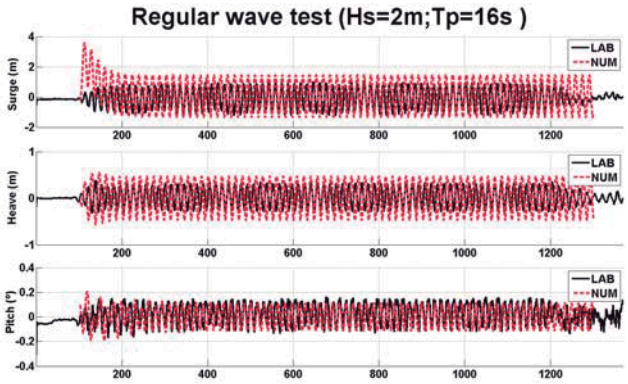

Figure 5.30: Regular wave test comparison.

5.4.3.3 **Irregular waves**

The last case is the comparison of irregular waves case. The results that are shown in this document correspond to a sea state of 12 m of significant wave height and a peak period of 17 seconds (figure 5.31).

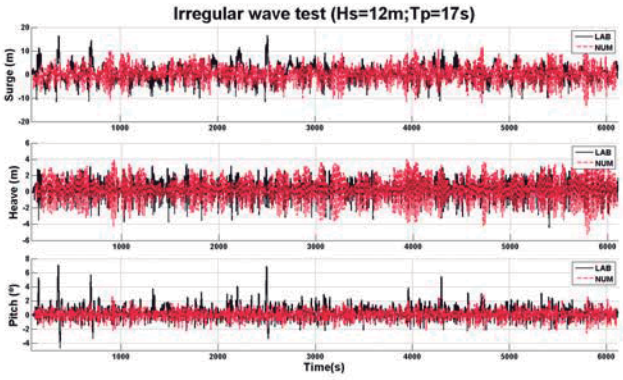

Figure 5.31: Irregular wave test comparison.

In the case of irregular sea states the direct comparison of the time series is not enough to validate the numerical model. Due to this, the loads on the mooring system (which is the final objective of this chapter) are shown in table 5.7.

5.4.3.4 Conclusions of calibration process

Results of the mooring system loads are based on a few statistical parameters. Furthermore, the results are shown for the four mooring lines. It is recalled that mooring lines 1 and 2 are at the front of the platform, facing directly the waves; and lines 3 and 4 are at the back of the structure. This layout implies that largest loads are recorded for the lines 1 and 2. The first parameter evaluated is the mean value of both time series: numerical simulations and laboratory records. It can be seen that mooring line 2 reaches the highest value and it is resembled closely by the numerical model. However, the numerical model is overestimating the mooring line 1 load. Moreover, it can be seen that lines 3 and 4 are recording loads whereas in the numerical model simulations show almost zero loads.

Maxima are not well estimated by the numerical model. It is noticed that in the laboratory tests the maximum loads registered are between two and three times the loads simulated by the numerical model. In order to reduce the weight of maxima, the analysis of the significant value of loads is included, which is the mean of the highest third sample. In this case, the maxima are filtered and results are improved. It can be seen that significant values are good enough for the methodology that is applied in this chapter. Furthermore, as final parameters of the analysis the quartiles are shown. In this case, due to the amount of zeros in the time series of mooring lines 3 and 4 their quartiles are always zero (these mooring lines rarely face the waves). However, results from mooring lines 1 and 2 are better. The behavior of these lines is better predicted.

Load (KN)	Catenary 1		Catenary 2		Catenary 3		Catenary 4	
	Num	Lab	Num	Lab	Num	Lab	Num	Lab
Mean	13.89	11.77	14.04	14.68	0.55	6.11	1.11	6.26
Max	214.8	677	247.2	674.15	207.6	633.9	241.1	545.17
F_s	20.39	17.03	23.4	24.98	1.66	8.96	3.35	8.4
	quartiles							
25%	10.01	8.93	8.41	8.93	0	4.46	0	5.14
50%	11.88	9.88	11.03	10.82	0	5.01	0	5.55
75%	14.94	11.36	15.72	13.80	0	6.09	0	6.22

Table 5.7: Statistical parameters of the mooring system loads for an irregular wave case ($H_s = 12m./T_p = 17s.$).

5.4.4 Mooring system loads variability

5.4.4.1 Met-Ocean Data

Wind Databases

SeaWind is a daily re-forecast for the Mediterranean and Euro-Atlantic region at 15 km resolution, providing wind-related variables with hourly frequency (Menéndez *et al.* (2014)). This product is produced by a mesoscale limited-area atmospheric model (WRF, Skamarock & Klemp (2008)) nested into ERA-Interim reanalysis data for the period 1989-2014. The focus of this work is on the accurate representation of hourly variability and, thus, a scheme with daily restarts from global reanalysis data was adopted in order to keep the model as close to the observed marine wind evolution as possible. The daily independent simulations also have the advantage of faster parallel computation, which was another requirement of the work, given the large domain simulated, the high resolution used and the long simulated period.

Waves Databases

In this work, wave data were taken from Global Ocean Waves 1.0 (GOW 1.0), an hourly wave reanalysis database for the period 1948-2014, with a spatial resolution of 1ºx1.5º (Reguero *et al.* (2012)). GOW 1.0 is generated using Wave Watch III model (WW3) and forced by winds from the NCEP/NCAR 40-year reanalysis

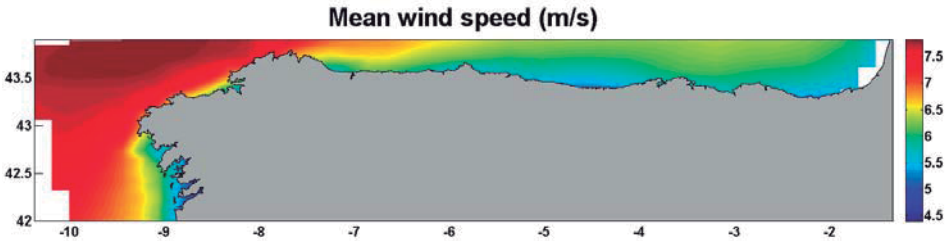

Figure 5.32: Mean wind speed (m/s).

project (Kalnay *et al.* (1996)).

The mean significant wave height and the mean peak period of waves are shown in figure 5.33 and figure 5.34, respectively, in order to correlate the mooring system loads with met-ocean characteristics. As it can be seen, the mean significant wave height is higher in the area of Galicia. It decreases along the North coast of Spain reaching the lowest values offshore the Basque Country. Near the coast the mean significant wave height is quite similar, around 1.8 meters.

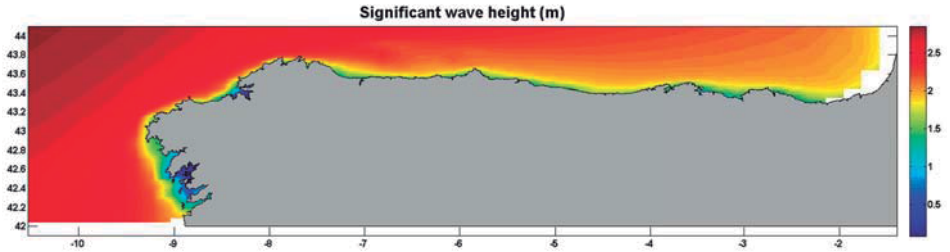

Figure 5.33: Mean significant wave height (m).

Another important variable that influences the hydrodynamic response of the floating platform is the peak period. In this case the mean peak period is around 9 and 10 seconds in all the area of study, but for the area close to the coast of Galicia. It is quite important to notice that the highest values are reached close to the coast, whereas lower values are reached offshore. This phenomenon might be due to the influence of sea waves. Winds from Northeast generating sea waves

have no effect on the West coast of Galicia due to the short fetch. Consequently, swell waves have more influence. Therefore, the mean peak period is higher in this area, as well as offshore the Basque Country.

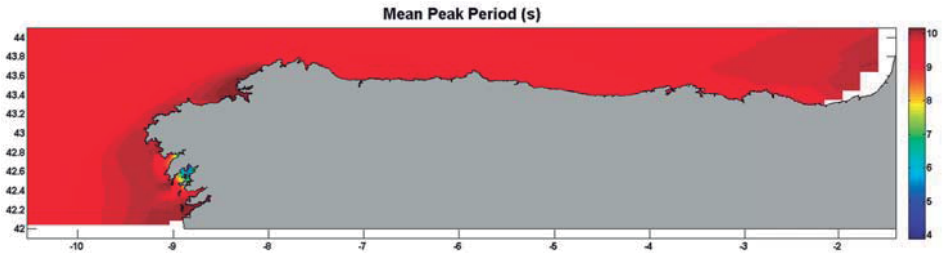

Figure 5.34: Mean peak period (s)

Currents Databases

GOS (Global Ocean Surges) is a dataset of 66-year (1948-2014) storm surge. The historical reconstruction of storm surge in the European region (Cid *et al.* (2014), Abascal *et al.* (2012)) has a spatial resolution of 1/8º (30km). GOS has been performed using the Regional Ocean Model System (ROMS), developed by Rutgers University (Shchepetkin & McWilliams (2003), Shchepetkin & McWilliams (2005)). ROMS is a three-dimensional, free-surface, bathymetry-following ocean model that solves the Reynolds-averaged Navier-Stokes equations using the hydrostatic vertical momentum balance and Boussinesq approximation.

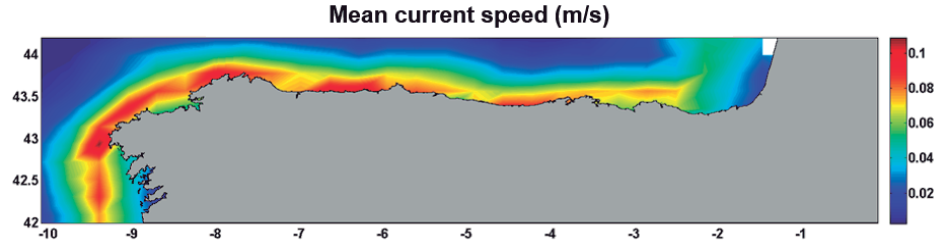

Figure 5.35: Mean current speed (m/s).

5.4.4.2 **Mooring system loads variability**

The mooring system loads variability analysis is based on the simulation of the 100 more representative sea states. This number of sea states is obtained by applying the Max-Diss algorithm (Camus *et al.* (2011b)) to 43 nodes preselected along the area of study (figure 5.36). This reduced number of nodes was chosen due to the length of the time series (more than 60 years) which implies a great use of computer memory during the application of the Max-Diss algorithm.

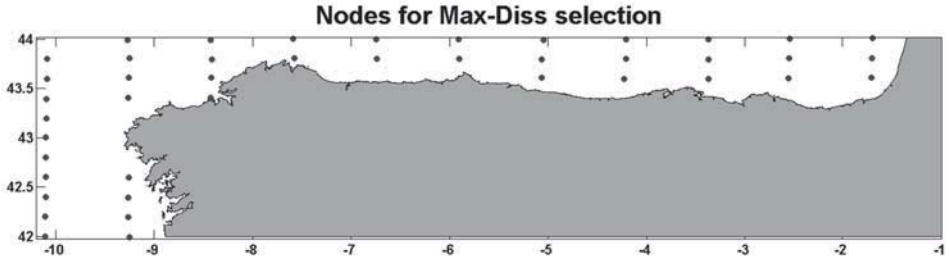

Figure 5.36: Selected nodes for Max-Diss application.

From each simulation the following parameters are calculated in order to characterize the mooring system load behavior (for the four catenary lines):

- Mean Load: mean value of the time series.
- Standard deviation: standard deviation of the time series.
- Mean value of load signal peaks: the peaks of the time series are chosen and their mean value calculated.
- Signal peaks standard deviation: following the same scheme, the standard deviation of the peaks of the signal is calculated.
- Significant Load: as it is used in waves statistical analysis, in this case the significant value of the loads is calculated.

It is important to notice that maximum values should be treated carefully due to FAST limitations. Therefore, statistical parameters from the load time series

peaks were used. The peaks mean value and their standard deviation were calculated as well as the significant peak load, which is the mean value of the greatest third part of the peaks.

Afterwards, the time series of these parameters at each node were reconstructed applying the RBF method (Camus *et al.* (2011a)). This allows reducing the total amount of cases simulated by the numerical model FAST and evaluating the spatial variability of mooring system loads.

In the following, the results of this process are described. Moreover, it must be noticed that results are presented as maps of different parameters along the area studied.

Firstly, the mean load value maps of the four catenary lines are shown in figure (5.37). It is clarified that catenaries 2 and 3 are the ones that face the waves. Therefore, they reach higher values at the most energetic areas, located offshore the coast of Galicia.

As it can be seen, the mean value spatial variability is small. In fact, catenary 1 load range is lower than 15 Tn as well as catenary 4. This fact might be due to its position in the layout (not facing the waves) or the reconstruction of load time series. Moreover, catenary 2 that reaches the highest mean loads (142 Tn), has a load range of around 10 Tn similar to catenary 3.

The highest mean loads are reached offshore the coast of Galicia in all the lines. Catenary 2 reaches values of 142 Tn whereas catenary 3 maximum mean value is 140 Tn. These values are 20 Tn higher than those from mooring lines 1 and 4 in the same area.

The response of all catenaries is clearly related to met-ocean variables. The peak period seems to be the one that influences the most the loads on the mooring system. This fact can be seen easily in catenaries 1 and 4. Surrounding Galicia (West) a strip is found where loads are higher than 130 Tn. corresponding to max-

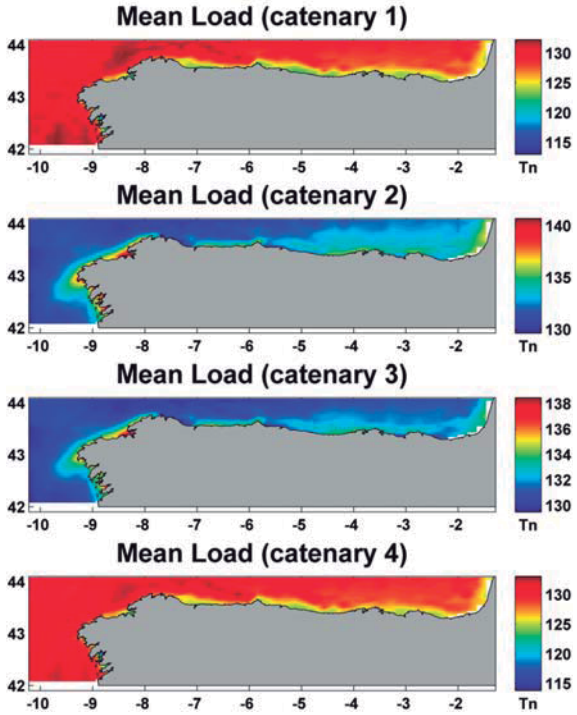

Figure 5.37: Mooring system loads - Mean value

imum mean peak periods in the area of study.

The next parameter that is analyzed is the standard deviation of the loads time series (figure 5.38). This parameter allows combining both spatial and temporal variability. The mean load deviation for the four mooring lines has a similar response. In this case, the catenary 4 reaches the highest values. The spatial pattern is quite similar to the mean load and to the peak period as well. It is interesting to highlight that maximum values are reached offshore the coast of Asturias (-8° lon -6°) which corresponds to a similar pattern in the mean peak period (figure 5.34).

The mean of maximum values of the loads time series is shown (figure 5.39) next. In this case, catenary 1 is reaching the lowest loads values. Catenary 4 has a similar behavior along the area of study but with values 30 Tn higher.

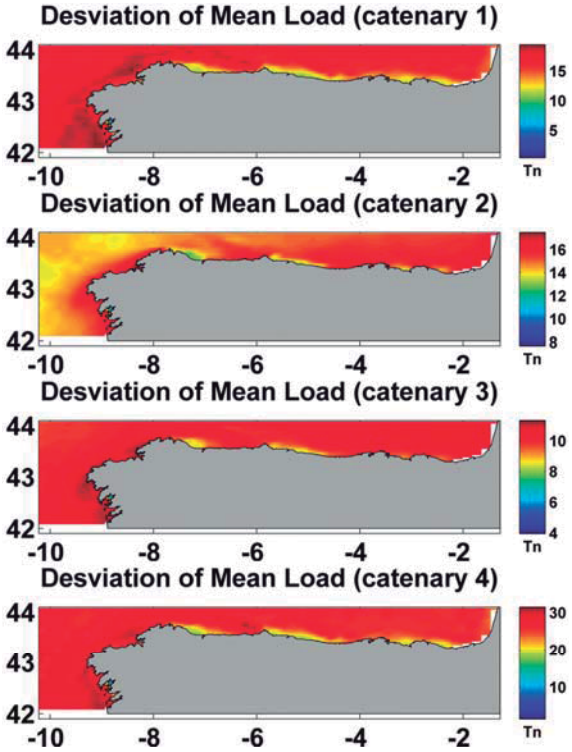

Figure 5.38: Mooring system loads - Standard Deviation

Catenary 2 and 3 are recording quite similar values, from 170 Tn in low energetic areas to 190 Tn in the more energetic areas in front of the coast of Galicia. The mean of maximum loads is influenced by the peak period.

The standard deviation of the peaks mean value is also included in this analysis. It can be noticed that four lines have a similar behavior in terms of spatial variability. In this case, the superposition of effects can be noticed. Firstly, the peak period pattern can be seen, as well as currents. However, in this parameter the effect of wind speed and significant wave height can be noticed as well. Catenary 1 and 4 (not facing the waves) reach values around 120 Tn, whereas catenary 2 and 3 that have also a similar behavior reach values around 90 Tn.

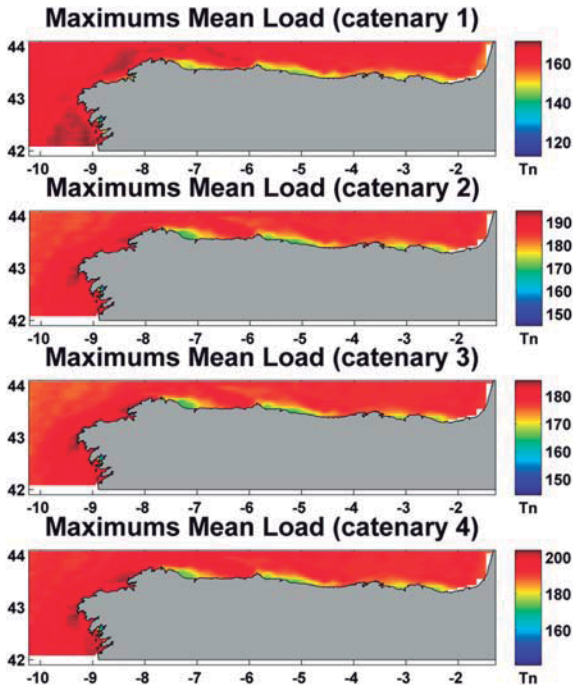

Figure 5.39: Mooring system loads - Peaks Mean value

The last parameter analyzed is the significant load. This parameter is included in the study in order to estimate the behavior of maxima without increasing the uncertainty due to FAST limitations.

In this case, all the mooring lines have a similar response. They reach the highest values offshore the coast of Galicia where peak period, wind speed, significant wave height and currents reach their maximum values. It can be noticed that all the catenary lines reaches maximum values around 150 Tn.

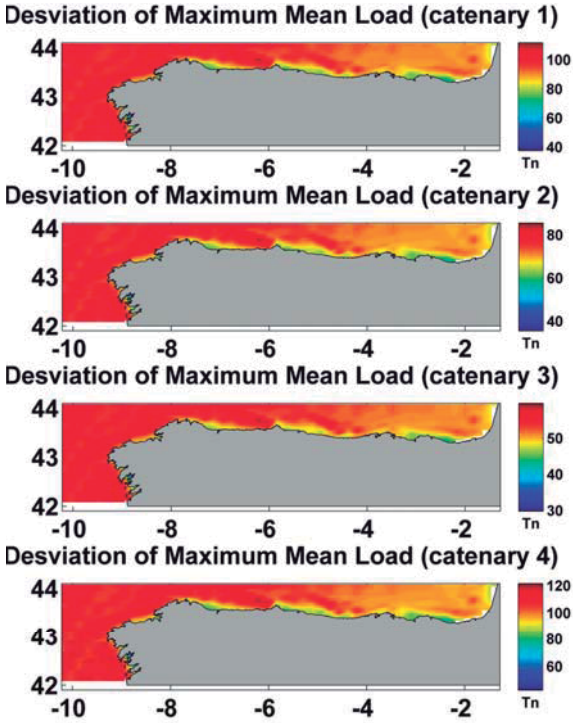

Figure 5.40: Mooring system loads - Peaks Standard Deviation

5.5 Conclusions

- Standards and guidelines propose a methodology for floating platform design. However, this methodology is based on the experienced gained from Oil&Gas technologies. Because of that, the methodologies proposed may be improved and adapted to the new challenges that offshore wind technology will face in the coming future.

- The mixed extreme method presented improves the estimation of the level of occurrence of met-ocean variables. It is based on the combination of instrumental data, which has good data related to extremes; and reanalysis data, which allows estimating the long-term behavior of the relevant variables due to its length.

- In this thesis, the IFORM method presented in Mínguez *et al.* (2014) is

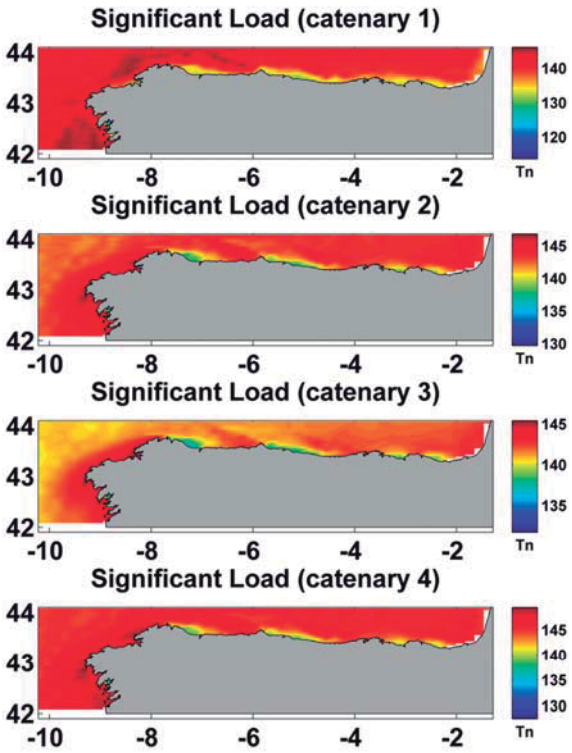

Figure 5.41: Mooring system loads - Significant Load

applied to several locations in order to estimate the impact of the improvements on the right tail of the distribution. Using Pareto distribution to fit the right tail of the distribution means that sea state long-term probability estimation gives better results. However, more efforts should be made in order to adapt the method to the data available providing more flexibility.

- The analysis of the spatial variability of loads in the area of study clarifies the difference of behavior of the four mooring lines. It is quite important to notice the influence of the met-ocean variables on the mooring lines loads. In this context the peak period seems to be very important as it can make the structure behave in different ways under different sea-states.

CHAPTER

6

Economic Feasibility Assessment

In this chapter, the influence of the wind conditions variability on the main financial estimators is evaluated. A life-cycle simulator model is developed and presented to obtain the variability of the main financial estimators. Moreover, a reference wind farm is described and used to simulate production and costs for the case study. The results of the simulations are related to financial estimators and their variability is discussed. This chapter is organized as follows:

- Introduction
- Life-cycle simulations
- Financial parameters description
- Case Study
- Results
- Conclusions

6.1 Introduction

6.1.1 Motivation

The investments required by offshore wind farms can be assumed to be in the range of 5M€/MW. Therefore, a methodology for economic analysis is required as an essential tool for assessing the potential feasibility of offshore wind farms and for assessing the effect of offshore wind conditions uncertainty on economic feasibility.

6.1.2 Objective of the chapter

In this chapter the objective is the evaluation of the influence of wind conditions variability on the economic feasibility.

6.1.3 Chapter structure

The chapter is organized as follows:

- Life-cycle simulation model
- Financial parameters
- Case Study
- Results
- Conclusions

6.2 Wind farm life cycle simulations

In this section the methodology followed to determine the distribution of the financial indicators is explained. The simulation of life-cycles has several steps (see figure 6.1):

1. 25 year wind speed time series are randomly generated using Markov chains method. These time series are, therefore, statistically significant.

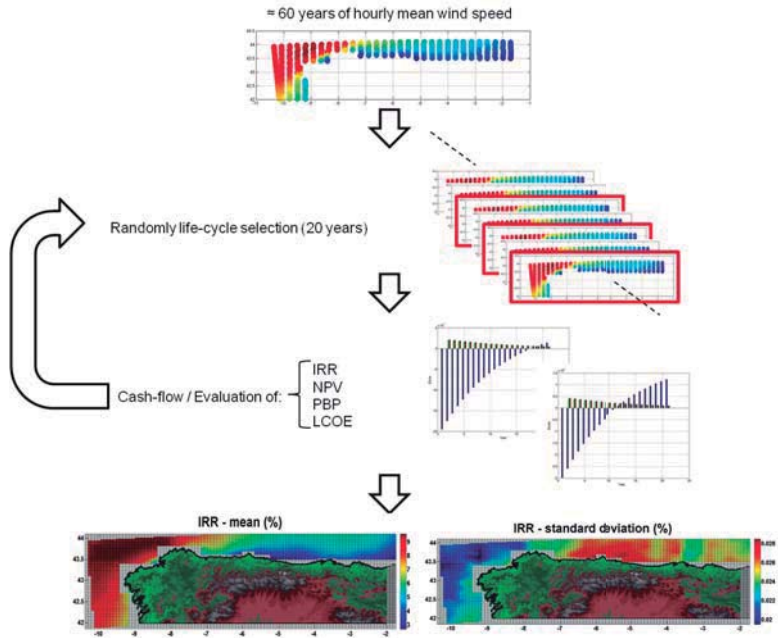

Figure 6.1: Cash-flow simulation diagram

2. Annual energy production (AEP) is evaluated at each node/location considering a specific wind turbine and wind farm.

3. The cashflow for the wind farm considered is calculated for each life-cycle. The construction costs, O&M costs, financial costs, the characteristics of the location and the income from energy production are taken into account.

4. The main financial indicators are obtained from each calculated cashflow.

5. Finally, statistical analysis of the financial indicators is carried out.

6.3 Financial Parameters

The cash flow analysis is based on the following financial formula:

$$PV = \frac{FV}{(1+r)^t} \tag{6.1}$$

where PV is the present value, FV stands to the future value, r represents the discount rate and t means the number of time periods.

The first indicator used to study the uncertainty related to the resource variability is the net present value (NPV) that is the sum of all the present values of the cash-flows corresponding to the project, measured at constant present prices.

$$NPV = \sum_{t=1}^{n_y} \frac{FV}{(1+r)^t} = \\ -I_0 + \sum_{t=1}^{n_y} \frac{AnnualRevenue - OperationCost}{(1+r)^t} \tag{6.2}$$

where Io represents the initial cost of the project assumed to the paid at time $t = 0$. $AnnualRevenue$ and $OperationCost$ refer to the annual income obtained by selling the energy generated at year t (q_t) at price pt, and to the annual operation and maintenance costs respectively and r refers to the discount rate.

The second indicator is the internal rate of return (IRR) that is the discount rate that makes the net present value equal to zero.

$$NPV = \frac{FV}{(1+IRR)^t} = 0 \tag{6.3}$$

The last financial indicator to take into account is the payback period (PBP), which provides the minimum number of years needed to recover the initial investment on a project.

$$\sum_{t=0}^{PBP} NPV \geq 0 \tag{6.4}$$

The cost of energy (COE) is considered in this work as the ratio between the total cost taking into account the discount rate and the energy produced in the lifetime.

$$COE = \frac{C_0 + \sum_{t=1}^{n_y} C_t}{\sum_{t=1}^{n_y} AEP} \tag{6.5}$$

where C_0 is the initial cost, C_t the O&M cost and AEP the annual energy production.

6.4 Case Study

6.4.1 Databases

6.4.1.1 Wind - SeaWind HR (High Resolution)

The coarse spatial resolution of global atmospheric databases is their most important inconvenient. Consequently, they cannot be applied to local characterization. Because of that, SeaWind HR (4.3.2) is used in this chapter.

In figure 6.2, the domain used in this work is shown. It can be seen that almost all the grid is located at offshore locations, but some included nodes are located onshore. This is due to the necessity of estimating the gradient of wind power from the coast to offshore locations.

6.4.1.2 Bathymetric data

The $GEBCO_{08}$ Grid is a continuous terrain model for ocean and land with a spatial resolution of 30 arc-seconds. The bathymetric portion of the grid has largely been generated from a database of ship-track soundings with interpolation between soundings guided by satellite-derived gravity data. However, in areas where they improve on the existing $GEBCO_{08}$ Grid, data sets generated by other methods have been included.

The bathymetric portion of the $GEBCO_{08}$ Grid was produced by combining the published Smith and Sandwell global topographic grid between latitudes 80N and 81S (version 11.1, September 2008) with a database of over 290 million ba-

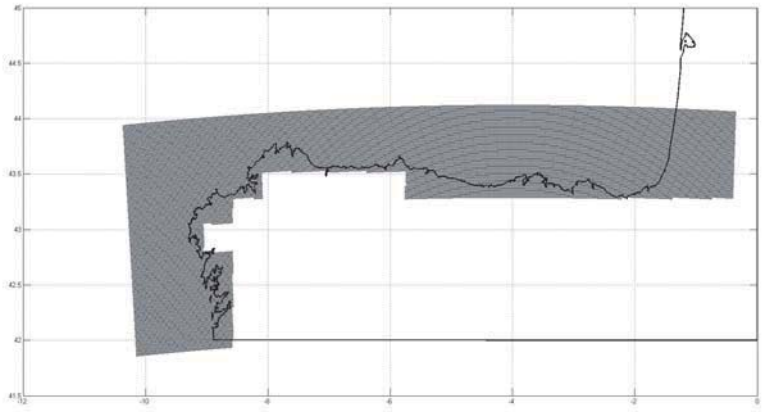

Figure 6.2: Grid points selected from SeaWind HR.

thymetric soundings.

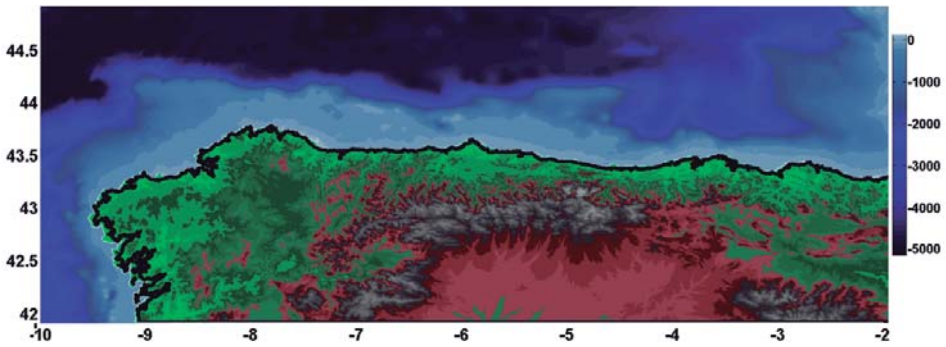

Figure 6.3: Bathymetry of the area of study.

The complete data sets give global coverage organized in files consisting of 21,600 rows x 43,200 columns, resulting in 933,120,000 data points. The data start at position 89 59' 45 "N, 179 59' 45" W. The data range eastward from 179 59' 45" W to 179 59' 45" E. The bathymetry of the area analyzed in this chapter is shown in figure 6.3.

6.4.2 **Floating wind turbine and wind farm description**

As it has been said in the introduction of this chapter, assuming a standard offshore wind farm allows focusing on the evaluation of the influence of the wind resource variability on the financial estimators.

In this case, a 500 MW installed capacity wind farm is selected (figure 6.4). To achieve this power capacity 100 turbines of 5 MW are chosen, with a squared layout of 10 x 10. The distance between turbines is around 800 meters. As it can be noticed, the offshore wind farm selected is quite simple in order to reduce the amount of variables to be analyzed.

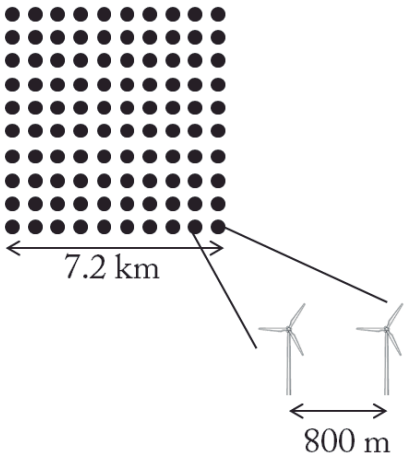

Figure 6.4: Wind farm layout.

Two important variables must be taken into account when the financial requirements for an offshore wind farm are analyzed (figure 6.5). These parameters are: i) distance to shore and ii) distance to port. The first one determines the length of the export cable, whereas the second one should be included in the analysis of transport, installation and O&M activities.

In this work, the distance to shore is evaluated by considering the distance

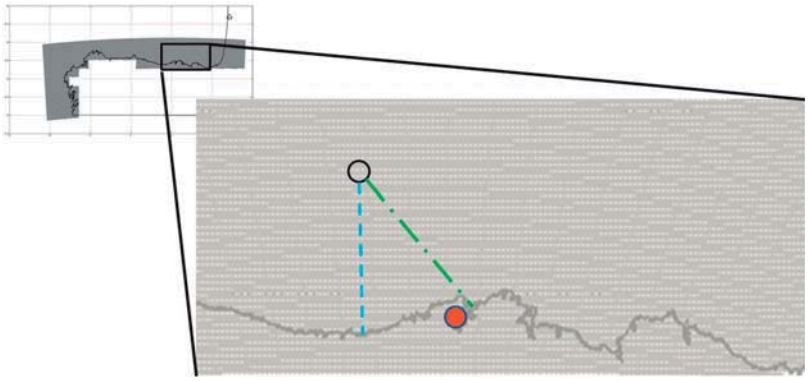

Figure 6.5: Distance to shoreline (blue line) and distance to harbour (green line)

between the wind farm and the nearest coastal point. This assumption does not take into account the points of the principal electrical capacity grid that allow the connection of 500 MW of electrical power. It is considered to be a problem out of the scope of this work.

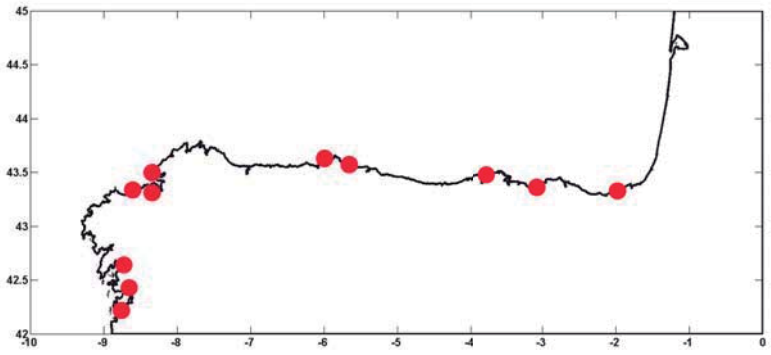

Figure 6.6: Harbours selected for the analysis

In the case of the distance to port, the most important harbors along the coast analyzed were considered (see figure 6.6). The distance for each node evaluated was selected as the minimum distance to harbor, which means that the distance

to every harbor was evaluated at every node and the minimum one was chosen as the distance to harbor. It is assumed that every harbor considered may be used as operations base.

A NREL 5 MW wind turbine is selected for this study (Jonkman *et al.* (2009)). The most important features of this wind turbine are publicly available and it is a representative utility-case multi-megawatt turbine. It has also been adopted as the reference model for the integrated European Union UpWind research program. This wind turbine is a conventional three-bladed, upwind, variable-speed, variable-blade-pitch-to-feather-controlled wind turbine.

6.4.3 **Cost breakdown**

The wind farm cost breakdown is a difficult task due to the lack of public available information. In our case, reference costs for the whole area of study were chosen based on the available literature information. It has to be highlighted that the more realistic the costs are the more accurate the analysis would be. Furthermore, the difference between locations are not dependent on the parameters and costs chosen, because they are considered common to all locations due to the limited extension of the region analyzed. Next, a summary of the breakdown cost is summarized.

6.4.3.1 **Wind Turbine**

Taking into account the proposed cost by Jonkman *et al.* (2009) of 1.2 M€/MW the wind turbine costs 6 M€. Systems on board and equipments are not included in this cost; therefore, a 5% of wind turbine and floating platform cost is added as Barturen *et al.* (2010) proposed.

6.4.3.2 **Floating Structure**

The floating structure cost is determined taking into account the amount of material and the cost of construction and transport. The material cost is 538€/Tn

(steel). Platform construction takes 64,000 hours with 45€/h.

As transport and installation specialized vessel cost 40,000€/day is used and 300,000€of mobilization. Two support vessel are used with a cost of 8,000€/day Barturen *et al.* (2010).

6.4.3.3 **Mooring lines**

A common catenary cost is assumed: 2.6 €/Kg. For the catenary length estimation it is applied the good practice rule that assumes the length on three times the depth. In this work, the depth is obtained from GEBCO database (http://www.gebco.net/). The mooring size considered is 70 mm. It is assumed that the mooring size is site independent. However, this is non certainly true it can be considered a good approach. In this study we assume that catenary installation for each platform takes 4 days.

6.4.3.4 **Anchoring system**

The anchoring system is 70,000€/catenary Barturen *et al.* (2010). The specialized vessel cost is 50,000€/day, with a mobilization cost of 250,000e and an installation cost of 200,000€. With these costs, the final cost per platform is 660,000€.

6.4.3.5 **Station keeping operations**

Anchoring system installation is supposed to take 4 days as the installation of the catenary system per platform. We propose to use a security factor of 3 days for these operations. As an example, for a 50MW installed capacity wind farm these operations would take 165 days if single set of vessels were used Barturen *et al.* (2010).

6.4.3.6 **Electrical infrastructure**

Three subsystems are identified in this work: i) internal system, ii) evacuation system and iii) inland system. For the internal and evacuation systems a cost of 100,000€/day is assumed for the specialized vessel and 100€/m for their installation. The cost of the material is 150€/m for internal system cable and 250€/m

for the external system cable Barturen *et al.* (2010).

For the inland electrical system a cost of 100€/m for the cable and 75€/m for the installation are assumed Barturen *et al.* (2010).

The offshore substation costs Barturen *et al.* (2010) related to equipment supply and installation are 221,667€/MW and 11,000€/MW. The cost of the structure supply is 17.333€/MW and for the installation is 28,667€/MW. Onshore substructure have costs of 216,000€/MW (supply) and 10,833€/MW.

6.4.4 Main assumptions and simplifications

Two different analysis are presented in the following sections.

- Test 1: It is focused on evaluating the financial estimators behavior in the area of study assuming a specific price of the energy.
- Test 2: In the second case, the internal return of rate expected by the investor is supposed as an input and the price of energy is derived.

1. Energy price defined as the cost of electricity is set to 0.5 €/KWh.
2. Real (net of inflation) interest rate is assumed to be 2%.
3. Construction costs are incurred and paid at year 0.
4. Financial and O&M costs are spread homogeneously during the lifetime.
5. OPEX is assumed to be 20% of CAPEX.
6. Annual revenues are collected at the end of each year.

6.5 Power production inter-annual and spatial variability

This section is divided into four subsections:

- Power production

	Component/Activity	Cost	Units
Wind Turbine	Turbine	1.2	M€/MW
	Systems on board	5	%
Floating Structure	Material	538	€/Tn
	Construction	45	€/day
	Transport Vessel	40,000	€/day
	Mobilization	30,000	€
	Support Vessel	8,000	€/day
Mooring Lines	Material	2.6	€/Kg
Anchoring System	Material	70,000	€/line
	Specialized Vessel	50,000	€/day
	Mobilization	250,000	€
	Installation	200,000	€
Electrical Infrastructure	Specialized Vessel	100,000	€/day
	Installation	100	€/day
	Internal system cable	150	€/m
	External system cable	250	€/m
	Inland system cable	100	€/m
	Inland system installation	75	€/m
	Offshore Substation	278,667	€/MW
	Onshore Substation	236,833	€/MW

Table 6.1: Summary of main costs.

- Cost of energy
- Test 1 results
- Test 2 results

The power production and the cost of energy are assessed independently, as they depend on the wind resource and the wind farm characteristics, respectively.

6.5.1 Power production inter-annual and spatial variability

The offshore wind energy farm profitability is directly related to its energy production. Due to this, it is quite important to analyze the energy production variability. In figure 6.7, the mean annual energy available, the mean annual energy produced by a single 5MW turbine and the corresponding capacity factor are shown. It can be seen that the maximum production values are achieved offshore Galicia, where the maximum wind yield is located. Moreover, wind power decreases along the coast until its minimum offshore the coast of the Basque Country.

The effect of the coastal topography can be seen properly in the area of Asturias, where the nearest nodes to the coast reach lower values of available energy than 1.8 MWh, whereas the next nodes reach values higher than 2MWh, resulting in a high gradient.

In order to evaluate wind energy inter-annual variability, five points along the area of study are selected. Afterwards, the AEP time series of a 500 MW wind farm are evaluated (Figure 6.8). In this case, the behavior of mean value follows the same pattern shown in figure 6.7 where the nodes in the coast of Galicia have more AEP than those located offshore Cantabria and the Basque Country. However, it can be said that the variability of the AEP is quite similar in these five cases, indeed in Galicia de scatter index (SI) (Table 6.2) is 6.6, whereas it is 8.1 in the Basque Country.

In table 6.2, the coordinates of the five points, as well as the mean value, the standard deviation and the scatter index are shown to evaluate the spatial and tem-

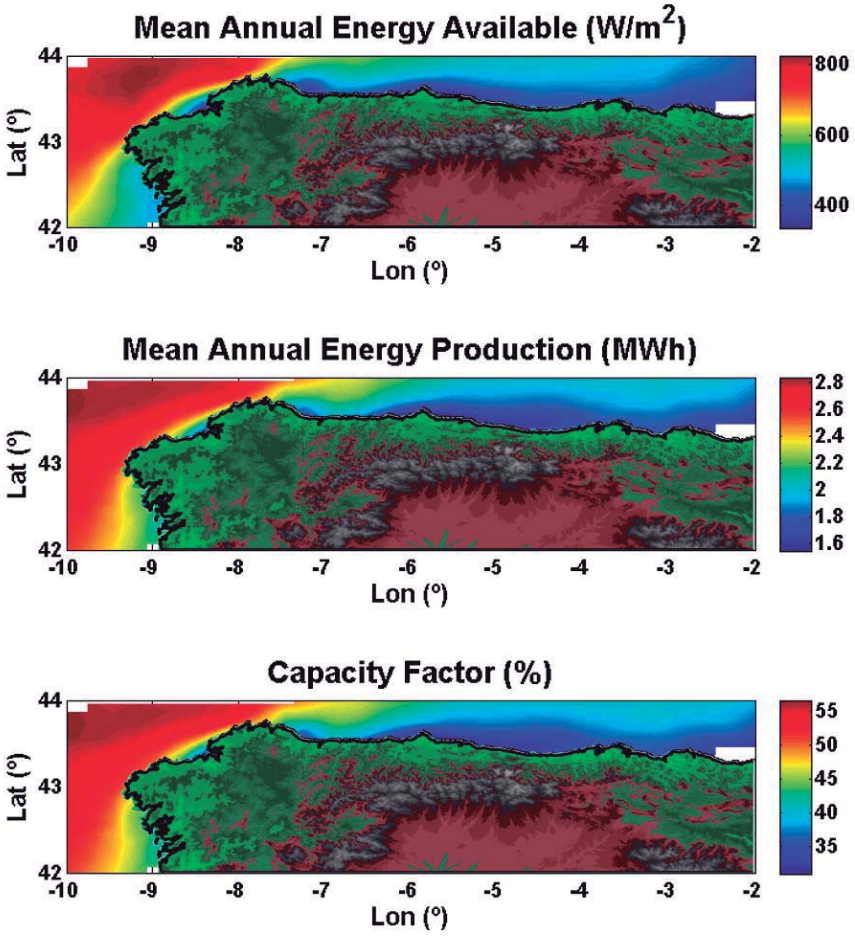

Figure 6.7: Mean wind energy available

poral variability along the North coast of Spain. The highest AEP value is reached at point 2 (yellow line in figure 6.8) in the Northwest coast of Galicia. Its mean value is 23307 GWh, its standard deviation is 1358 GWh and the scatter index is 5.8%. The other four locations have lower values of AEP and their scatter index are higher, which means that their variability is higher as well.

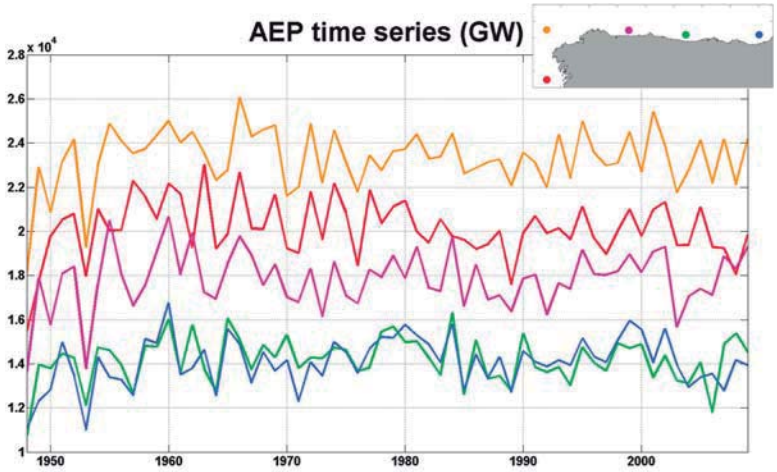

Figure 6.8: AEP time series in GW

	Point 1	Point 2	Point 3	Point 4	Point 5
latitude	42.25	43.75	43.75	43.6	43.6
longitude	-9.5	-9.5	-6.5	-4.5	-2
$\overline{P}(GW)$	20136	23307	17830	14178	14078
$\sigma(GW)$	1328	1358	1336	1058	1135
SI(%)	6.6	5.8	7.5	7.5	8.1

Table 6.2: Mean energy produced, standard deviation and scatter index at each point.

6.5.2 Cost Of Energy

The COE parameter is not independent from the discount rate because it is defined in this paper as the result of dividing the total cost of the wind farm (construction and O&M), which depends on the discount rate considered, by the total amount of energy produced. Consequently, there are two ideas to be considered: i) the further from the coast the wind farm is located the COE is greater mainly due to the export cable and the depth and ii) the greater the resource is the lower the COE is. Therefore, it may be reached a balance between both and an optimal location

may be found.

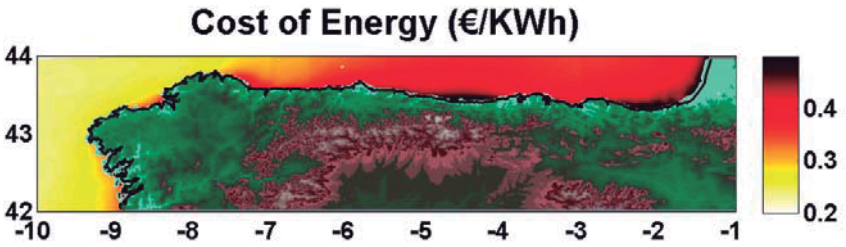

Figure 6.9: mean LCOE

In figure 6.9, the COE mean value is shown. It can be seen how the influence of the resource is higher than the influence of the distance to shore because lower values of COE are reached at the Atlantic coast (longitude $<$ °-7.5°), while higher values are located in the North ($-7° <$ longitude), due to the coastal topography influence in the case of Asturias and the low resource available in the case of Cantabria and Basque Country. The lower values, located in Galicia, are around 0.25-0.3 €/KWh, while higher values reached at Asturias and Basque Country are around 0.5 €/KWh.

6.5.3 Financial estimators assessment for Test 1

In this section the financial estimators are analyzed along the area of study. They have been obtained following the assumptions presented in section 6.4.4.

6.5.3.1 Internal Rate of Return

In figure 6.10, the mean value of the internal return rate at the area of study is shown. The Atlantic coast (longitude $<$ -7.5) shows IRR values higher than 15% while eastern region show lower rates, even 0% near the coast of Asturias and Basque Country. The IRR factor follows the same pattern as the wind power available, which means that wind power available is the factor that influences the most the internal rate of return.

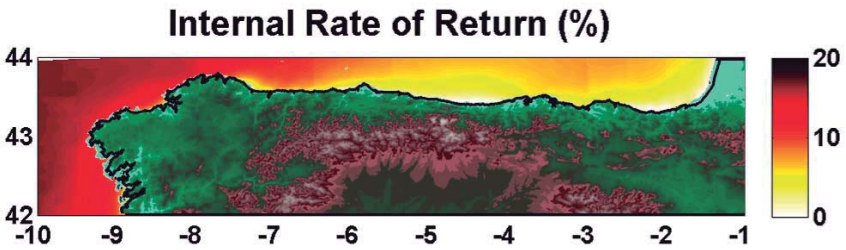

Figure 6.10: mean IRR

6.5.3.2 **Net Present Value**

Net present value is influenced by the discount rate, in contrast to IRR. Furthermore, in this section, the NPV for a discount rate of 2% is shown in order to analyze the spatial behavior of this parameter along the area of study.

In figure 6.11 the mean value of NPV is shown. It can be noticed that the NPV is higher where the wind resource power is higher. Consequently, it is following the same pattern as the IRR. Along the coast of Asturias ($-7^{\circ} <$ longitude $< -4.5^{\circ}$), Cantabria (around -3° of longitude) and Basque Country (longitude $> -3^{\circ}$) several areas are reaching negative values of NPV, which means, that these areas are not profitable for an offshore wind farm in the scenario assumed (around 10% of the total area analyzed).

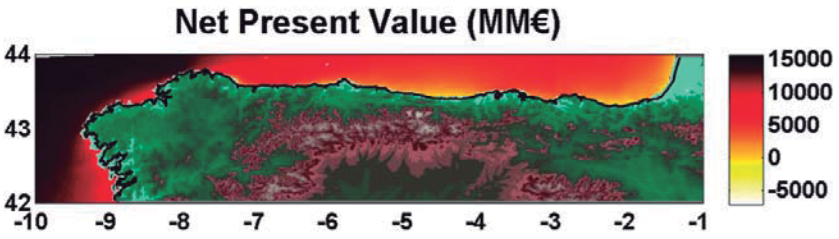

Figure 6.11: mean Net Present Value

6.5.3.3 **Pay-Back Period**

The PBP mean value is shown in figure 6.12. It can be seen that almost the whole area of study is characterized by a PBP lower than the lifetime of the wind farm,

which means that the project will be feasible. Some dark color zones along the coast of Asturias ($-7° <$ longitude $< -4.5°$) and Basque Country (longitude $> -3°$) can be noticed, this fact means that the PBP is higher than the lifetime, therefore, the investment would not be recovered. Values at the coast of Galicia (longitude $< -7.5°$) are around 12 years, so the investment is recovered at the mid-lifetime of the wind farm.

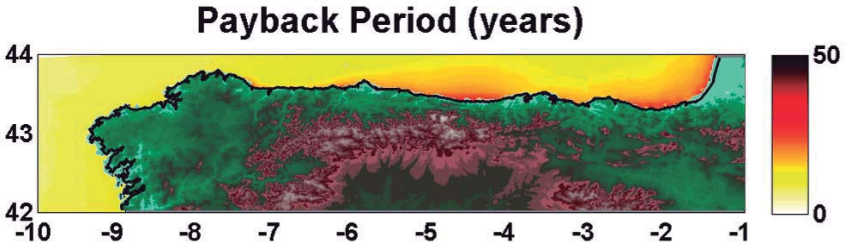

Figure 6.12: mean PBP

6.5.4 Energy price of test 2

In test 2, the energy price in c€/KWh for a 10% IRR is analyzed. Assuming this investment return implies an energy cost from 15c€/KWh in Galicia to 75c€/KWh in some areas of Asturias and Basque Country.

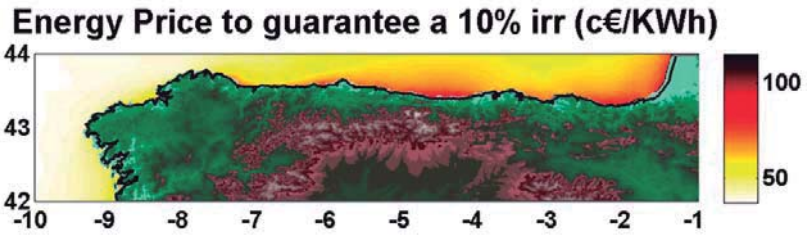

Figure 6.13: Energy price to guarranty a 10% irr

6.6 Conclusions

- The economical model applied in this study may be considered as a simple model. Due to this it must be improved in some areas. The main improvements may be done in the O&M model, the mooring system deployment costs and the power production time series construction.
- The spatial scale determines the impact of the main assumptions chosen during the analysis. In this case, some of them may reduce the applicability of the methodology as they are overestimated.
- The principal financial indicators give information to decision makers during the first steps of the design. In this study, the analysis allow selecting the optimal locations to implement an offshore wind farm.
- As it has been shown, the coast of Galicia seems to be the optimal area for floating offshore wind farms. This is mainly due to the high offshore wind resource.

CHAPTER

7

Conclusions

In this document the analysis of met-ocean conditions variability in offshore wind farms has been carried out. Firstly, the most significant contributions to date were selected to perform the review of the state of the art (chapter 2) related to offshore wind energy concepts treated in this work. This task allowed pointing out potential gaps in knowledge and proposing some objectives to be addressed in this research and selecting the methodology to achieve those objectives (chapter 3).

In chapter 4, wind conditions assessment at deep waters and very deep waters sites has been carried out. In first place, the long-term error due to the movement of floating met-mast has been analyzed. The numerical analysis is based on specific characteristics of a real floating meteorological mast (Guanche *et al.* (2011)) and the generation of synthetic wind time series. Afterwards, main sources of error due to the movement of the device were studied (heave, tilt and velocity). This study allow reducing the uncertainty related to instrumental measurements used in the rest of the work. Next, high resolution reanalysis data, as well as instrumental data from meteorological buoys and floating met-masts were used to characterize the spatial and temporal variability of wind conditions in the North coast of Spain.

One key point considered in this research was the influence of coastal topography and its relation to the wind flowing patterns and the wind shear in the transition zone between the coast and the ocean. Moreover, seasonal and annual analysis were also carried out.

As an important issue related to offshore deep and very deep water wind energy, in chapter 5 the floating platform performance assessment was carried out. Based on some gaps highlighted in the standards and guidelines, some improvements and updates were proposed in extreme characterization. The main objectives were related to the design parameters from extreme sea-states. Therefore, IFORM and Mixed Extreme Value models were studied. In the first case, the methodology proposed in Mínguez *et al.* (2014) was validated and applied to the North of Spain in order to analyze the spatial variability of 50-year return level H_S and V states. In the second case, a mixed extreme value model was updated to be able to work with shorter instrumental time series, which seems to be the common scenario in the future of deep and very deep water locations. This extreme model was also used to study the spatial variability of extreme loads on mooring systems. Numerical models and laboratory tests served for characterizing and simulating the dynamic response of the semisubmersible floating platform selected for supporting a wind turbine.

In chapter 6, the economic feasibility assessment of the implementation of an offshore floating wind farm was performed. The review of the literature was carried out to determine realistic methodologies and costs models to simulate random life-cycles. Applying this methodology to a reference wind farm, based on floating semisubmersible platforms and 5MW wind turbines, allowed characterizing the influence of met-ocean variability on the main financial estimators (NPV, IRR, PBP and COE).

In the following, the main conclusions of the Thesis are presented taking into account the general structure of the document:

- Deep waters wind conditions assessment

- The analysis of long-term error related to the floating met-mast carried out in chapter 4 shows that floating met-masts can be considered a competitive alternative to monitor met-ocean variables. This is supported by the low maximum error within the operational wind speeds range of a wind turbine. In the case of the floating met-mast analyzed numerically this error is nearly 0.5%.

- From the numerical and instrumental databases analysis it can be concluded that the combination of both improves the quality and the final assessment of wind resource and wind conditions. Instrumental measurements can be used to validate numerical databases in order to increase the area of study allowing characterizing the whole area of potential wind farms. Moreover, the pros and cons of the two databases were clarified and validated in this Thesis.

- The analysis of coastal topography influence addressed the objective proposed and served to understand how the orography can influence the wind flow. In the area of study in this work, southerly winds are really affected by coastal topography, creating a regional pattern that determines the best suited sites for the implementation of offshore wind farms. The methodology used to characterize this influence may be directly applied to other sites of interest.

- In the wind conditions temporal variability analysis the synoptic states methodology has been applied resulting in a more specific and useful information for the wind conditions assessment. The approach allows reducing the amount of data standing out the most important pieces of information for the analysis. This advantage was emphasized when seasonal and annual variability were analyzed.

• Floating platform performance assessment

  - The first and most important conclusion is that offshore wind energy

guidelines and standards have still room for improvement. They can be better adapted to the future challenges that wind energy farms will face in the foreseeable future.

– In this work, a calibration process for numerical modeling is shown. During the process it was noticed that there are some gaps in the assumptions and methods commonly used. Because of that, numerical tools combining aerodynamics, structural, hydrodynamics, etc. aspects still have a margin of improvement.

– In the case of extreme, more effort can be made to improve their characterization. In this work, one method has been updated to be applied to short time series of field measurements, which is expected to be the most common situation in offshore wind developments. Therefore, the extreme characterization needed for design purpose may have a great level of uncertainty and this updated method implies the use of bigger samples to estimate design parameters, reducing the uncertainty.

– The importance of the application of these extreme methods to the design process has been shown. Extreme load cases are based on long return level parameters. Because of that, more effort can be made to improve the extreme characterization. In this work, one method proposed by Mínguez *et al.* (2014) has been applied at different sites with different sources of data.

– It is noticed that a flexible methodology should be developed in order to be able to generalize its application. For instance, IFORM updated method proposed in Mínguez *et al.* (2014) requires strict characteristics of the data as it is a method based on fitting extreme distributions to the available samples of data.

- The implementation of extreme distribution to the mixed extreme model improved the estimation of occurrence level of met-ocean variables. It allows working with shorter instrumental time series which seems to be expected in future developments.

- Economical feasibility assessment
  - The life-cycle simulator model developed and applied to the reference scenario assumed at the North coast of Spain gives useful results for the analysis of economical feasibility assessment including the influence of wind conditions variability. Using long numerical databases to simulate wind farm life-cycles improves the characterization of the wind farm financial behavior. In this work, it was used to evaluate the spatial distribution of the main financial estimators and the influence of coastal topography.

CHAPTER

8

Future Research Lines

This Thesis tried to address the spatial and temporal variability related to some aspects of offshore wind energy due to the influence of met-ocean variables. Some important aspects were put aside because either they were out of the specific scope of this Thesis or because they were discovered while this research was being carried out. All the topics put aside compose the future research lines of this Thesis and they are presented following the same pattern of the Thesis and presented in the following:

- Deep waters wind conditions assessment
  - In this work, the numerical analysis of the movements of a floating met-mast has been carried out. However, the next step is to analyze the method developed in a real situation. Furthermore, it would add value to account of a fixed reference to evaluate accurately the short and long term error due to the movement.
  - Reanalysis databases have numerous advantages, such as their temporal length and their accuracy in mean terms. However, many efforts should be put in developing models that will be able to simulate

accurately extreme situations to reduce the dependency of expensive instrumental measurements.

- Another way to reduce the dependency from offshore instrumental data is the development and analysis of the correlation between onshore and offshore wind. It is proposed to advance in the understanding of the behavior and relation between wind at coastal locations and wind conditions offshore.

- Floating platform performance assessment
  - Currently, research projects are considering the possibility of combining different renewable energy sources or uses in the same floating platform. This will require the development or update of standards and guidelines.
  - Methods for the characterization of extreme states must be adapted to become more flexible. Consequently, they would give better results depending on the available data.
  - In the case of mixed extreme value model it is important to determine the minimum requirements for time series length. Therefore, it is proposed to evaluate the sensitivity of the model to the instrumental and reanalysis databases length.

- Economical feasibility assessment
  - Life-cycle simulator has been applied to the economical feasibility assessment to evaluate the spatial and temporal variability of the main financial indicators. The implementation of a better characterization of climate conditions, as well as a more complex O&M costs model are proposed to increase the accuracy of the economical model.

Bibliography

(2007). Dnv os-j101 design of offshore wind turbine structures. 59

(2010). Levelized cost of new generation resource in the annual energy outlook 2011. Tech. rep., Energy Information Administration (EIA). 70

(2013). Renewable energy outlook - world energy outlook 2013. Tech. rep., International Energy Agency (IEA). 23

Aamo, O. & Fossen, T. (2001). Finite element modelling of moored vessels. *Mathematical and Computer Modelling of Dynamical Systems*, **7**, 47–75. 61

Abascal, A., Castanedo, S., Fernández, V. & Medina, R. (2012). Backtracking drifting objects using surface currents from high-frequency (hf) radar technology. *Ocean Dynamics*, **62**, 1073–1089, cited By 7. 175

Alarcón, M. & Alonso, S. (2001). Computing 3-d atmospheric trajectories for complex orography: application to a case study of strong convection in the western mediterranean. *Computers & Geosciences*, **27**, 583–596. 48

Alewine, K. (2011). *Wind Turbine Generator Failure Modes*. Ph.D. thesis, Shermco Industries. 69

Alewine, K. & Zeglinski, D. (2013). Awea operation and maintenance recommended practices. *Washington, DC*. 69

Andersen, O.J. & Løvseth, J. (2006). The frøya database and maritime boundary layer wind description. *Marine Structures*, **19**, 173 – 192. 89

Arent, D., Sullivan, P., Heimiller, D., Lopez, A., Eurek, K., Badger, J., J, H.E., Kelly, M., Clarke, L. & Luckow, P. (2012). Improved offshore wind resource assessment in global climate stabilization scenarios. Tech. rep., National Renewable Energy Laboratory (NREL). xvii, 24, 25

Barturen, R., Couñago, B. & Díaz, I. (2010). Estudio técnico financiero sobre la construcción de un parque eólico marino flotante en el litoral español. In *Congreso Ingeniería Naval*, Bilbao. xxiii, 70, 191, 192, 193

Beran, M. & Nozdryn-Plotnicki, M. (1977). Estimation of low return period floods. *Hydrological Sciences Journal*, **22**, 275–282. 156

Blanco, M.I. (2009). The economics of wind energy. *Renewable and Sustainable Energy Reviews*, **13**, 1372–1382. 69

Braam, H., Obdam, T., van de Pieterman, R. & Rademakers, L. (2011). Properties of the o&m cost estimator (omce). *ECN-E-11-045*. 69

BVGA (2010). A guide to an offshore wind farm. Tech. rep., The Crown State. 8, 66

Caires, S. & Sterl, A. (2005). A new nonparametric method to correct model data: application to significant wave height from the era-40 re-analysis. *Journal of Atmospheric and Oceanic Technology*, **22**, 443–459. 56

Camus, P., Méndez, F.J. & Medina, R. (2011a). A hybrid efficient method to downscale wave climate to coastal areas. *Coastal Engineering*, **58**, 851 – 862. 96, 168, 177

Camus, P., Méndez, F.J., Medina, R. & Cofiño, A.S. (2011b). Analysis of clustering and selection algorithms for the study of multivariate wave climate. *Coastal Engineering*, **58**, 453 – 462. 11, 17, 88, 168, 176

Carrasco-Díaz, M., Rivas, D., Orozco-Contreras, M. & Sánchez-Montante, O. (2015). An assessment of wind power potential along the coast of tamaulipas, northeastern mexico. *Renewable Energy*, **78**, 295–305. 48

Castillo, E. (1988). *Extreme value theory in engineering*. New York: Academic Press. 55

Castro-Santos, L. & Diaz-Casas, V. (2015). Economic influence of location in floating offshore wind farms. *Ocean Engineering*, **107**, 13 – 22. 65, 67, 68

Cavaleri, L. & Sclavo, M. (2006). The calibration of wind and wave model data in the mediterranean sea. *Coastal Engineering*, **53**, 613–627. 56

Chujo, T., Minami, Y., Nimura, T. & Ishida, S. (2013). Experimental study for spar type floating offshore wind turbine with blade-pitch control. In *ASME 2013 32nd International Conference on Ocean, Offshore and Arctic Engineering*, V008T09A034–V008T09A034, American Society of Mechanical Engineers. 63

Cid, A., Castanedo, S., Abascal, A.J., Menéndez, M. & Medina, R. (2014). A high resolution hindcast of the meteorological sea level component for southern europe: the gos dataset. *Climate Dynamics*, **43**, 2167–2184. 175

Coles, S., Bawa, J., Trenner, L. & Dorazio, P. (2001). *An introduction to statistical modeling of extreme values*, vol. 208. Springer. 55

Cordie, A. (2010). State-of-the-art in design tools for floating offshore wind turbine. upwind project. Deliverable report, Garrad Hassan and Partners Ltd. 57

Couñago, B., Barturen, R. & Díaz, I. (2010). Estudio técnico-financiero sobre la construcción de un parque eólico marino flotante en el litoral español. *Ingeniería naval*, **LXXIX**, 85–105, iSSN 0020-1073. 8, 18, 66

de Prada Gil, M., Gomis-Bellmunt, O. & Sumper, A. (2014). Technical and economic assessment of offshore wind power plants based on variable frequency operation of clusters with a single power converter. *Applied Energy*, **125**, 218–229. 68

Dee, D.P. & co authors, . (2011). The era-interim reanalysis: Configuration and performance of the data assimilation system. *Quart. J. R. Meteorol. Soc.*, **137**, 553–597. 108

Dicorato, M., Forte, G., Pisani, M. & Trovato, M. (2011). Guidelines for assessment of investment cost for offshore wind generation. *Renewable Energy*, **36**, 2043–2051. xxiii, 65, 67, 68

Doyle, J.D. (1996). The influence of mesoscale orography on a coastal jet and rainband. *Monthly Weather Review*, **125**, 1465–1488. 48

EWEA (2013). Deep water, the next step for offshore wind energy. Tech. rep., European Wind Energy Association. xvii, 3, 24, 25, 26, 29

Faltinsen, O.M. (1990). *Sea Loads on Ships and Offshore Structures.*. Cambrigde University Press, Cambrigde, United Kingdom. xvii, 59

Faulstich, S., Hahn, B., Lyding, P. & Tavner, P. (2009). Reliability of offshore turbines–identifying risks by onshore experience. *Proc. of European Offshore Wind*. 69

Forsythe, G., Malcolm, M. & Moler, C. (1977). In Prentice-Hall, ed., *Computer Methods for Mathematical Computations*, Englewood Cliffs, New Jersey. 156

Gibson, P.B. & Cullen, N.J. (2015). Synoptic and sub-synoptic circulation effects on wind resource variability - a case study from a coastal terrain setting in new zealand. *Renewable Energy*, **78**, 253–263. 49

González-Longatt, F., Medina, H. & González, J.S. (2015). Spatial interpolation and orographic correction to estimate wind energy resource in venezuela. *Renewable and Sustainable Energy Reviews*, **48**, 1–16. 48

Grelle, A. & Lindroth, A. (1994). Flow distortion by a solent sonic anemometer: Wind tunnel calibration and its assessment for flux measurements over forest and field. *J. Atmos. Oceanic Technol.*, **11**, 1529–1542. 43

Guanche, R., Vidal, C., Piedra, A. & Losada, I. (2011). Idermar meteo. offshore wind assessment at high and very high water depths. In *OCEANS, 2011 IEEE - Spain*, 1–8. 9, 46, 49, 79, 88, 89, 203

Guanche, R., de Andrés, A., Simal, P., Vidal, C. & Losada, I. (2014a). Uncertainty analysis of wave energy farms financial indicators. *Renewable Energy*, **68**, 570 – 580. 11, 87, 96

Guanche, R., de Andrés, A., Simal, P., Vidal, C. & Losada, I. (2014b). Uncertainty analysis of wave energy farms financial indicators. *Renewable Energy*, **68**, 570–580. 69

Guanche, R., Meneses, L., Sarmiento, J., Vidal, C. & Losada, I.J. (2014c). Methodology to obtain the life cycle mooring loads on a semisubmersible wind platform. In *OMAE - 34th International Conference on Ocean, Offshore and Artic Engineering*, San Francisco, California. 10, 11, 79

GWEC (2012). Global wind energy outlook 2012. Tech. rep. 3, 23

Hall, M. & Goupee, A. (2015). Validation of a lumped-mass mooring line model with deepcwind semisubmersible model test data. *Ocean Engineering*, **104**, 590 – 603. 61

Hansen, M. (2008). *Aerodynamics of wind turbines*. Earthscan, London, UK. 58

Hansen, M., Sorensen, J., Voutsinas, S., Sorensen, N. & Madsen, H. (2006). State of the art in wind turbine aerodynamics and aeroelasticity. *Progress in Aerospace Sciences*, **42**, 285 – 330. 58

Heptonstall, P., Gross, R., Greenacre, P. & Cockerill, T. (2012). The cost of offshore wind: Understanding the past and projecting the future. *ENERGY POLICY*, **41**, 815–821. 69

Hirth, L., Ueckerdt, F. & Edenhofer, O. (2015). Integration costs revisited - an economic framework for wind and solar variability. *Renewable Energy*, **74**, 925–939. 49

Hsuan, C.Y., Tasi, Y.S., Ke, J.H., Prahmana, R.A., Chen, K.J. & Lin, T.H. (2014). Validation and measurements of floating lidar for nearshore wind resource assessment application. *Energy Procedia*, **61**, 1699 – 1702, international Conference on Applied Energy, {ICAE2014}. 43, 45

Hu, C., Sueyoshi, M., Liu, C., Kyozuka, Y. & Ohya, Y. (2013). Numerical and experimental study on a floating platform for offshore renewable energy. In *ASME 2013 32nd International Conference on Ocean, Offshore and Arctic Engineering*, vol. 8. 62

Iijima, K., Kawai, M., Nihei, Y., Murai, M. & Ikoma, T. (2013). Conceptual design of a single-point-moored fowt and tank test for its motion characteristics. In *ASME 2013 32nd International Conference on Ocean, Offshore and Arctic Engineering*, vol. 8. 62

IRENA (2012). Renewable energy technologies: Cost analysis series: Wind power. Tech. rep., International Renewable Energy Agency. 68

Izaguirre, C., Méndez, F.J., Menéndez, M., Luceño, A. & Losada, I.J. (2010). Extreme wave climate variability in southern europe using satellite data. *Journal of Geophysical Research: Oceans (1978–2012)*, **115**. 56

Jaynes, D. (2009). Lidar validation and recommendations for wind resource assessments. In *Proceedings of the AWEA WINDPOWER 2009 Conference*. 45

Jaynes, D.W., McGowan, J.G., Rogers, A.L. & Manwell, J.F. (2007). Validation of doppler lidar for wind resource assessment applications. In *AWEA Windpower Conference*, Los Angeles CA. 44

Jonkman, J., Butterfield, S., Musial, W. & Scott, G. (2009). *Definition of a 5-MW Reference Wind Turbine for Offshore System Development*. 16, 191

Jonkman, J.M. (2009). Dynamics of offshore floating wind turbinesmodel development and verification. *Wind Energy*, **12**, 459–492. 16, 59, 80, 166

Kaimal, J. & Finnigan, J.J. (1994). *Atmospheric Boundary Layer Flows. Their Structure and Measurement*. 43

Kalnay, E., Kanamitsu, M., Kistler, R., Collins, W., Deaven, D., Gandin, L., Iredell, M., Saha, S., White, G., Woollen, J., Zhu, Y., Leetmaa, A., Reynolds, R., Chelliah, M., Ebisuzaki, W., Higgins, W., Janowiak, J., Mo, K.C., Ropelewski, C., Wang, J., Jenne, R. & Joseph, D. (1996). The ncep/ncar 40-year reanalysis project. *Bull. Amer. Meteor. Soc.*, **77**, 437471. 96, 174

Karimirad, M., Koushan, K., Weller, S., Hardwick, J. & Johanning, L. (2015). Applicability of offshore mooring and foundation technologies for marine renewable energy (mre) device arrays. xvii, 40

Katzenstein, W. & Apt, J. (2012). The cost of wind power variability. *Energy Policy*, **51**, 233–243. 49

Kraan, C. & Oost, W.A. (1989). A new way of anemometer calibration and its application to a sonic anemometer. *Journal of Atmospheric and Oceanic Technology*, **6**, 516–524. 43

Kubik, M., Brayshaw, D., Coker, P. & Barlow, J. (2013). Exploring the role of reanalysis data in simulating regional wind generation variability over northern ireland. *Renewable Energy*, **57**, 558–561. 49

Landberg, L., Myllerup, L., Rathmann, O., Petersen, E.L., Jørgensen, B.H., Badger, J. & Mortensen, N.G. (2003). Wind resource estimationan overview. *Wind Energy*, **6**, 261–271. 6, 47

L.Kristensen (1998). Cup anemometer behaviour in turbulent environments. *J. Atmos. Ocean. Technol.*, **15**, 5–17. 43

López-Pavón, C., Watai, R.A., Ruggeri, F., Simos, A.N. & Souto-Iglesias, A. (2013). Influence of wave induced second-order forces in semi-submersible fowt mooring design. In *ASME 2013 32nd International Conference on Ocean, Offshore and Arctic Engineering*, American Society of Mechanical Engineers. 63

Makridis, C. (2013). Offshore wind power resource availability and prospects: A global approach. *Environmental Science & Policy*, **33**, 28–40. 69

Manwell, J., Mcgowan, J. & Rogers, A. (2009). *Wind Energy Explained. Theory, Design and Application.*. Second edition edn. xvii, 36, 37

Menéndez, M., Méndez, F.J. & Losada, I.J. (2009). Forecasting seasonal to interannual variability in extreme sea levels. *ICES Journal of Marine Science: Journal du Conseil*, **66**, 1490–1496. 56

Menéndez, M., García-Díez, M., Fita, L., Fernández, J., Méndez, F. & Gutiérrez, J. (2014). High-resolution sea wind hindcasts over the mediterranean area. *Climate Dynamics*, **42**, 1857–1872. 9, 96, 173

Mínguez, R., Méndez, F., Izaguirre, C., Menéndez, M. & Losada, I.J. (2010). Pseudo-optimal parameter selection of non-stationary generalized extreme value models for environmental variables. *Environmental Modelling & Software*, **25**, 1592–1607. 56

Mínguez, R., Reguero, B.G., Luceño, A. & Méndez, F.J. (2011). Regression models for outlier identification (hurricanes and typhoons) in wave hindcast databases. *J. Atmos. Oceanic Technol.*, **29**, 267–285. 56

Mínguez, R., Guanche, Y. & Méndez, F.J. (2013a). Point-in-time and extreme-value probability simulation technique for engineering design. *Structural Safety*, **41**, 29–36. 7, 16

Mínguez, R., Tomás, A., Méndez, F. & Medina, R. (2013b). Mixed extreme wave climate model for reanalysis databases. *Stochastic Environmental Research and Risk Assessment*, **27**, 757–768. 56, 81, 153

Mínguez, R., Guanche, Y., Jaime, F., Méndez, F. & Tomás, A. (2014). Filling the gap between point-in-time and extreme value distributions. In *Safety, Reliability, Risk and Life-Cycle Performance of Structures and Infrastructures*, 2595–2602–, CRC Press. 15, 17, 22, 55, 63, 76, 80, 142, 143, 146, 181, 204, 206

Mortensen, N. & Hojstrup, J. (1995). *The Solent sonic - response and associated errors*, 501–506. American Meteorological Society. 43

Mortensen, N. & Larsen, S. (1994). Flow-response characteristics of the kaijo denki omni-directional sonic anemometer (dat 300/tr-61b). 43

Overland, J.E. & Bond, N. (1993). The influence of coastal orography: The yakutat storm. *Monthly Weather Review*, **121**, 1388–1397. 6, 48

Overland, J.E. & Bond, N.A. (1995). Observations and scale analysis of coastal wind jets. *Monthly Weather Review*, **123**, 1388–1397. 48

P. B. MacCready, J. (1965). Dynamic response characteristics of meteorological sensors. *Bull. Am. Meteorol. Soc.*, **46**, 533–538. 43

Palm, J., Paredes, G. & Eskilsson, C. (2013). Simulation of mooring cable dynamics using a discontinuous Galerkin method. In B. Brinkmann & P. Wriggers, eds., *V International Conference on Computational Methods in Marine Engineering*, Hamburg, Germany. 61

Parish, T.R. (1982). Barrier winds along the sierra nevada mountains. *Journal of Applied Meteorology and Climatology*, **21**, 925–930. 6, 48

Philippe, M., Courbois, A., Babarit, A., Bonnefoy, F., Rousset, J.M. & Ferrant, P. (2013). Comparison of simulation and tank test results of a semi-sumersible floating wind turbine under wind and wave loads. In *ASME 2013 32nd International Conference on Ocean, Offshore and Arctic Engineering*, vol. 8. 62

Rademakers, L. & Braam, H. (2002). O&m aspects of the 500 mw offshore wind farm at nl7. *DOWEC project*. 65, 67, 69

Reguero, B., Menéndez, M., Méndez, F., Mínguez, R. & Losada, I. (2012). A global ocean wave (gow) calibrated reanalysis from 1948 onwards. *Coastal Engineering*, **65**, 38 – 55. 96, 173

Rodrigo, J.S. (2010). State-of-the-art of wind resource assessment. wind resource assessment audit and standarization (waudit). Tech. rep., CENER. 47

Rosenblatt, M. (1952). Remarks on a multivariate transformation. *Ann. Math. Statist.*, **23**, 470–472. 55

Santos-Alamillos, F., Pozo-Vázquez, D., Ruiz-Arias, J. & Lara-Fanego, V. (2014). A methodology for evaluating the spatial variability of wind energy resources: Application to assess the potential contribution of wind energy to baseload power. *Renewable Energy*, **69**, 147–156. 49

Schepers, G. & Van Garrel, A. (2006). Awsm: Free wake lifting line model for wind turbine aerodynamics. 58

Sempreviva, A., Barthelmie, R. & Pryor, S. (2008). Review of methodologies for offshore wind resource assessment in european seas. *Surveys in Geophysics*, **29**, 471–497. 24, 41

Shampine, L.F. (2008). Vectorized adaptive quadrature in matlab. *Journal of Computational and Applied Mathematics*, **211**, 131–140. 155

Shchepetkin, A.F. & McWilliams, J.C. (2003). A method for computing horizontal pressure-gradient force in an oceanic model with a nonaligned vertical coordinate. *J. Geophys. Res.*, **108**, 3090. 175

Shchepetkin, A.F. & McWilliams, J.C. (2005). The regional ocean modeling system: A split-explicit, free-surface, topography following coordinates ocean model. *Ocean Modelling*, **9**, 347–404. 175

Shin, H., Kim, B., Dam, P.T. & Jung, K. (2013). Motion of oc4 5mw semi-sumersible offshore wind turbine in irregular waves. In *ASME 2013 32nd International Conference on Ocean, Offshore and Arctic Engineering*, American Society of Mechanical Engineers. 63

Shu, Z., Li, Q. & Chan, P. (2015). Investigation of offshore wind energy potential in hong kong based on weibull distribution function. *Applied Energy*, **156**, 362–373. 49

Skamarock, W.C. & Klemp, J.B. (2008). A time-split nonhydrostatic atmospheric model for weather research and forecasting applications. *Journal of Computational Physics*, **227**, 3465 – 3485, predicting weather, climate and extreme events. 96, 108, 173

Snarey, M., Terrett, N.K., Willett, P. & Wilton, D.J. (1997). Comparison of algorithms for dissimilarity-based compound selection. *Journal of Molecular Graphics and Modelling*, **15**, 372 – 385. 11, 88

Standridge, C.R., Zeitler, D., Nordman, E., Boezaart, T. & Edmonson, J. (2013). Laser wind sensor performance validation with an existing gage. Tech. rep., Grand Valley State University. 44

Torres, C.R., Lanz, E.E. & Larios, S.I. (2015). Effect of wind direction and orography on flow structures at baja california coast: A numerical approach. *Journal of Computational and Applied Mathematics*. 48

Van Bussel, G. & Schöntag, C. (1997). Operation and maintenance aspects of large offshore windfarms. In *EWEC-CONFERENCE-*, 272–275, BOOKSHOP FOR SCIENTIFIC PUBLICATIONS. 69

Van Bussel, G. & Zaaijer, M. (2001). Reliability, availability and maintenance aspects of large-scale offshore wind farms, a concepts study. In *Proceedings of MAREC*, vol. 2001. 69

Vogt, S. & Thomas, P. (1994). Test of a phased array sodar by intercomparison with tower data. *J. Atmos. Oceanic Technol.*, **11**, 94–102. 45

Vogt, S. & Thomas, P. (1995). {SODAR} a useful remote sounder to measure wind and turbulence. *Journal of Wind Engineering and Industrial Aerodynamics*, **54–55**, 163 – 172, third Asian-Pacific Symposium on Wind Engineering. 44

Wiggelinkhuizen, E., Verbruggen, T., Braam, H., Rademakers, L., Xiang, J., Watson, S., Giebel, G., Norton, E., Tipluica, M.C., MacLean, A., Christensen, A.J., Becker, E. & Scheffler, D. (2007). Conmow: Condition monitoring for offshore wind farms. *Proceedings of the 2007 EWEA european Wind Energy Conference (EWEC 2007) Milan, Italy*. 69

Yamaguchi, A. & Ishihara, T. (2014). Assessment of offshore wind energy potential using mesoscale model and geographic information system. *Renewable Energy*, **69**, 506–515. 48

Young, E.. (2009). Cost of and financial support for offshore wind. Tech. rep., Ernst & Young Report for the Department of Energy and Climate Change, DECC, London. 7, 65